

Structural Bamboo - Mechanical Properties and Potential Fields of Application



M-4-06/2015

Philipp Leitner
Institut für Holzbau und Holztechnologie
Technische Universität Graz



Philipp Leitner, BSc

STRUCTURAL BAMBOO – Material Properties and Fields of Application

MASTER'S THESIS

to achieve the university degree of
Diplom-Ingenieur
Master's degree programme: Civil Engineering – Structural Engineering

submitted to
Graz University of Technology

Supervisors

Univ.-Prof. Dipl.-Ing. Dr.techn. Gerhard Schickhofer
Institute of Timber Engineering and Wood Technology

Ass.Prof. DI(FH) Dr.techn. Reinhard Brandner
Institute of Timber Engineering and Wood Technology

DI Bernhard Wallner
Institute of Timber Engineering and Wood Technology

Graz, June 2015

EIDESSTATTLICHE ERKLÄRUNG

AFFIDAVIT

Ich erkläre an Eides statt, dass ich die vorliegende Arbeit selbstständig verfasst, andere als die angegebenen Quellen/Hilfsmittel nicht benutzt, und die den benutzten Quellen wörtlich und inhaltlich entnommenen Stellen als solche kenntlich gemacht habe. Das in TUGRAZonline hochgeladene Textdokument ist mit der vorliegenden Masterarbeit identisch.

I declare that I have authored this thesis independently, that I have not used other than the declared sources/resources, and that I have explicitly indicated all material which has been quoted either literally or by content from the sources used. The text document uploaded to TUGRAZonline is identical to the present master's thesis.

Datum / Date

Unterschrift / Signature

Danksagung

Ich möchte mich an dieser Stelle bei all jenen Personen bedanken, die mich während meiner Studienzeit begleitet, angespornt und unterstützt haben.

Ein großer Dank gilt allen Mitarbeitern des Instituts für Holzbau und Holztechnologie sowie der holz.bau forschung GmbH für die Hilfsbereitschaft und nette Gesellschaft beim Verfassen dieser Masterarbeit wie auch während des gesamten Studiums.

Besonders möchte ich mich auch bei meinen beiden Betreuern DI Reinhard Brandner und DI Bernhard Wallner für die Unterstützung bei dieser Arbeit sowie für die anregenden Gespräche und Diskussionen bedanken.

Bei Herrn Prof. Gerhard Schickhofer möchte ich mich für die interessante Gestaltung der Lehrveranstaltungen bedanken, welche mein Interesse am Holzbau geweckt und gefördert haben. Außerdem für seine begeisterungsfähige Art und sein offenes Ohr für die Studierenden.

Ein riesiges Dankeschön an Ing. Bernd Heissenberger für die Hilfsbereitschaft, die Herstellung der Prüfkörper sowie die Unterstützung bei der Durchführung der Versuche.

Für die Bereitstellung des Materials und jeglicher Informationen möchte ich mich auch bei der Moso-International B.V. bedanken.

Danke Andrea für das Korrekturlesen und den Feinschliff meines Englisch.

Mein größter Dank gilt meiner Familie, vor allem meinen Eltern Eva und Hermann, für die immerwährende Unterstützung, dass sie es mir ermöglicht meinen Weg zu gehen, meine Interessen zu entfalten und ich mich in jeder Lebenslage auf sie verlassen kann.

Außerdem möchte ich mich bei all meinen Freunden, besonders bei meiner WG in der Rechbauerstraße, bedanken. Für die Erlebnisse und Unternehmungen die meine Studienzeit zu einem unvergesslichen und lustigen Abschnitt meines Lebens gemacht haben.

Abstract

Due to the increasing social awareness for sustainable constructions and thus the increasing demand for using environmentally friendly materials, renewable building materials are currently being discovered or rediscovered. One of these resources is bamboo. Bamboo is biodegradable and its mechanical characteristics, strength properties in particular, are promising.

The present study deals with growth habits, macro- and microstructure of the plant as well as the mechanical properties of bamboo relevant for structural applications. Furthermore, the state of the art regarding the production of engineered bamboo as structural beams or boards are pointed out. The central issue of this master thesis is the performance, evaluation and interpretation of tests used for determining selected moduli of elasticity and strength properties of laminated bamboo lumber (LBL). The results provide information about the strengths and weaknesses of this structural material. Based on these findings the potential fields of application of bamboo-products as structural element are discussed and outlined.

Kurzfassung

Aufgrund des steigenden gesellschaftlichen Bewusstseins für nachhaltiges Bauen und der damit einhergehenden Nachfrage nach natürlichen Baumaterialien, werden zurzeit nachwachsende Baustoffe neu oder wieder entdeckt. So auch Bambus, dem zusätzlich vielversprechende mechanische Eigenschaften, insbesondere Festigkeiten, zugesprochen werden.

In der vorliegenden Arbeit wird auf das Wachstum, die Struktur und die mechanischen Eigenschaften von Bambus, relevant für den konstruktiven Einsatz, eingegangen und der Stand der Technik zur Verarbeitung des Rohstoffes Bambus zu stab- sowie flächenförmigen Bauprodukten aufgezeigt. Kern dieser Masterarbeit ist die Durchführung, Auswertung und Interpretation ausgewählter Versuche an Laminated Bamboo Lumber (LBL) zur Bestimmung ausgewählter Elastizitätsmoduln und Festigkeitskennwerte. Die Ergebnisse geben Aufschluss bezüglich der Stärken und Schwächen dieses Werkstoffes auf Basis dessen Möglichkeiten zum Einsatz von Bambus als konstruktives Bauelement aufgezeigt werden.

TABLE OF CONTENTS

CHAPTER 1: INTRODUCTION	1
1-1 MOTIVATION	1
1-2 BACKGROUND ON BAMBOO.....	1
1-2.1 Structure	1
1-2.2 Mechanical Properties	5
1-2.3 Geographical distribution.....	10
1-2.4 Growth	10
1-3 STATE OF THE ART – ENGINEERED BAMBOO	11
1-3.1 Process of Production	12
1-3.1.1 Method 1: Strips to boards to beams/LBL	12
1-3.1.2 Method 2: Parallel strand bamboo (PSB)/bamboo scrimber/SWB	14
1-3.1.3 Method 3: Plate or roller flattened bamboo as base material	15
1-3.1.4 Method 4: Bamboo Mat Boards (BMB)/glulam.....	17
1-3.1.5 Method 5: Other bamboo based boards.....	18
1-3.2 Production Efficiency	18
1-3.3 Standardization.....	19
CHAPTER 2: MATERIALS & METHODS	20
2-1 GENERAL LAY-UP OF THE TEST SPECIMENS.....	20
2-2 GENERAL TEST METHODS	21
2-2.1 Determination of the specimen dimensions.....	21
2-2.2 Determination of the specimen moisture content	21
2-2.3 Determination of the specimen density	21
2-2.4 Air-conditioning of the specimen	21
2-3 TESTING MACHINES	22
2-4 GUIDELINES FOR THE DETERMINATION OF MECHANICAL PROPERTIES	22
2-5 BENDING	22
2-5.1 Basis of calculation.....	23
2-6 COMPRESSION PERPENDICULAR TO THE GRAIN	24
2-6.1 Basis of calculation.....	25
2-7 TENSION PERPENDICULAR TO THE GRAIN	26
2-7.1 Basis of calculation.....	27

2-8	TENSION PARALLEL TO THE GRAIN.....	28
2-8.1	Basis of calculation.....	29
CHAPTER 3: RESULTS.....		30
3-1	TEST RESULTS OF SERIES B – BENDING.....	30
3-1.1	Sample B-A1 (FW).....	30
3-1.2	Sample B-A2 (EW).....	31
3-2	TEST RESULTS OF SERIES C90 – COMPRESSION PERPENDICULAR TO THE GRAIN.....	33
3-2.1	Sample C90-H1 (EW).....	33
3-2.2	Sample C90-H2 (FW).....	34
3-3	TEST RESULTS OF SERIES T90 – TENSION PERPENDICULAR TO THE GRAIN.....	34
3-3.1	Sample T90-G1 (EW).....	34
3-3.2	Sample T90-G2 (FW).....	35
3-4	TEST RESULTS OF SERIES T-C AND PT-T0– TENSION PARALLEL TO THE GRAIN.....	37
3-4.1	Sample T-C.....	37
3-4.2	Sample PT-T0.....	37
CHAPTER 4: DISCUSSION.....		40
4-1	STRESS STRAIN RELATIONSHIPS IN BAMBOO.....	40
4-2	STRENGTH CHARACTERISTICS IN WOOD.....	41
4-3	BENDING.....	43
4-4	COMPRESSION PERPENDICULAR TO THE GRAIN.....	46
4-5	TENSION PERPENDICULAR TO THE GRAIN.....	51
4-5.1	E_{90} – Characteristic value.....	53
4-6	TENSION PARALLEL TO THE GRAIN.....	54
4-7	JOINTS.....	56
4-8	COMPARISON OF PROPERTIES.....	58
CHAPTER 5: CONCLUSION.....		59
5-1	PRACTICAL RELEVANCE & POTENTIAL APPLICATION.....	59
APPENDIX A: DIRECTORIES.....		I
A-1	References.....	I
A-2	List of Figures.....	IV
A-3	List of Tables.....	VI

APPENDIX B:TEST RESULTS.....		VIII
B-1	Sample B-A1 (FW)	VIII
B-2	Sample B-A2 (EW)	IX
B-3	Sample C90-H1 (EW).....	X
B-4	Sample C90-H2 (FW).....	XI
B-5	Sample T90-G1 (EW).....	XII
B-6	Sample T90-G2 (FW)	XIII
B-7	Sample T-C	XIV
APPENDIX C:FORCE VS. DISPLACEMENT DIAGRAMS		XVI
C-1	Sample B-A1 (FW)	XVI
C-2	Sample B-A2 (EW)	XVII
C-3	Sample C90-H1 (EW).....	XVIII
C-4	Sample C90-H2 (FW).....	XIX
C-5	Sample T90-G1 (EW)	XX
C-6	Sample T90-G2 (FW)	XXI
C-7	Sample T-C	XXII
C-8	Sample PT-T0	XXIV
APPENDIX D:IMAGES OF FRACTURE.....		XXV
D-1	Sample B-A1 (FW)	XXV
D-2	Sample B-A2 (EW)	XXIX
D-3	Sample T90-G1 (EW).....	XXXIII
D-4	Sample T90-G2 (FW)	XL

CHAPTER 1: INTRODUCTION

1-1 MOTIVATION

In recent years, the approach of environmentally friendly buildings has become more popular. So-called “Green buildings” aim attention to better insulation and more efficient heating to reduce energy consumption during the building’s lifetime. In addition, they focus on the decline of embodied energy of the materials and products installed as well as on the insurance of a healthy living environment for the inhabitants. Because of this trend and its excellent characteristics such as mechanical properties, being biodegradable, sustainable and removing carbon from the atmosphere due to photosynthesis process, wood gained importance (Falk, 2010). Nevertheless, as resource demands increase, it is becoming more crucial to find new fabrics and to develop products. One attempt to fulfil all these requirements is working with bamboo. Bamboo belongs to the family of grasses and its nature ranges from type of wood to bamboo herb. For structural application the woody bamboo is of special interest. It is a renewable and sustainable resource with mechanical properties comparable to some wood species. To use these advantages and to improve the application of bamboo in construction, engineered structural bamboo products are developed with the aim to reduce the variation in mechanical properties and geometry. Besides, bamboo-forests are widely distributed all over the world and grow in regions where woods for structural timber are limited (Ramage, et al., 2014). According to the International Network for Bamboo and Rattan there are about 1,250 species of bamboo worldwide. It is known as the fastest growing plant of all.

1-2 BACKGROUND ON BAMBOO

1-2.1 STRUCTURE

The bamboo culm has a cylindrical shape, with a larger diameter (d) and wall thickness (a) near the ground decreasing with height. On both sides, the culm wall is covered with a special tissue. The epidermis, the outer layer, with its high silica content resists insects and prevents the living stem from moisture loss. A waxy layer, which is also watertight, covers the inside. Longitudinally, the culm is separated into sections by nodes (solid diaphragms) that run transversely through the cross section. The longitudinal parts between these nodes are called internodes (Dixon & Gibson, 2014). Within the internodes, all cells are axially oriented and no radial cells, such as rays, exist (Liese, 1985). However, at the nodes, the parallel cell structure branch out which means some fibres enter the node and others head toward the upper intersection. Inside the nodes the fibres are randomly arranged, which aims for an isotropic behaviour within the node. The nodal diaphragms provide a horizontal connection of the fibres and vascular bundles and act as a prevention of buckling of the culm because of bending (Amada, et al., 1995). The nodes, which divide the culm into sections, are not at regular intervals. In most cases, the length (L) of the internodes increases up to a maximum at about the midpoint of the culm’s total length and then decreases again. Figure 1 outlines the structure

of two-year old Moso bamboo (or *Phyllostachys edulis*) culms. The height was between 16-20 m and the maximum diameter was about 13 cm (Amada, et al., 1995).

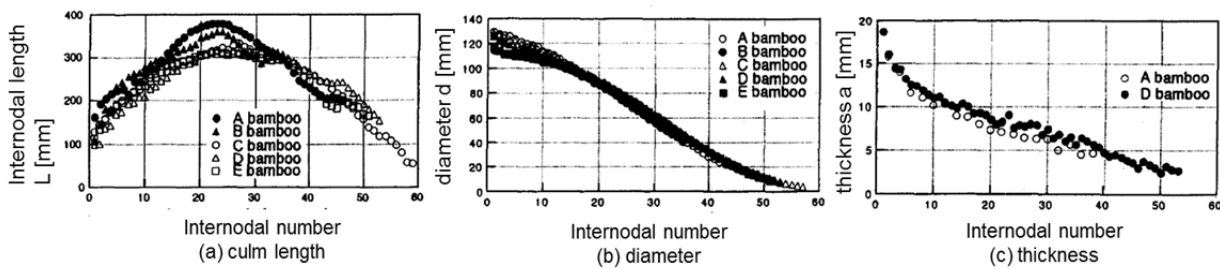


Figure 1: Macroscopic geometry of Moso bamboo (Amada, et al., 1995)

The number, size, arrangement and shape of the dark spots, which are the vascular bundles, mostly characterize the cross section of an internode. These vascular bundles are composed of two hollow metaxylem vessels, which serve water and mineral transportation, the phloem, consisting of sieve tubes (transportation of sugars) and companion cells, plus the supporting sclerenchyma fibres. The fibres occur as sheaths of the vascular bundle. In some species, there are additionally isolated fibre strands. The vascular bundles are embedded in the ground tissue that is made up of parenchyma cells. In general, the large portion of the culm consists of parenchyma (about 50 percent). About 40 percent by volume and 60-70 percent by weight of the total culm tissue consist of fibres. The conducting tissue (sieve tubes with companion cells and vessels) make up around 10 percent by volume (Liese, 1985).

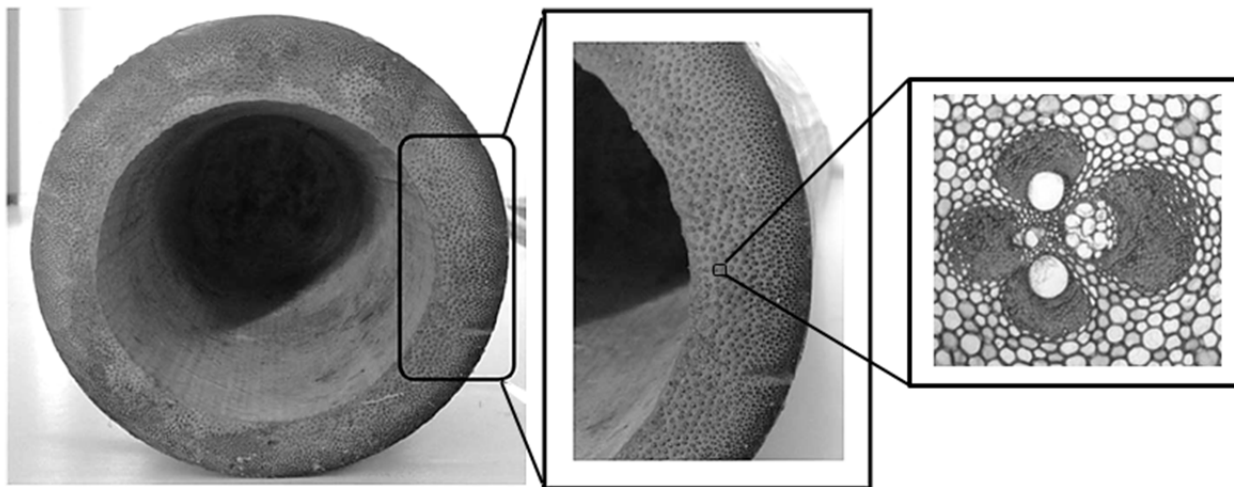


Figure 2: Cross section of a bamboo culm; fibre distribution in the culm wall; vascular bundle [left and middle image adopted from (Sharma, et al., 2014), right image adopted from (Schröder, 2014)]

In comparison to wood, bamboo has a more heterogeneous structure (Liese, 1992) as it mainly consists of the ground parenchyma and the ingrained vascular bundles. The sclerenchyma tissue that surrounds the hollow vessels consists of long thick-walled fibres, which are much denser, stronger and stiffer than the ground tissue. The vascular bundles are not evenly distributed within the culm wall but the volume fraction increases even though the size of the vascular bundles decreases with distance from the lacuna (Obataya, et al., 2007). As the vessels within the vascular bundles become smaller from the inside to the outside the solid fraction increases. Therefore, bamboo is a plant with a highly developed architecture or otherwise known a plant with a functionally graded structure, as the fibre distribution

corresponds to the stress distribution due to the bending moment generated by wind loads (Amada, et al., 1995). Figure 3 shows a cross section through the culm wall and pictures of the vascular bundles in different radial positions.

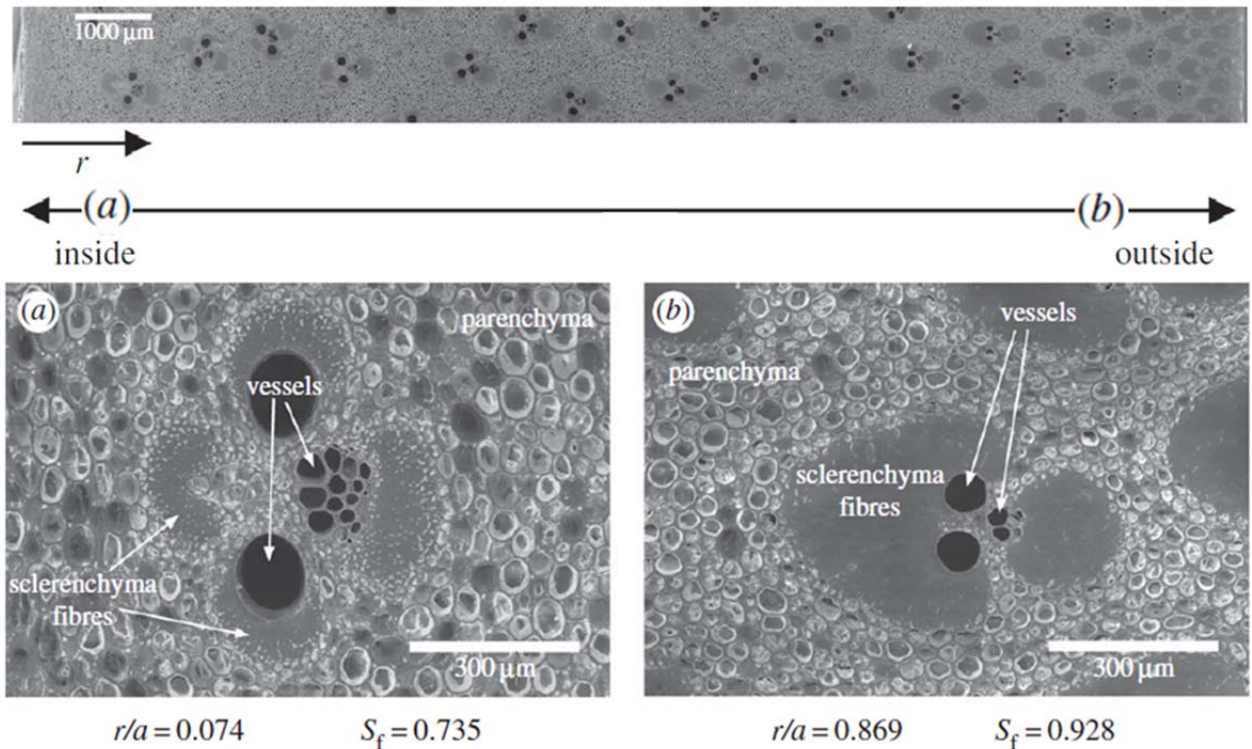


Figure 3: Micrographs; (above) over entire culm wall thickness; (below): a) of inner b) of outer vascular bundles

“Both the increasing volume fraction of vascular bundles, and the increasing volume fraction of solid within each vascular bundle lead to a pronounced radial density gradient in the bamboo culm, with denser tissue towards the outer part of the culm” (Dixon & Gibson, 2014)

The structure of an annual growth ring in a softwood tree, like Norway spruce, is similar as the early wood layer has about one third of the density of the late wood layer.

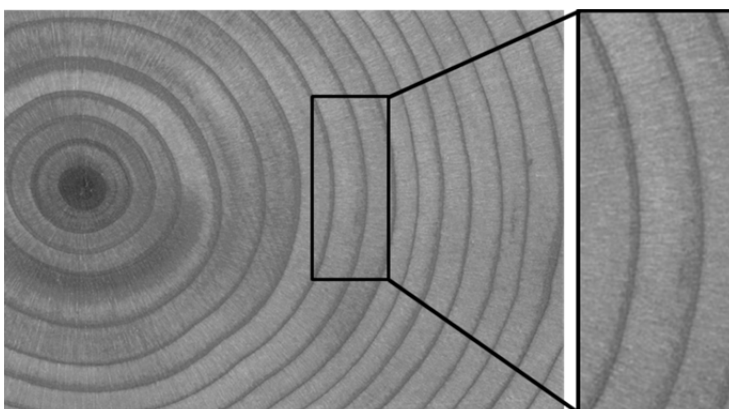


Figure 4: Annual growth rings in softwood

The fibre density also increases along the height of the bamboo culm but this trend is more moderate. However, there have been several studies on how the effect of density fraction within a culm affects the mechanical properties (Nogata & Takahashi, 1995; Amada, et al., 1995;

Nugroho & Ando, 2001; Li, 2004; Dixon & Gibson, 2014). Figure 5 shows the density of the small size specimens cut from different internodes (IN 5, 11 and 14; numbering started with zero at the base of the culm) and regions within the culm wall. On the axis of abscissas, the radial position (r) is normalized by the culm wall thickness (a) (Dixon & Gibson, 2014).

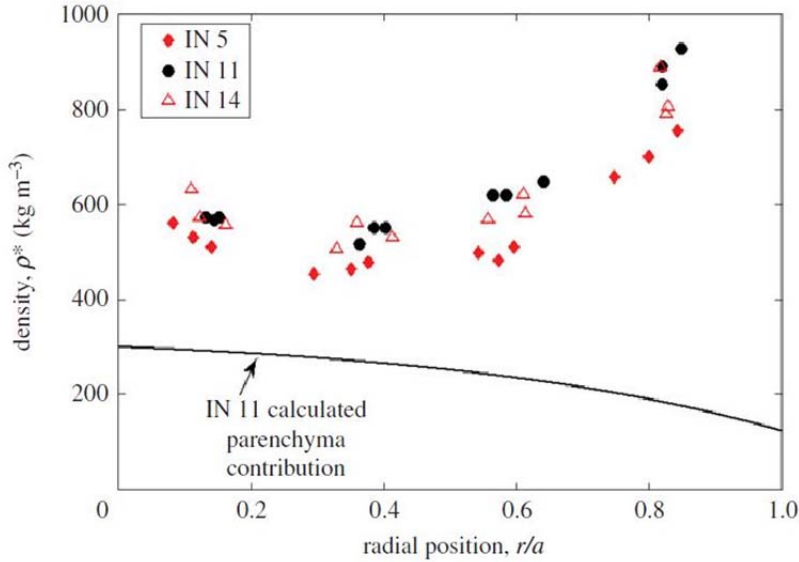


Figure 5: Density of internodes 5, 11 and 14 vs. radial position

Subsequently, Dixon and Gibson (2014) measured the volume fraction of vascular bundles (V_{vb}) from culm cross sections from internodes in various heights (Internode (IN) 3, 5, 7, 11, 14) and plotted it as a function against normalized radial position (r/a). As a next step, they measured the solid fraction (S_f) within the vascular bundles and found out that it increases from the inside to the outside of the culm wall but not with the height of the internode (see Figure 6).

The solid fraction of the parenchyma is 0.22 ± 0.03 and can be considered as constant throughout the culm wall. The average density of this ground tissue is 330 kg/m^3 , supposing that the solid cell wall material has the same density than that of wood (1500 kg/m^3). The material examined was a dried Moso bamboo culm (Dixon & Gibson, 2014).

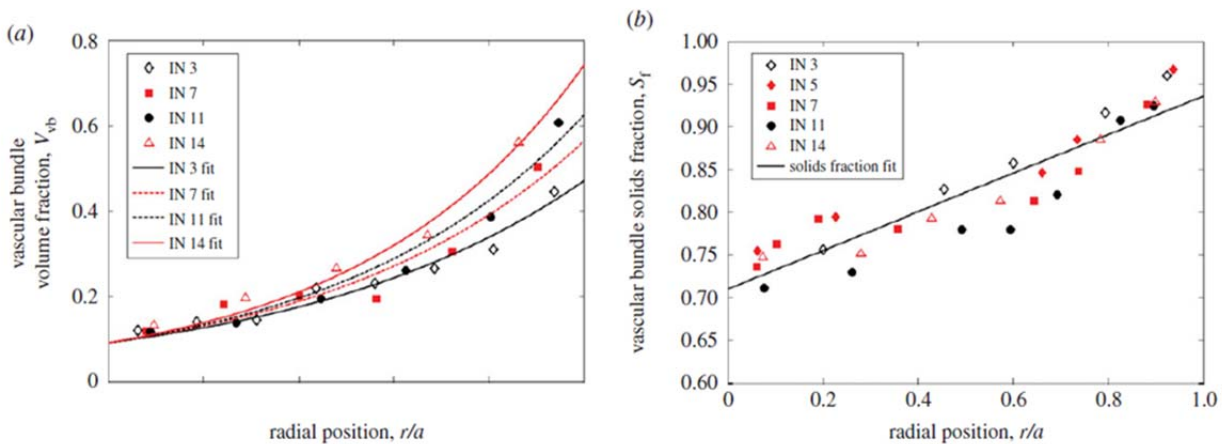


Figure 6: (left) Volume fraction of vascular bundles (V_{vb}); (right) solid fraction (S_f) plotted against normalized radial position (Dixon & Gibson, 2014)

The chemical composition of bamboo is similar to that of wood. It consists to more than 90 percent of the total mass of lignin (ground tissue), hemicellulose and cellulose (fibres). Additionally, bamboo contains other organic composition such as starch, fat, deoxidized saccharide and protein. As the microstructure varies between and within the species, so does the chemical makeup. Furthermore, it is affected by the condition of growth and the age of the culm (Liese, 1985).

1-2.2 MECHANICAL PROPERTIES

Just as with wood the strength is strongly dependent on the load direction, as the orientation of the cell fibres is in direction of the stem axis. As well, the cohesion of the vascular bundles among themselves (by the ground tissue) is lower than the strength of the single fibre. Strictly speaking, it is in bamboo as in wood an anisotropic material behaviour. However, an orthotropic material behaviour is for engineering purposes a sufficiently detailed approximation. Thus, the material properties are distinguished in the orthogonal directions (axial, radial, and tangential).

In bamboo research, most attention was paid to the mechanical properties in axial direction and therefore especially to the fibres. The allocation of the vascular bundles with their sclerenchyma sheaths varies with respect to position in the culm wall, and so do the physical and mechanical properties. Moreover there are many factors, such as age, moisture, season, soil, species, etc., that influence the characteristics of bamboo (Lee, et al., 1994).

Many studies have been carried out on the mechanical properties of bamboo and there are various approaches to understand and describe the relationship between structure and properties. Ghavami and Marinho (2001) determined the mean density of a whole Moso bamboo cane to be 666 kg/m^3 and the mean tensile strength to be 153 MPa. The result for mean bending strength was 135 MPa and for the mean modulus of elasticity 13.5 GPa (Ghavami & Marinho, 2001). Dizman Tomac, et al. (2011) state that the specific gravity within a bamboo cane, measured over the entire wall thickness, ranges from 700 to 840 kg/m^3 . Compression strength parallel to the grain varied from 47.3 to 62.5 MPa, bending strength from 93.1 to 186.2 MPa and modulus of elasticity from 13.1 to 18.9 GPa. The high variations originate due to the location along the cane, the "age" of the culm (the specimens have been subjected to accelerated aging procedure according to ASTM D 1037–89, 1989) and the presence or absence of nodes in the specimen tested. Since the fibres in nodal areas do not all run parallel to the direction of growth, it is a weak spot within the structure and strength properties decrease (Dizman Tomak, et al., 2011).

In other articles the structure of bamboo was modelled as fibre composite material in which the fibre ("reinforcement") is embedded in the matrix material. In Bamboo the vascular bundles that are surrounded by the bundle sheaths act as fibre and the parenchyma represents the matrix (Amada, et al., 1995; Dixon & Gibson, 2014). Obataya, et al. (2007) describe the structure of bamboo as a fibre-foam composite.

To determine the axial tension strength distribution of the bamboo's culm Amada, et al. (1995) tested thin slices ($12 \times 1 \text{ mm}^2$) from various locations of a two-year old culm of a *Phyllostachys edulis*, better known as Moso bamboo. The minimum axial tensile strength of 80 MPa was measured at the inner slice. The strength increased with radial distance from the lacuna and reached its maximum value of about 450 MPa in the outermost region. They plotted the relation from the test results for tensile strength against the fraction of the fibre volume and furthermore

described this relation with an equation, assuming that the mixture principle for composites can be applied, see Eq. (1.1)

$$f_{t,0} = f_{t,0,f} \cdot V_f + f_{t,p} \cdot (1 - V_f) \quad (1.1)$$

with $f_{t,0,f}$ as the tensile strength of the fibre and $f_{t,p}$ of the parenchyma-matrix, set with 610 MPa and 50 MPa, respectively. This model can also be applied on Young's modulus ($E_f = 46$ GPa, $E_p = 2$ GPa) and density ($\rho_f = 1,160$ kg/m³, $\rho_p = 670$ kg/m³). The density indicated for the parenchyma is, compared to other studies (see Table 1) relatively high and not comprehensible, as the average density of the whole bamboo culm is approximately 670 kg /m³.

Nogata and Takahashi (1995) performed tension tests on very small specimens with cross sectional area of about 0.25 mm², which were taken from nine different radial locations and in two different heights of a bamboo culm. The specimens were selected from a Moso bamboo and tested within 48 hours after it was taken from the field. The authors found out that the variation of tensile strength follows the variation of volume density of the fibres. They determined 25 MPa for the tensile strength of the parenchyma and 810 MPa of the fibre. The modulus of elasticity was estimated to be 55 GPa for the fibres and 2 GPa for the ground tissue, also using the rule of mixture.

Dixon & Gibson (2014) studied the microstructure of the culm (see subchapter 1-2.1) but also performed three-point bending tests and compression tests in axial, radial and tangential directions. The specimens for the bending tests were taken from different internodes and in various radial positions within the culm wall. The beams size was between 100 and 130 mm length, 6 and 12 mm width in tangential direction and 1 to 4 mm in thickness. The specimens were tested with the outer side, having the higher fraction of fibres, facing upwards (compression zone). The authors report that at all specimens the ultimate failure occurred in the tension zone. With the test results they found out following equations as a function of density for the bending modulus of elasticity and strength:

$$E_m = 1.27 \cdot E_s \cdot \left(\frac{\rho}{\rho_s}\right) - 10.57 \quad (1.2)$$

$$f_m = 1.25 \cdot f_s \cdot \left(\frac{\rho}{\rho_s}\right) - 117.5 \quad (1.3)$$

E_m	bending modulus of elasticity in [GPa]
f_m	bending strength in [MPa]
ρ	density of the specimen [kg/m ³]
ρ_s	density of the solid cell wall [1500 kg/m ³]
E_s	bending modulus of elasticity of solid cell wall material [39,8 GPa]
f_s	bending strength of solid cell wall material [472 MPa]

Furthermore the authors investigated the compressive strength of bamboo. The cuboids for the compression tests had a thickness to width to height (loading direction) ratio of 1:2:2 and tests were performed in axial, radial and tangential direction. Unlike the radial and the tangential compressive strength (f_r and f_t), that are almost independent of density (approximately 20 MPa; see Figure 7), the axial strength rises linear with density (ρ).

$$f_{c,0} = 1.20 \cdot f_{c,s} \cdot \left(\frac{\rho}{\rho_s}\right) - 49.69 \quad (1.4)$$

The compressive strength of the solid cell wall was estimated to be $f_{c,s} = 248$ MPa.

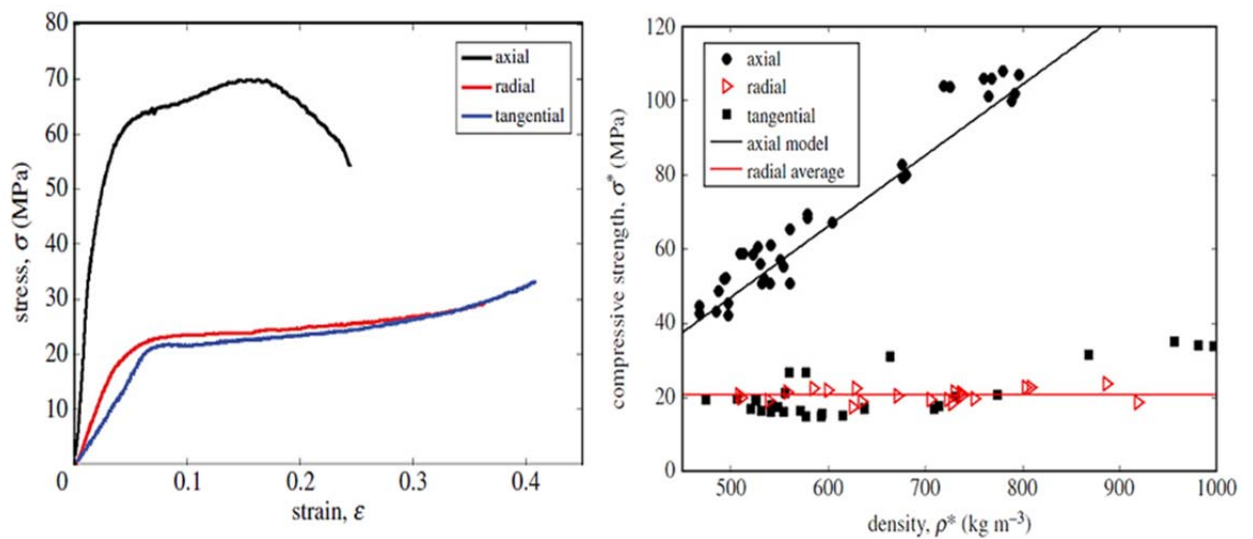


Figure 7: (left) Typical compressive stress-strain curves; (right) compressive strength vs. density (Dixon & Gibson, 2014)

Additionally, radial compression tests were performed, in which the pressure piston was stopped at certain positions. At this point pictures were taken with a scanning electron microscope (SEM) to better understand the failure mechanism due to compression perpendicular to the grain. The micrographs in Figure 8 clearly show the collapsing of the vessels within the vascular bundles and only the Parenchyma stressed. Due to that investigation the independence of density can be explained, as the volume fraction of the hollow vessels ($V_{vessels}$) is roughly constant with radial position.

$$V_{vessels} = V_{vb} \cdot (1 - S_f) \sim const. \quad (1.5)$$

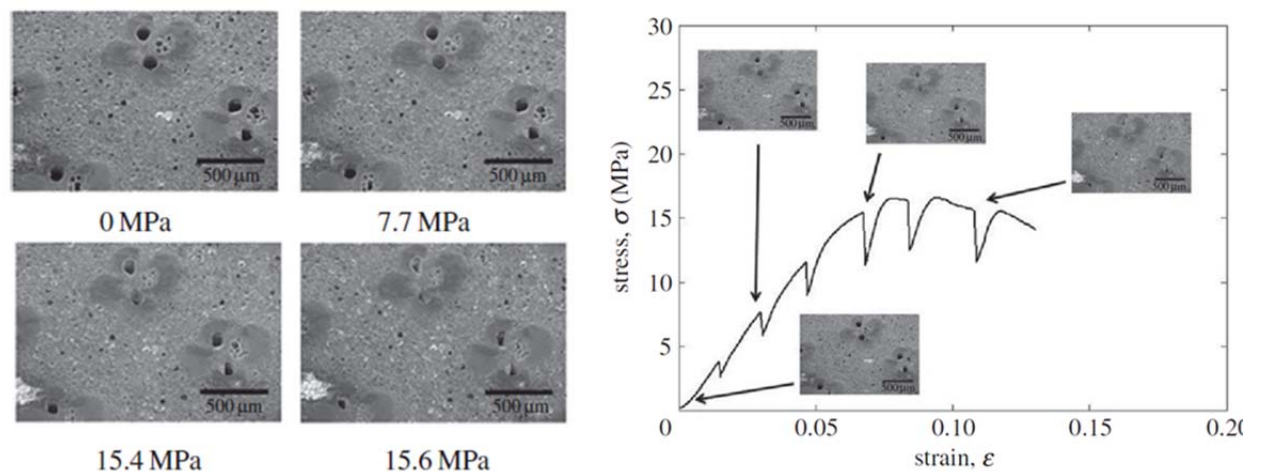


Figure 8: (left) Photomicrographs of the specimen compressed in radial direction; (right) accompanying stress-strain curve (Dixon & Gibson, 2014)

A study by Obataya, et al. (2007) also deals with mechanical properties of a split bamboo culm. Here an internode of a three-year-old Moso bamboo was cut into strips and further separated into three parts along the radial direction. The specimens were conditioned at 20 °C and 60 % relative humidity for a period of six months.

The effective span (along the grain) for the four-point bending tests was 170 mm and the density of the specimens varied from 670 to 1,040 kg/m³ due to the increasing fibre quantity

within the culm wall from the inside to the outside. Two different types of tests were performed: first, load applied to the inner side (type I) and second, load applied to the outer denser part (type II). Interestingly the modulus of elasticity was between 15 and 16 GPa, regardless of which side was strained. The maximum relative deflection was much higher when the softer inner part was compressed and the denser outer part was stretched. Consequently, the way of how the specimen is loaded has a big impact on flexural ductility but not on the stiffness. The higher deformation is due to a more distinct plastic load bearing behaviour of the type I beams when the proportional limit is exceeded. The diagram in the middle of Figure 9 shows the relationship between bending moment (M) and the relative curvature (l/r) of the bamboo and wood specimens. The radius of the deflection was calculated with the measured strains on the compression and the tension side and the height of the specimen. Simplified, at a small strain level, the modulus of elasticity can be calculated with Eq. (1.7)

$$r = h/(\varepsilon_t - \varepsilon_c) \quad (1.6)$$

$$M = E \cdot I/r \quad (1.7)$$

The authors state that the type of failure varied of the two test samples. As in type-I-bending, the fibre-bundles were gradually pulled out from the bottom side of the beam while the fibres remained straight. They concluded that the bending strength of the bamboo specimen depends rather on the cohesion of the fibre bundles among each other than on the ultimate tensile strength of the fibres themselves. The description of the fracture behaviour is not clearly comprehensible, as the fibre can not be pulled out without being ruptured in axial direction. The observed failure mode is rather caused by a combination of bending tensile stress and tension stress perpendicular to the grain that occurs after the first crack as the fibre bundles seek to go back to their initial straight position, as shown in Figure 9. The failure in type-II-bending was caused by a combination of tensile plus shear stress as the first crack always occurred just below the loading point on the down face of the beam.

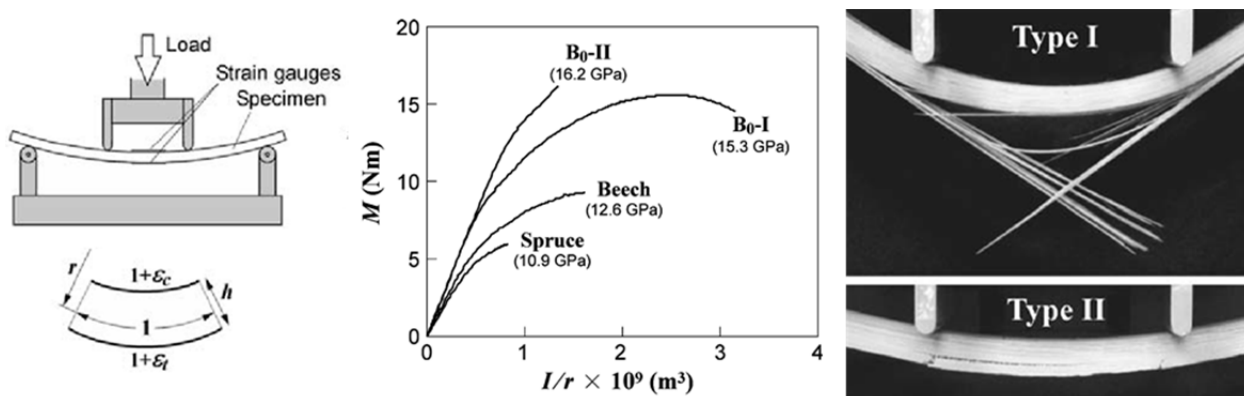


Figure 9: (left) Experimental setup; (middle) M plotted vs. I/r ; (right) types of failure (Obataya, et al., 2007)

The authors state that the ground tissue plays an important role in the bending ductility due to its high compressibility. Thus, the longitudinal compression strength of bamboo was analysed in more detail. Whereas the stress in the specimen of the inner third (B_3) of the culm remained rather constant above a strain from 3 to 10 %, the stress in the cuboid made of the fibre-rich outer part (B_1) dropped at a strain of 2 % due to buckling of the fibres. However, the maximum stress recorded was about twice as high.

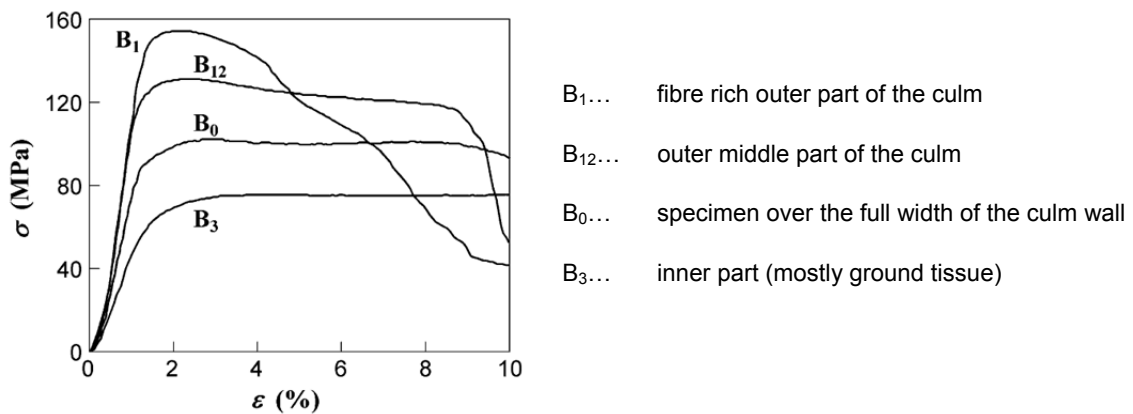


Figure 10: axial compression stress-strain diagram (Obataya, et al., 2007)

Even though the Parenchyma cells do not contribute to bamboo's stiffness they can absorb large compressive distortion and prevent the fibre bundles from large scale buckling. Table 1 summarizes the values for density, modulus of elasticity and tensile strength of the fibres and the parenchyma ground tissue found in various studies.

Table 1: Characteristics of sclerenchyma fibres and parenchyma ground tissue

	Fibre			Parenchyma		
	ρ_f [kg/m ³]	$E_{t,of}$ [GPa]	$f_{t,o}$ [MPa]	ρ_p [kg/m ³]	$E_{t,p}$ [GPa]	$f_{t,p}$ [MPa]
Amada, et al., 1995	1,160	46	610	670	2	50
Nogata&Takahashi,1995	--	55	810	--	2	25
Dixon & Gibson, 2014	1500	39.8	472*	330	1.92	14.6*
Obataya, et al., 2007	1,570	48	498	450	0.26	73

*bending tensile strength

1-2.3 GEOGRAPHICAL DISTRIBUTION

According to FAO's Forest Resource Assessment 2010 there are about 31.5 million hectares of bamboo worldwide. About 60 percent of the global distribution of bamboo are in China (absolute: 5.7 million ha), Brazil (5.4 million ha) and India (9.3 million ha) (Food and agriculture organization of the United Nations, 2010). Of the more than 1,200 species, the woody bamboo is of interest for structural applications.

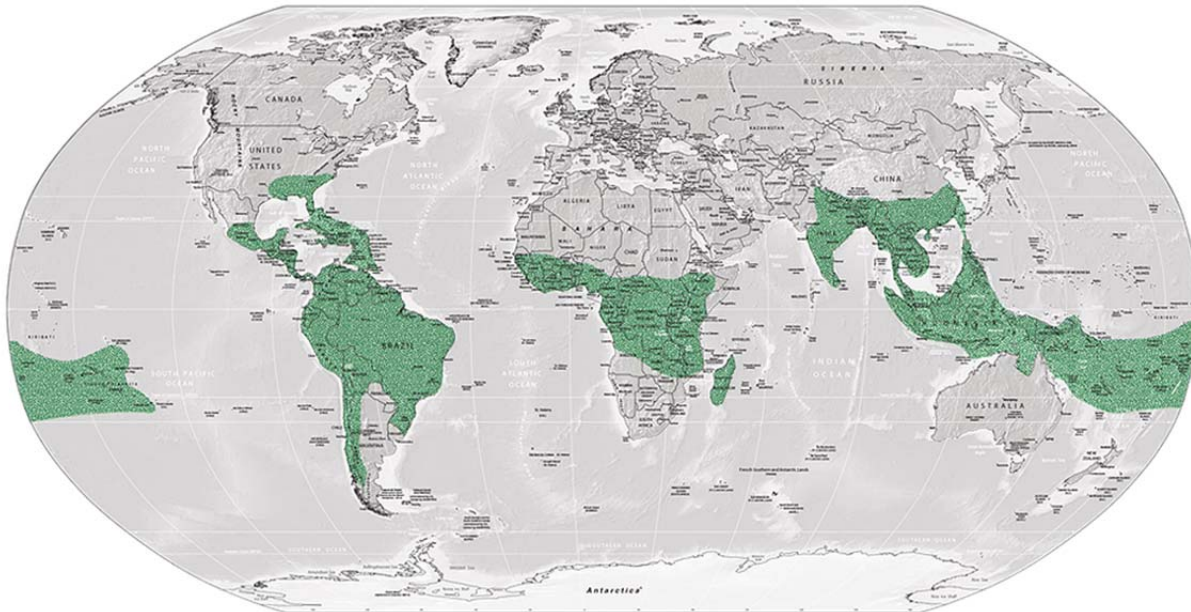


Figure 11: Distribution of woody bamboo (Lambo Inc., 2015)

Guadua, which is native to Central Latin America, and the genera *Phyllostachys* and *Dendrocalamus*, which are native to Asia, have the best structural properties. All three genera belong to the group of tropical woody bamboo (Bambuseae) (Hollee, 2013).

1-2.4 GROWTH

The growth characteristic of bamboo plants is very unique. Bamboos combine growth properties of grass, leaf-bearing tree and palm. Typically for grass is the tubular blade, structured in nodes and internodes. Like leaf-bearing trees, they drop their leaves every year and they increase their crown by throwing out new branches. The growth habit of the culm is similar to that of palm tree, as both have a definitive diameter when they emerge from the soil. Unlike all needle- and leaf-bearing trees, they do not increase their circumference (Dunkelberg, 1985).

Bamboo is split into two main groups, the monopodial and the sympodial bamboo plants (see Figure 12), depending on the nature of the rootstock (rhizome). Sympodial bamboo forms short and thick rhizomes from whose apex a shoot grows into a culm. Such culms grow in close proximity to each other as a clump. In monopodial bamboo, each culm grows at a distance from each other, although it is part of a root system. It forms long, thin and horizontally extending rhizomes from whose buds shoots sprout in steady intervals. The roots continue to extend, about 1 to 6 m/year, if they are not controlled (Holzmann, et al., 2012).

All nodes and internodes are present in the bud (see Figure 12). The young shoot is protected by sheaths, which shed off, when the plant grows. Many species have tiny hairs on the protective culm sheaths, sharp enough to pierce human skin or toxic enough to cause skin

irritations. The expansion of the culm results from elongation of the different cell types within the individual internodes. The bamboo culm reaches its full length (3 to 30 m) within a few months (Liese & Weiner, 1995).

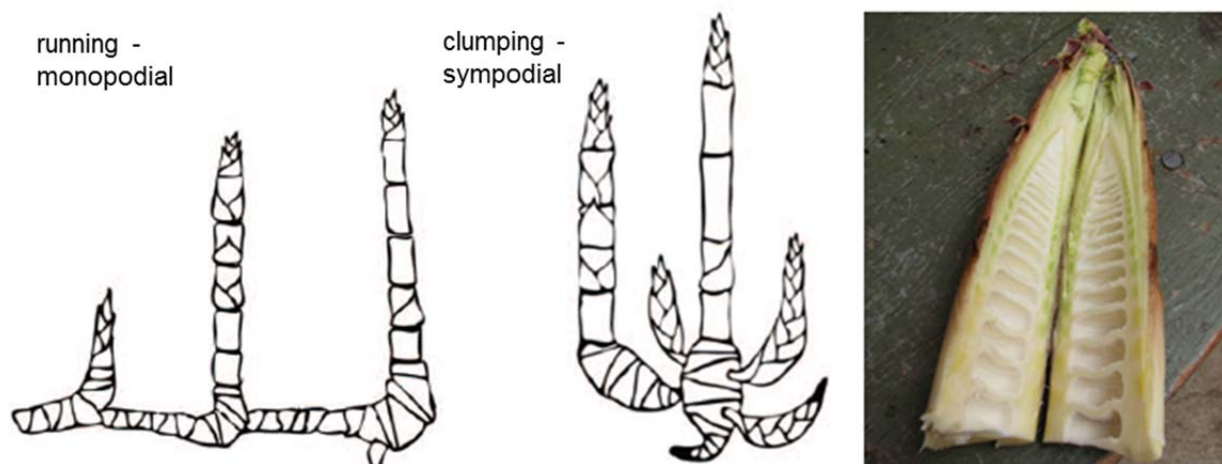


Figure 12: (left) bamboo rhizomes (Sharma, et al., 2014); (right) longitudinal section of a young bamboo shoot (Bamboo Garden, 2006)

During lifetime of a culm, the structure and consequently properties and utilization change. This ageing process, especially in the maturation period of 3-4 years, induces a thickening of the cell walls of the fibres and of the parenchyma cells. The thickening of the cell wall is caused by subsequent lignification, where additional lamellae are deposited on the existing wall layers. This process causes an increase of density and strength properties. Additionally the moisture content decreases distinctly during the maturation phase. However, this natural ageing causes a blocking-off the sieve tubes and the water conducting vessels that makes it functional inefficient and so causes the dying of an individual culm (Liese, 2003).

According to Van der Lugt (2008) the best age to fell a Moso bamboo culm that is going to be used for structural application is about four years (and about five to six years for Guadua). Thus, maximum sustainable income can be achieved. If the bamboo is used for applications where the fibre function is less important, such as for handicraft work, pulping or the production of paper, the stems can be harvested at an earlier age. It has to be noted that the age of a culm has to be distinguished from the age of the bamboo plant, as the bamboo plant consists of various culms and reproduces new shoots each year (van der Lugt, 2008).

1-3 STATE OF THE ART – ENGINEERED BAMBOO

In countries where bamboo is native, it is used as structural building material for houses, bridges and scaffoldings in its natural form. The big issue of natural bamboo is that geometry, structure and the mechanical properties vary from culm to culm but also within a single cane, a circumstance generally observable in renewable, natural materials. Moreover, the naturally varying diameter and shape of its tubular form makes joints and connections challenging. Engineered bamboo products resolve deficiencies like dispersion of the material properties. Furthermore, there is the ability to create standard sections and joints (Sharma, et al., 2014). Due to the lack of appropriate building standards bamboo has been mainly applied for non-structural purposes like flooring, panels and veneer for furniture production and as decking for terraces.

1-3.1 PROCESS OF PRODUCTION

China is the leading producer and exporter of bamboo based products (the mainly used resource for production of industrial bamboo products is the species Moso). The bamboo industry is efficiently organised as almost the whole bamboo culm is used for a certain product. The standard length of the bamboo for further processing is 2.66 m, to which the whole Chinese bamboo industry is standardized. This dimension was chosen based on the international standard dimension for boards (1.22 x 2.44 m) plus tolerance. Usually the bottom eight metres (3 x 2.66 m; this corresponds to a calculated average volume of 0.014 m³ of solid material per stem) of the stem is used for the fabrication of bamboo materials such as solid beams or boards. The upper part of the culm is processed to smaller bamboo products such as chopsticks. In Latin America, Guadua is the most important bamboo species. Currently the production of engineered bamboo products in South America is negligible compared to China, though the potential for this purposes is high in the future, due to the higher annual yield and larger dimensions of Guadua. Therefore it is assumed, that four segments in a length of 2.66 m can be derived from a stem, which corresponds to 0.024 m³ of solid material per stem (van der Lugt, 2008).

1-3.1.1 Method 1: Strips to boards to beams/LBL

LBL is most likely comparable to the structural timber product glulam – glue laminated lumber. The shortened culm is split in the radial direction (depending on the diameter of the stem 8 or 12 rough strips can be derived) and the diaphragms are removed to get straight bamboo slices. Then the inner and the outer layers, that contain wax and silica, are removed with a planer or through tangential splitting. When the letter is practised, the outermost bamboo silver can be used to manufacture bamboo curtains or mats whereas the bigger inner split is the base material for LBL (or another engineered bamboo product as will be described later). The next step in production is to make the material less prone to insect attack, rot or fungi and to affect the desired colour tone. A common treatment is bleaching of the raw material, where the slices are immersed into a chemical solution, e.g. a hydrogen peroxide (H₂O₂) bath at a temperature of 70 to 80 °C. As an alternative, the bamboo slices can be carbonized, whereby steam is used to put the strips under high pressure and a temperature of approximately 130 °C to melt the sugars in the bamboo. This treatment gives the bamboo a deeper brown, caramelized colour. In both processes, colouring and preservation take place at the same time. After drying, the slices are passed through a polishing machine to obtain the laminae with rectangular cross section. Each lamina has an average width of 15 to 25 mm and a thickness ranging from 5 to 10 mm. Furthermore, the laminae are glued and pressed together to form one-layer boards, although it distinguishes between horizontal and vertical lamination (see Figure 13). The glue and the glue spread rate vary from the different products and requirements. The one-layer board is sanded again and can then be compounded and fitted to the demanded cross section (van der Lugt, 2008).

The finished product with all laminae oriented in the same direction is called laminated bamboo lumber, short LBL. Mechanical properties such as stiffness and strength values can be found in Table 2. Boards with two cross laminated layers are often used in flooring whereas three layered solid panels can be applied as kitchen worktops and for furniture. This product resembles a three-layer solid wood panel and is frequently referred as plybamboo.

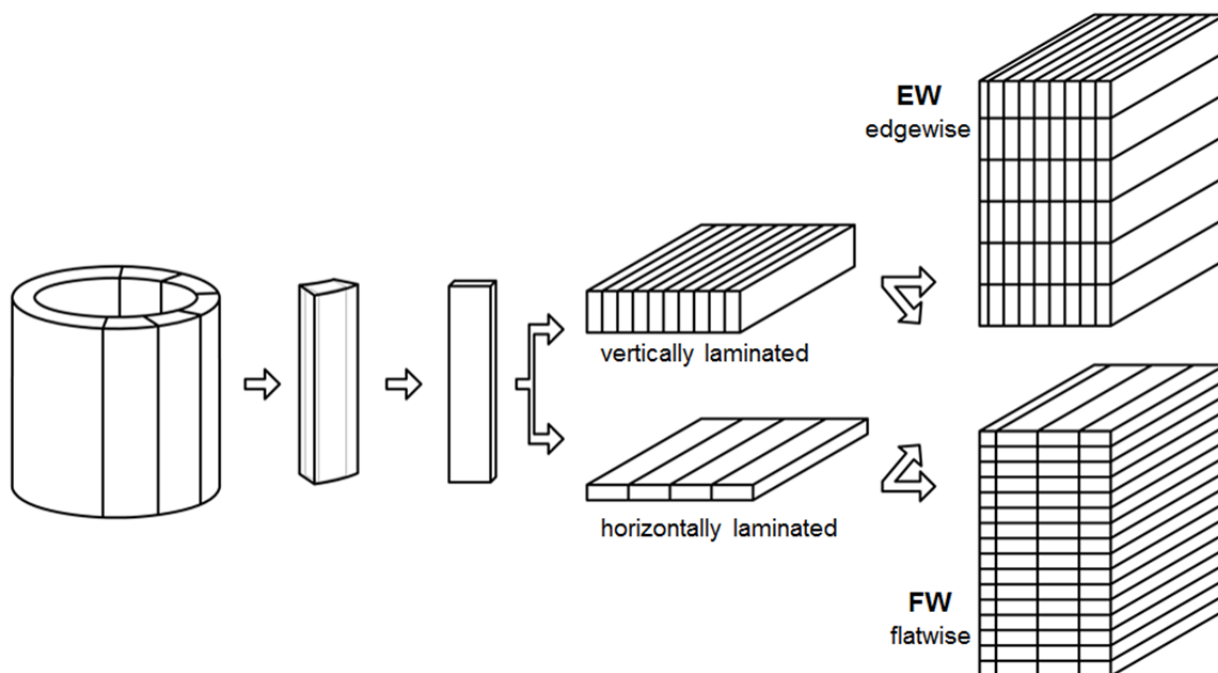


Figure 13: Production process

Besides, bamboo veneer can be obtained from laminated bamboo, in that way as slices with a thickness of 0.6 mm are sawn from a laminated bamboo block (van der Lugt, 2008).

Processing effects: Thermal treatment

Thermal treatment in timber causes an alteration in chemical composition and it is used to reduce moisture, improve durability and to increase dimensional stability and processability. However, it is known that (extensive) thermal treatment reduces the tensile and bending properties as well as it makes the material more brittle in comparison to untreated timber. As bamboo has a similar chemical composition than wood, the influence on mechanical properties is likely. Sharma et al (2014) carried out a study on laminated bamboo lumber made from Moso and compared the mechanical properties of semi-caramelized (steam treatment but with a shorter treatment time than for the (full-) caramelized product) and bleached bamboo (Sharma, et al., 2015). Before that, a study was performed to investigate the mechanical properties of bamboo parallel strand bamboo (see method 2 in section 1-3.1.2) and caramelized LBL (Sharma, et al., 2015). The specimens that had been carbonized by pressurised steam had a higher average density despite of lower moisture content, compared to the semi caramelized and bleached bamboo.

Anyway, the higher average density of the carbonized material is not due to thermal treatment, as this process causes the exact opposite: a mass loss (Zhang, et al., 2013).

In tension, all specimens indicate a linear behaviour prior to failure, though the bleached material had a higher tensile strength. On the contrary, it exhibits the lowest strength in compression parallel to grain. All materials demonstrated a similar bilinear behaviour in compression and the typical failure was overall section buckling. A shear failure along a local shear plane (kinking) was not observed. The specimens' size for the tension test was 25 mm / 25 mm / 460 mm, for the compression test 20 mm / 20 mm / 60 mm. However, for the bending tests full-size specimens with dimensions of $l / h / w = 2,400 \text{ mm} / 120 \text{ mm} / 60 \text{ mm}$

were used (according to EN408 $l \geq 19 \times h$). All specimens were built up from vertically laminated bamboo boards. To distinguish the influence of lamellae-orientation the results presented in Table 2 come from FW orientation of the strips within the beam cross-section. All failures occurred at the tension face of the beams near mid-span although all specimens exhibited longitudinal shear failures. The modulus of elasticity is much the same of the bleached and the semi-caramelised material whereas the caramelised exhibits a significantly higher stiffness.

Table 2: Mechanical properties of structural bamboo (Sharma, et al., 2015)

processing method	density	moisture	compression*	tension**	bending***	
	ρ [kg/m ³]	u [%]	f_{cII} [N/mm ²]	f_{tII} [N/mm ²]	f_m [N/mm ²]	E_m [N/mm ²]
bleached	644	8	55	124	79	10,471
COV	n/s	n/s	9 %	15 %	7 %	6 %
semi-caramelised	673	7	60	116	79	10,440
COV	1 %	n/s	4 %	20 %	12 %	8 %
caramelised	686	6	77	90	83	12,900
COV	5 %	n/s	5 %	26 %	8 %	6 %

* according BS 373; ** according ASTM D143; *** according EN 408

COV stands for coefficient of variation and is defined as standard deviation to mean value

The experimental results display that thermal processing has an influence on the mechanical properties of the materials but to fully capture the changes due to procession further research is needed.

1-3.1.2 Method 2: Parallel strand bamboo (PSB)/bamboo scrimber/SWB

Bamboo scrimber, also known as strand woven bamboo (SWB), is manufactured from crushed strips. Its structure resembles the structure of parallel strand lumber (PSL), but which is better known under the brand name Parallam. The requirement for the geometry of the strips is not as high as it is for the strips used for laminated bamboo. For this reason, also the upper sections of the culm with smaller diameter and wall thickness serve as base material allowing for a higher yield of harvested material for production of engineered products. However, the strips are planed to remove the inner and the outer layer, which would seriously harm the internal bond strength of the bamboo-adhesive composite. In another way, the inner and outer skin is removed during splitting the stem into slender strips. Flattening is not necessary. Depending on the area of application and the desired appearance, the strips can be bleached by immersing into a boron solution, or carbonized in an autoclave. Anyway, the bamboo strips are saturated in resin, e.g. phenol formaldehyde, and then placed into a steel mould in which the saturated strips are compressed for about five minutes and with a high pressure to form the beams. The beams, which are still in the mould, are then taken into an oven where the resin is activated at a temperature of about 150 °C (van der Lugt, 2008). Another forming process that is mainly used for the production of sheets is hot pressing. After assembling the bamboo strands parallel in the hot press-mould it is compressed between two hot plates. The pressure and a temperature of 140 °C is kept until the board is cured (Yu, et al., 2015).



Figure 14: Cross section of bamboo scrimber: (left) natural (right) carbonized (Yu, et al., 2015)

Due to compression and high glue content, the density of SWB is higher than natural bamboo and LBL and varies from about 1,050 to 1,250 kg/m³ (Yu, et al., 2015). According to van der Lugt (2008), 1.54 times more raw bamboo material is used to make the beams. The material properties of SWB-products can be found in Table 3. Sharma et al. investigated the mechanical bending properties on beams with the dimensions $l / h / w = 800 \text{ mm} / 40 \text{ mm} / 40 \text{ mm}$. Yu et al. tested 360 mm / 15 mm / 50 mm beams resected from a board that was produced in hot-pressing process. Another experimental study was performed on PSB beams with a 80 mm · 110mm cross section and a free span of 1400 mm (Zhou & Bian, 2014).

Table 3: Mechanical properties of strand woven bamboo

	ρ [kg/m ³]	$f_{t,0}$ [MPa]	$f_{c,0}$ [MPa]	E_m [Gpa]	f_m [MPa]
Sharma, et al. (2015)	1,163	120	86	13	119
Yu, et al. (2015)	1,150	--	--	12-15	150-180
Zhou & Bian (2014)	--	--	--	12.7	89



1-3.1.3 Method 3: Plate or roller flattened bamboo as base material

The finished product, made from flattened bamboo strips, is also referred as LBL. However, it is none of the processes currently practiced (Xiao & Yang, 2012).

A technique, investigated by Lee et al. (1998), forms a composite, which is similar constructed to laminated veneer lumber, laminating quasi-flattened Moso bamboo. Each culm section is split in halves and then placed between the plates of a hydraulic press. After applying a pressure of 0.69N/mm² for one to four minutes, depending on the thickness of the culm wall, the quasi-flattened splits are passed through a planer to take off the inner and the outer layer. Only after that, the material is taken to the dryer. The dry splits are then applied with adhesive and assembled to form the desired dimensions. One layer is between 3.8 and 6.4 mm thick. Until the adhesive is cured, a pressure of 1.38 N/mm² is applied to the beams. The density of the LBL specimens cut from the boards produced varied in a range of 620 to 660 kg/m³. It is important to note that this manufacturing process was conducted in a laboratory. The flattening of the stem section and lamination of the beams took place at room temperature and there was no manufacturing step like thermal treatment or bleaching. The mechanical properties were determined on small-scale specimens (25.4 mm / 25.4 mm / 406.4 mm) and can be found in Table 4. A distinction is made between vertically (V-beam) and horizontally laminated (H-beam; see also Figure 13).

The study analysed the effect of initial moisture content of the flattened bamboo strips, as one group was conditioned to 10 % and the other one to 15 % equilibrium moisture content. Additionally the influence of the glue spread rate (220 to 420 g/m²) was examined. The authors found out, that both, the modulus of elasticity and bending strength increased with increasing glue spread rate. The trend of the effect of initial moisture content was not consistent (Lee, et al., 1998).

Table 4: Mechanical properties (Lee, et al., 1998)

	E_m [Gpa]		f_m [Mpa]		H-beam 	V-beam 
	H-beam	V-beam	H-beam	V-beam		
min	7.4	8.0	67.7	85.3		
max	9.2	9.1	98.6	107.2		

Another method to gain flat sheets was carried out by Nugroho and Ando (2001). After splitting the culm into quarters, the splits were passed through a roller press crusher. Further, this bamboo sheets were pre-treated by a hot-press method and planed to remove the epidermal layers. After application of the adhesive, four sheets were carefully stacked on top of another to form LBL. A factor of interest was the influence of the alignment of the layers (Nugroho & Ando, 2001).

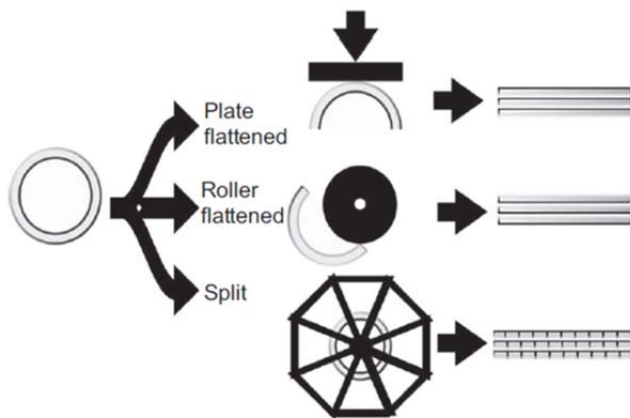


Figure 15: Techniques to receive base-material for LBL (Sharma, et al., 2014)

A completely different approach to produce LBL was made by Mahdavi et al. (2011) who describe a very simple, low-technology method that can be done without sophisticated fabrication equipment. First of all the outer surface of the bamboo stem was removed, using coarse sand paper. A dry culm can be easily split in longitudinal direction, which makes further flattening by hammering easier. Because the outside of the culm wall is more resistant to mechanical attack, the split should be placed on a flat and hard surface with the inner side facing down. Then the wax and silica of the inner surface was removed, using a rotary sander. However, many longitudinal gaps occurred, which weakens the cross section and makes horizontal shear failure more likely. In this study, the strips were wrapped with nylon stings to apply a lateral pressure during flattening and so reduce the size of the longitudinal gaps. Further processing is like in the other methods: glue application, stacking and pressing to form the LBL (Mahdavi, et al., 2012).

1-3.1.4 Method 4: Bamboo Mat Boards (BMB) / glubam

As a first production step, the bamboo culm is split into thin strips during which progress the skin of the bamboo is removed. Due to the small cross sections of the strips, there is no need for a further process like flattening and additionally there is less restriction on the wall thickness of the bamboo stems. After the preservative treatment, the dry bamboo strips are either sting netted parallel (unidirectional) or woven (bidirectional) to large mats. These mats (the thickness is approximately 2 mm) are the basic material for the production of glubam sheets. After the mats are saturated in resin and dried again, they are stacked one above each other. The number and layout of the bamboo mats (parallel, orthogonally, mats with an equal amount of strips in both directions) can be adapted due to the respective strength design and desired fibre orientation. A method to form the sheet is hot pressing, where the mats are pressed together for 15 to 20 min, at a temperature of 150 °C and a pressure of 20 MPa in a hydraulic pressure machine. In China glubam-sheets are often used for concrete formworks. Through post-processing like cutting, finger-jointing, stacking and compressing, different structural elements can be formed (Xiao & Yang, 2012; Xiao, et al., 2013). The boards can also be pressed into molds of various shapes, what is e.g. done to produce corrugated roof sheets in China and India (van der Lugt, 2008). According to Xiao the density ranges from 800 to 980 kg/m³. Van der Lugt states 1,030 kg/m³ as the average density, which is similar to that of SWB and makes the two products comparable in terms of production efficiency.



Figure 16: (left) Bamboo mat board (Foshan Ying plus earnings Wood Co, 2013); (right) roof sheet made from bamboo mats (Schröder, 2014)

The mechanical properties depend on the layout of the boards / beams. Xiao et al. (2010) tested ten meter long girders manufactured from bamboo veneer sheets (2,440 x 1,220 mm² and 28 mm thick). The sheets contained bidirectional mats with the same amount of bamboo strips oriented in longitudinal and in transverse direction. The longitudinal joints were made with finger joints as the boards among each other were bonded with adhesive. The experimental results delivered values for the modulus of elasticity ranging from 9,200 to 11,900 N/mm² and a bending strength ranging from 27.1 to 45.8 N/mm² (Xiao, et al., 2010).

In a later study 30 mm thick glubam sheets (with a layout of 12 bamboo curtain layers oriented in the longitudinal direction and 3 in transverse direction) were tested. The free span in the bending test was only 240 mm and the cross section was 30 x 30 mm². The mean modulus of elasticity measured was 9,400 N/mm² and the tensile strength was on average 99 N/mm² and the mean in plane compressive strength was 51 N/mm² (Xiao, et al., 2013).

1-3.1.5 Method 5: Other bamboo based boards

Like in the production of wood materials, the base materials are fibres (e.g. MDF, hardboard), chips (e.g. chipboard) or strands (e.g. OSB) to form large sized boards. These elementary units are dried and mixed with a certain amount and type of resin and waterproofing compound. These base materials are then scattered on the treadmill either randomly arranged or with a specific direction after which they are pressed (depending on product and production method at a proper temperature and with proper pressure) (Suhaily, et al., 2013). Hardboards (the elementary unit is fibres) are often wet-formed.

1-3.2 PRODUCTION EFFICIENCY

Bamboo materials are often marketed as environmentally friendly. Van der Lugt (2008) conducted a life cycle analysis (LCA) on various bamboo materials and found out, that bamboo products, produced in China and used in Western Europe, score worse in terms of Eco-costs than locally grown wood but in general better than wood harvested in other continents. (Eco-cost is a unit in a LCA based method to describe the environmental burden of a product in a single indicator). Largely this is due to transportation as the transport from harbour to harbour by trans-oceanic freight ship (Shanghai to Rotterdam) accounts for more than one quarter of the total Eco-cost of a laminated bamboo product. Among Eco-costs, the annual yield plays a key role in evaluating the environmental sustainability of bamboo. Of course, material losses due to processing have to be taken into account. The production efficiency depends on the product manufactured. Van der Lugt differentiates class A products (high value added but little yield), such as sawn timber, laminated bamboo boards (see section 1-3.1.1), strand woven bamboo (SWB; see section 1-3.1.2) or veneer, and class B Products (low value added but high yield) such as any kind of board materials (MDF, chipboards). It is to be noted that class A materials are semi-finished materials used as input in construction or interior decoration industries. The production efficiency is high if a large portion of the harvested material ends up in the semi-finished material. For laminated bamboo the demands on quality are the highest and only a portion of the felled culms meets the quality requirements for LBL-boards. During the production process of selected stems into laminated bamboo lumber, about 60 % of the material is lost. For bamboo scrimber, as the strips are compressed in the final product, the quality requirements on the input material are lower. The author states a production efficiency of 70 %. The residual material in both processing types is in practice used for biofuel in the factory itself. Hypothetically, the material rejected during production of A-quality products can be used as input in B-class materials (e.g. MDF). The production efficiency for the manufacturing of bamboo based medium dense fibreboards is assumed to be 80 percent (van der Lugt, 2008).

Table 5 outlines the estimated volume of semi-finished materials that can be gained annually from one hectare of bamboo. The average number of stems per hectare in a *Guadua* plantation was guessed at 5,000 culms. Since the bamboo stems of this species mature in six years, the annual yield is 1 / 6, which corresponds to 833 culms / ha. About 3,000 Moso culms per hectare grow in a typical plantation on China. If per year 1 / 4 of the culms are harvested, this results in an annual yield of 750 stems per hectare. The calculated number for semi-finished LBL boards is rather theoretical as only a small portion of the stems meets the quality requirements. For the production of bamboo scrimber the amount for the input material is 1.54 times more in volume than the final product since the material is compressed (see 1-3.1.2). For MDF the assumed

density was 1,050 kg/m³, which meets to a compression factor of 1.5 times. All input data was taken from Pablo van der Lugt (2008).

Table 5: Material costs and estimated yield per cubic meter of semi-finished material

raw material	method	product	ρ of semi-finished material	$\emptyset V$ / culm	production efficiency	culms per m ³ semi-finished material	semi-finished material
			[kg/m ³]	[m ³]	[%]	[#]	[m ³ /ha/a]
Moso	1	LBL	700		40	179	4.2
	2 + 4	SWB/BMB	1,080	0.014	70	157	4.8
	5	MDF	1,050		80	134	5.6
Guadua	1	LBL	700		40	104	8.0
	2 + 4	SWB/BMB	1,080	0.024	70	92	9.1
	5	MDF	1,050		80	78	10.7

To put this numbers into relation it is compared to common timber and hardwoods. According to the Forestry Commission's website, the annual yield class of Sitka spruce is 14. The "yield class" describes the amount of solid stem material in cubic meters per hectare per year. The yield class given for beech is 7, and 6 for oak (Forestry Commission, 2008). Depending on which product is to be manufactured the material losses vary. According to Puettmann and Wilson (2006) the production efficiency of glulam production in North America is about 82 % (Puettmann & Wilson, 2006).

1-3.3 STANDARDIZATION

The International Organization for Standardisation made the first step to standardize bamboo in 2004 by publishing three standards on bamboo construction:

- ISO 22156 Bamboo – Structural design (ISO, 2004a)
- ISO 22157-1 Bamboo – Determination of physical and mechanical properties – Part 1: Requirements (ISO, 2004b)
- ISO 22157-2 Bamboo – Determination of physical and mechanical properties – Part 2: Laboratory manual (ISO, 2004c)

Mainly these standards address the structural application of the full cane but "plybamboo" is mentioned and explained as sheets processed like bamboo mat boards (production method 4) or LBL (method 1). When it comes to mechanical properties of this material, the standard refers to the national standards for plywood.

Another approach, besides independent standardization of bamboo, is to integrate bamboo products to standards and codes for structural composite lumber. This is done in ASTM D5456: "Standard specification for evaluation of structural composite lumber" (ASTM International, 2013) which recognises LBL as structural material. Using timber or wood standards to evaluate bamboo products has the benefit of providing a comparison to known timber products as well as it broadens engineered bamboos products' potential market (Gat6o, et al., 2014).

CHAPTER 2: MATERIALS & METHODS

2-1 GENERAL LAY-UP OF THE TEST SPECIMENS

The test specimens consist of a sub-structure of laminated Bamboo (Moso bamboo) strips which are oriented in edgewise (EW) or flatwise (FW) direction. Therefore, the descriptions EW and FW are made for the orientation of the lamellae within the beam, but which is independent of the orientation of the beam itself. Referring to Chapter 1-3.1 the specimens were fabricated according to method 1 with vertical laminations. The Bamboo strips of the main test series are produced with special joints in longitudinal direction (see Figure 17). However, the material used in the pre-tests did not have any longitudinal joints but each lamella was from one piece. The results from the pre-tests are later used as reference in order to show the effectiveness of the joint.

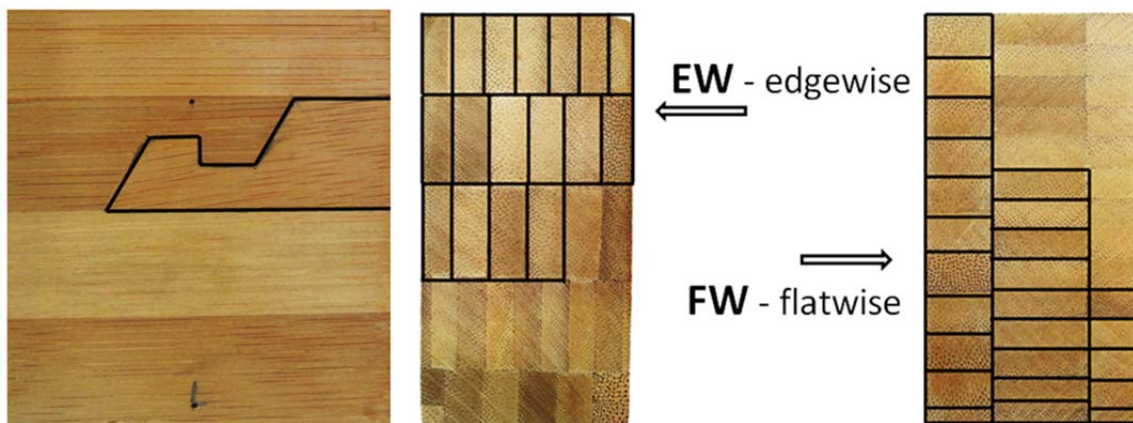


Figure 17: (left) Geometry of the Joint; (right) orientation of lamellae



Figure 18: Beams with joints highlighted

No regularity of the distances and distribution of the joints were found but a number of 60 strips was investigated to find out the approximate average distance between the joints. The average number of joints per lamella is 1.47, which corresponds to a distance of 1.66 m from joint to joint.

Table 6: Investigation of joint-distribution

# of joints per lamella	# of lamellae	# of joints
0	6	0
1	21	21
2	32	64
3	1	3
sum:	60	88

Furthermore, the materials differ from the adhesive used. As the bamboo beams used in the pre-tests are indoor quality, the strips were laminated to one layer board with Melamine Formaldehyde (MF). However, the materials produced for the full testing were outdoor quality using a Phenol Formaldehyde (PF) resin to form the cross section.

2-2 GENERAL TEST METHODS

2-2.1 DETERMINATION OF THE SPECIMEN DIMENSIONS

The dimensions of the specimens were determined with an error less than 1 %. All measurements were carried out directly before conducting the tests. The measurements of the cross section (width and thickness) were obtained by taking the mean value of three measurements along the specimen. The length was measured once per specimen.

2-2.2 DETERMINATION OF THE SPECIMEN MOISTURE CONTENT

The moisture content of the laminated Bamboo elements was determined according to ÖNORM ISO 3130 (CEN, 1994). An adaptation of the density and the local modulus of elasticity according to ÖNORM EN 384 (CEN, 2010) to a moisture content of 12 % was not conducted.

$$u = \frac{m_1 - m_0}{m_0} \cdot 100 \quad (2.1)$$

- u ... moisture content of the specimen [%]
- m_1 ... mass of the specimen before drying [g]
- m_0 ... mass of the dry specimen [g]

2-2.3 DETERMINATION OF THE SPECIMEN DENSITY

The density was obtained based on the (average) dimensions and the mass of the specimen.

2-2.4 AIR-CONDITIONING OF THE SPECIMEN

Until the tests, the specimens were stored in a climate chamber at standardized conditions (temperature of 20 °C and relative air humidity of 65 %).

2-3 TESTING MACHINES

All tests, except the tests on tension parallel to the grain, were carried out utilizing the universal testing machine Zwick Universal 275 (Lignum U_275), which allows a continuously manageable, displacement- and/or force-controlled introduction of forces until a maximum of 275 kN. The employed loading device made a measurement of the applied load with an error less than 1 % possible.

The tension tests parallel to the grain were carried out utilizing a tension testing machine (Lignum Z_850), which allows a continuously manageable, semi load-controlled introduction of loads until a maximum of 850 kN. The employed loading device made measurements of the applied load with an error less than 1 % possible.

2-4 GUIDELINES FOR THE DETERMINATION OF MECHANICAL PROPERTIES

The mechanical properties were determined according to ÖNORM EN 408 “Timber structures – Structural timber and glued laminated timber – Determination of some physical and mechanical properties” (CEN, 2010).

The characteristic strength values were determined according to ÖNORM EN 14358 “Timber structures – Calculation of characteristic 5-percentile values and acceptance criteria for a sample” (CEN, 2007).

2-5 BENDING

Name of the specimens, dimensions and the orientation of the lamellae within the cross section are provided in Table 7. 22 specimens of each type (EW/FW) were tested. The parameters of the testing configuration are provided in Table 8 (see also Figure 19).

Table 7: Sample B-A1, B-A2 – bending

name of sample	orientation of the bamboo strips [-]	dimensions l / h / w [mm ³]	# of delivered / # tested [-/-]
B-A1	flatwise	2440/140/90	22/22
B-A2	edgewise		

Table 8: Parameters of the test configuration for sample B-A1 and B-A2

Description	Variable [-]	Value [mm]	Comment [-]
free span	l	2,240	$16 \cdot h$
measuring length for local E-modulus	l_1	700	$5 \cdot h$
distance support to load introduction	a_1	700	$5 \cdot h$
distance of the load introduction points	a_2	840	$6 \cdot h$
length	L	2,440	$\geq 17 \cdot h$
width of the support	b_a	70	$\leq h/2$

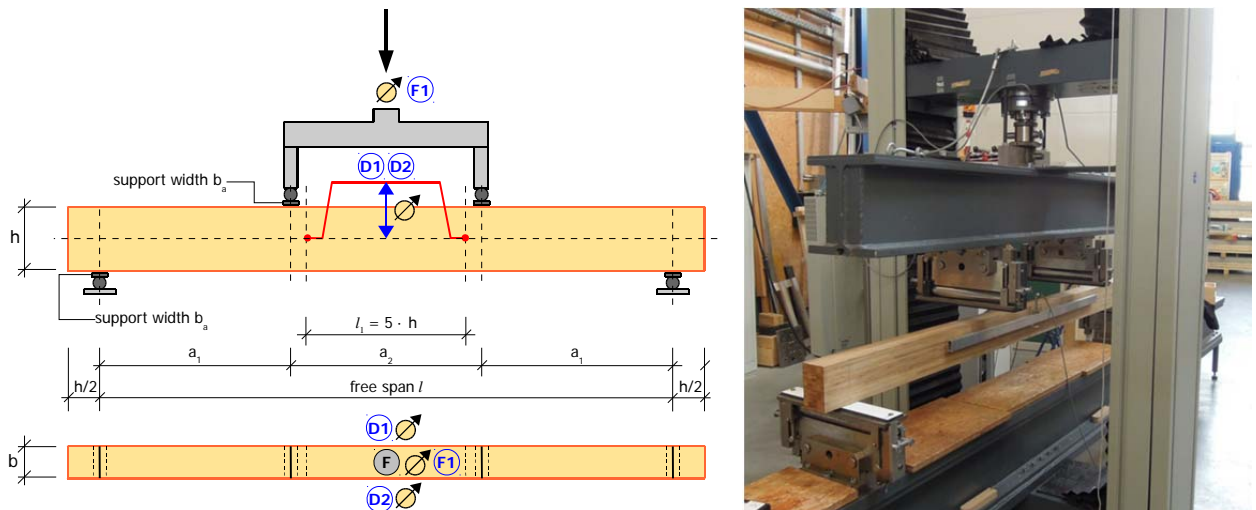


Figure 19: Test setup for bending according to ÖNORM EN 408

The local displacement measurements at the midpoint of the reference beam were realized with inductive displacement sensors of type WA 10 (see Figure 19). The rate of movement of the loading head was chosen so that the testing time until F_{max} and thus failure was reached within 300 ± 120 s.

2-5.1 BASIS OF CALCULATION

The local bending modulus of elasticity is determined according to Eq. (2.2).

$$E_{m,l} = \frac{a \cdot l_1^2 \cdot (F_2 - F_1)}{16 \cdot I \cdot (w_2 - w_1)} \quad (2.2)$$

- a ... distance between load introduction point and nearest support
- l_1 ... measuring length for local E-modulus
- I ... second moment of inertia of the specimen cross section
- $F_2 - F_1$... increase of the load in the range where the regression line has a correlation coefficient of 0.99 or better
- $w_2 - w_1$... corresponding rise in displacement

The bending strength is determined according to Eq. (2.3).

$$f_m = \frac{3 \cdot F_{max} \cdot a}{b \cdot h^2} \quad (2.3)$$

- F_{max} ... maximum load attained in the test
- a ... distance between load introduction point and nearest support
- b ... width of the specimen
- h ... height of the specimen

2-6 COMPRESSION PERPENDICULAR TO THE GRAIN

The test specimens of sample C90-H1 have Bamboo strips in edgewise orientation and the specimens of sample C90-H2 have a flatwise orientation of the lamellae. 21 tests per each sample C90-H1 (EW) and C90-H2 (FW) were made. The dimensions of the specimens equal the dimensions required for the testing of structural timber (see Table 9). The parameters of the testing configuration are provided in Table 10 (see also Figure 20).

Table 9: Sample C90 – compression perpendicular to the grain

name of sample	orientation of the bamboo strips [-]	dimensions l / w / h [mm ³]	# of delivered / # tested [-/-]
C90-H1	edgewise	70 / 45 / 90	22 / 21
C90-H2	flatwise		

Table 10: Parameters of the test configuration for sample C90-H1 and C90-H2

Description	Variable [-]	Value [mm]	Comment [-]
testing length = height	h	90	--
measuring length for local E-modulus	h_0	54	$0,6 \cdot h$
length	l	70	--
width	w	45	--
height	h	90	--

Before testing, the surface areas loaded were flattened with the circular saw to secure parallel planes. The local displacement measurements at reference length were realized with inductive displacement sensors of type DD1.

C90-H1 (EW)

C90-H2 (FW)

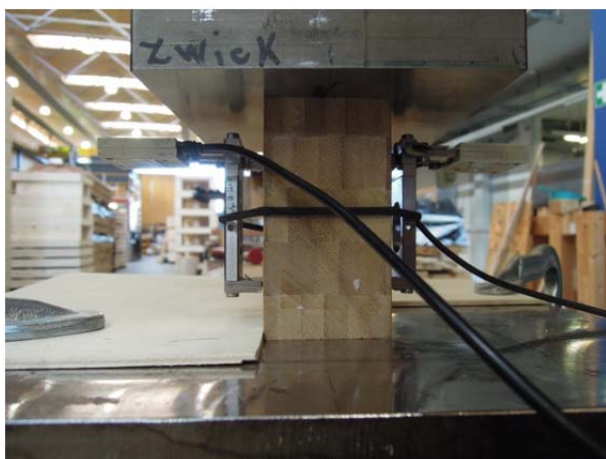


Figure 20: Test setup for compression tests perpendicular to the grain

2-6.1 BASIS OF CALCULATION

The compression modulus of elasticity perpendicular to the grain is determined according to Eq. (2.4). The definition of the boundary conditions $0,1 \cdot F_{c,90,max}$, $0,4 \cdot F_{c,90,max}$ and $F_{c,90,max}$ is obtained from Figure 21.

$$E_{c,90} = \frac{(F_{40} - F_{10}) \cdot h_0}{(w_{40} - w_{10}) \cdot b \cdot l} \quad (2.4)$$

- $F_{40} - F_{10}$... load increase between $0,1 F_{max,est}$ and $0,4 F_{max,est}$
- $w_{40} - w_{10}$... corresponding rise in displacement
- h_0 ... measuring length
- b ... width of the specimen
- l ... length of the specimen

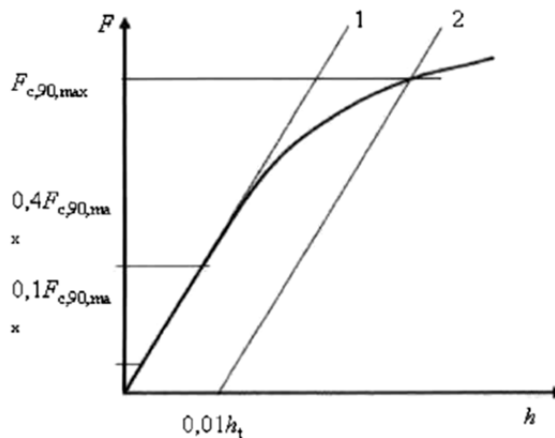


Figure 21: Load plotted against deformation to determine $F_{c,90,max}$ according to ÖNORM EN 408 (CEN, 2010)

The compression strength perpendicular to the grain is determined according to Eq. (2.5).

$$f_{c,90} = \frac{F_{c,90,max}}{b \cdot l} \quad (2.5)$$

- $F_{c,90,max}$... load obtained by iterative process
- b ... width of the specimen
- l ... length of the specimen
- h_t ... = h_0

2-7 TENSION PERPENDICULAR TO THE GRAIN

22 test specimens of sample T90-G1 are produced with Bamboo strips in edgewise direction and another 22 test specimens of sample T90-G2 are produced with Bamboo strips in flatwise direction. Dimensions of the specimens are provided in Table 11. The parameters of the testing configuration are provided in Table 12 (see also Figure 23)

Table 11: Sample T90 – tension perpendicular to the grain

name of sample	orientation of the bamboo strips [-]	dimensions l / w / h [mm ³]	# of delivered / # tested [-/-]
T90-G1	edgewise	70/45/180	22/20
T90-G2	flatwise		

Table 12: Parameters of the test configuration for sample T90-G1 and T90-G2

Description	Variable [-]	Value [mm]	Comment [-]
testing length = thickness	h	180	--
measuring length for local E-modulus	h_0	54*	$0,3 \cdot h^*$
length	l	70	--
width	w	45	--
thickness	t	180	--

* The measuring length of the local modulus of elasticity is not according ÖNORM EN 408 ($h_0 = 0,6 \cdot h$). The chosen length is the same than for compression tests perpendicular to the grain for comparing the results

In order to minimize error interferences due to load introduction, the bamboo test specimens were bonded on pieces of Norway spruce with a PUR-adhesive (PURBOND HB S 309). The adhesive was applied on both surfaces (Norway spruce and laminated Bamboo). The specimens were then fixed on steel elements with six fully-threaded self-tapping screws (8.0 x 160.0 mm) directly before the test, to be built into the testing machine. The local displacement measurements at reference length were realized with inductive displacement sensors of type DD1. The measuring length was chosen the same than for the tests samples C90, which does not meet the value of $0,6 \cdot h$ that is suggested in ÖNORM EN 408.



Figure 22: Manufacturing process of the samples for the T90-tests

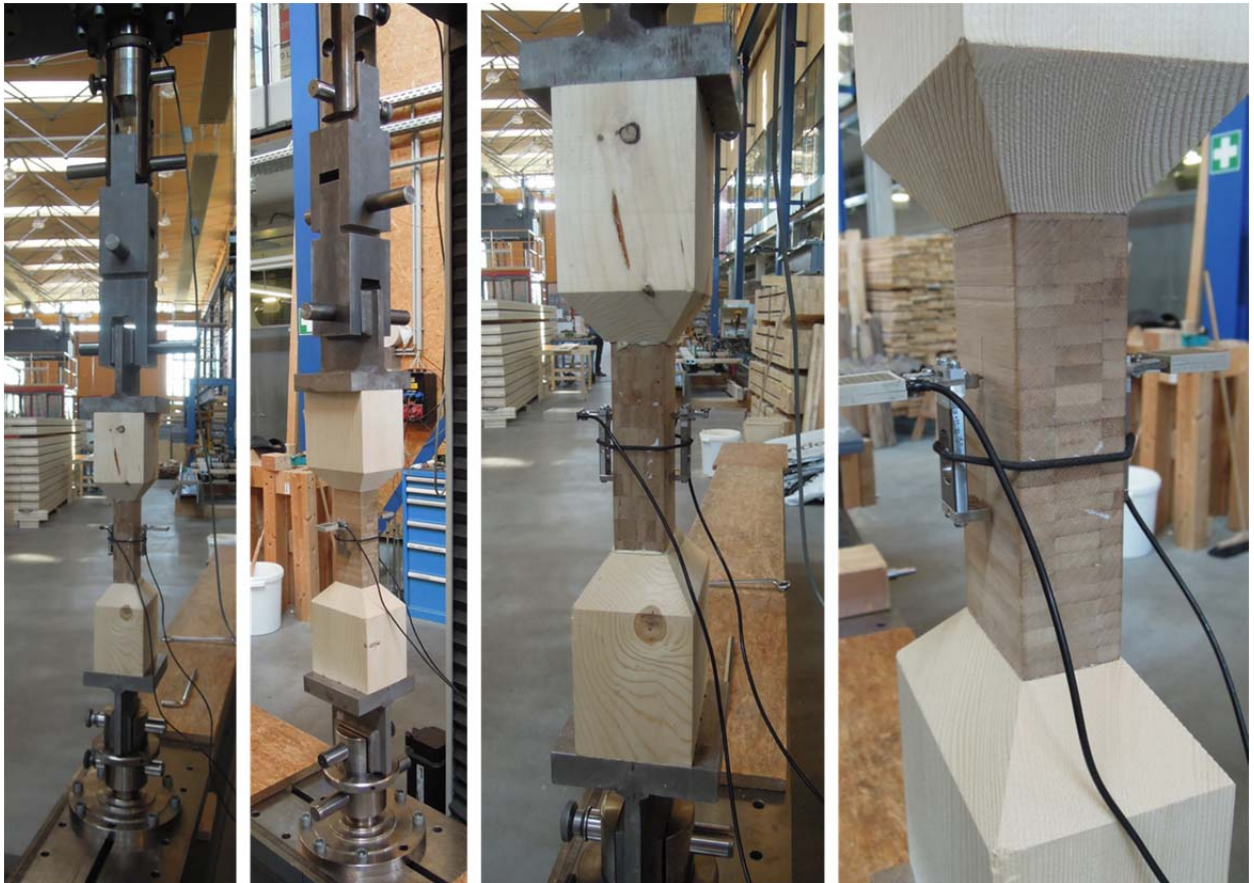


Figure 23: Test setup for tension tests perpendicular to the grain

2-7.1 BASIS OF CALCULATION

The tension modulus of elasticity perpendicular to the grain is determined according to Eq. (2.6).

$$E_{t,90} = \frac{(F_{40} - F_{10}) \cdot h_0}{(w_{40} - w_{10}) \cdot b \cdot l} \quad (2.6)$$

- $F_{40} - F_{10}$... load increase between $0,1 F_{max,est}$ and $0,4 F_{max,est}$
- $w_{40} - w_{10}$... corresponding rise in displacement
- h_0 ... measuring length
- b ... width of the specimen
- l ... length of the specimen

The tension strength perpendicular to the grain is determined according to Eq. (2.7).

$$f_{t,90} = \frac{F_{t,90,max}}{b \cdot l} \quad (2.7)$$

- $F_{t,90,max}$... maximum load attained in the test
- b ... width of the specimen
- l ... length of the specimen

2-8 TENSION PARALLEL TO THE GRAIN

An amount of 44 laminated Bamboo specimens for determination of the tension properties parallel to the grain was tested. Another ten specimens have been resected from the beams delivered as pre-test material. These specimens can be considered as “defect-free” as there are no longitudinal joints in the bamboo strips. Dimensions of the specimens are provided in Table 13. The specimens tested were one layer vertically laminated boards. The parameters of the testing configuration are provided in Table 14.

Table 13: Samples T-C and PT-T0 – tension parallel to the grain

name of sample	orientation of the bamboo strips [-]	dimensions l / w / t [mm ³]	# of delivered / # tested [-/-]
T-C	edgewise	2440/140/18	44/44
PT-T0	edgewise	2440/120/19	10/10

Table 14: Parameters of the test configuration for samples T-C and PT-T0

description	variable [-]	value [mm]	comment [-]
free span	l	1740	$12,4 \cdot w$
measuring length for local E-modulus	l_1	700	$5 \cdot w^*$
width	w	140 (PT120)	--
thickness	t	18 (PT 19)	--
length	L	2440	--
length of the clamping	l_{cl}	320	--

* the measuring length of 700 mm was adopted for the pre-tests ($> 5 \cdot w$)

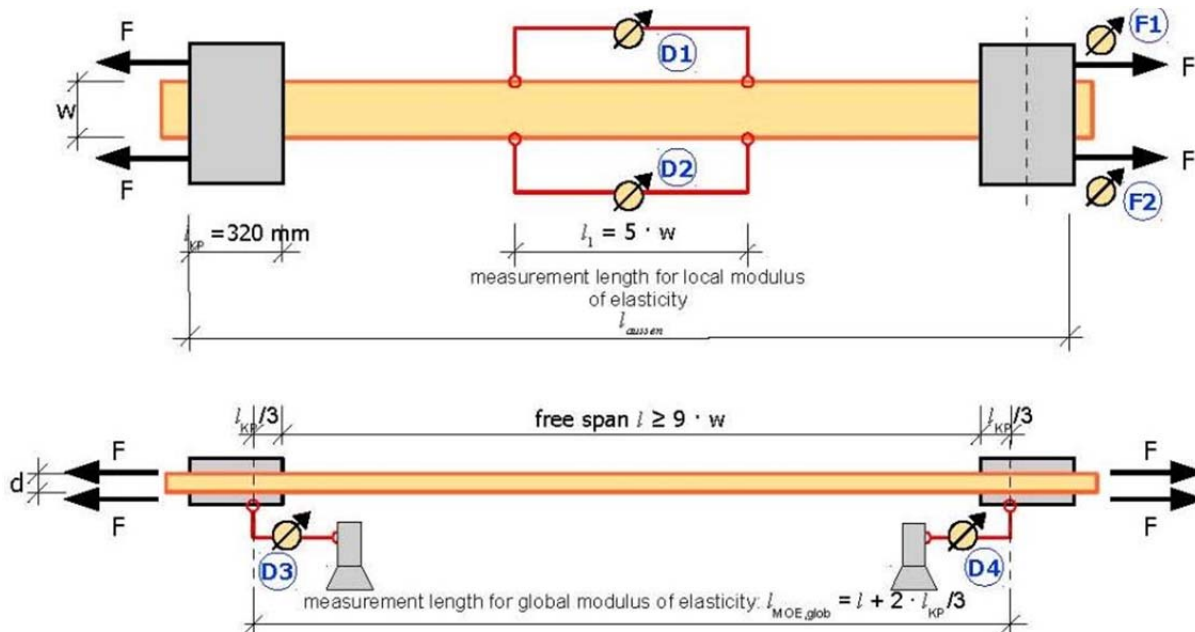


Figure 24: Test setup for tension test parallel to the grain according to EN 408

Inductive displacement sensors of type WA 10 (see Figure 24 and Figure 26) were used for the local displacement measurements. Due to the machines geometry the measuring length was

not exactly in middle of the free span as the displacement sensors had to be removed from the specimen before failure. The distance from the end grain was 99 cm on the side with the fixed clamping and 75 cm ($> 2 \cdot l_{cl} = 64$ cm according to EN 408) on the side with the moving clamping (Figure 25). The local displacement measurement was carried out until a load level of approximately 50 % of the estimated failure load. At this point, the tests were interrupted shortly to remove the displacement sensors.



Figure 25: Specimen with mounted rods as base line for measuring the local deformation

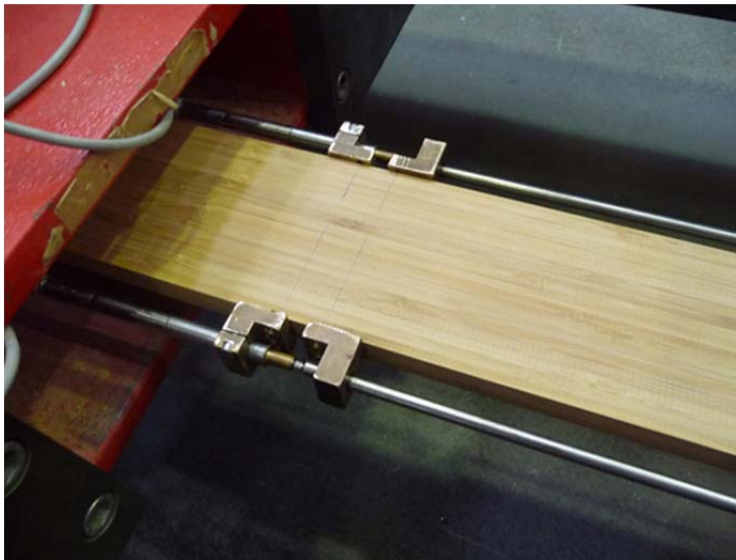


Figure 26: Displacement sensors WA 10

2-8.1 BASIS OF CALCULATION

The tension modulus of elasticity is determined according to Eq. (2.8).

$$E_{t,0} = \frac{l_1 \cdot (F_2 - F_1)}{A \cdot (w_2 - w_1)} \quad (2.8)$$

- l_1 ... measuring length for E-modulus
- A ... cross sectional area
- $F_2 - F_1$... increase of the load in the range where the regression line has a correlation coefficient of 0.99 or better
- $w_2 - w_1$... corresponding rise in displacement

The tension strength parallel to the grain is determined according to Eq. (2.9).

$$f_{t,0} = \frac{F_{t,0,max}}{A} \quad (2.9)$$

- $F_{t,0,max}$... maximum load attained in the test
- A ... cross sectional area

CHAPTER 3: RESULTS

This chapter summarises the determined material properties of each sample. Detailed results for each series are provided in Appendix B. Load vs. displacement diagrams are shown in Appendix C and images of the failure of the bending and tension perpendicular to the grain test samples are shown in Appendix D.

3-1 TEST RESULTS OF SERIES B – BENDING

3-1.1 SAMPLE B-A1 (FW)

At time of testing, the average moisture content of sample B-A1 was 8.7 %. In 17 of 22 test specimens, an unclenching of the longitudinal joints in the tension zone of the beam was clearly visible. This was indicative for the failure of the specimen. The remaining five specimens did not show an obvious gaping in the joint but it can be assumed that the breakage also started with the failure of the longitudinal joints.

All test specimens are considered in the analysis and satisfied the demanded testing time of 300 ± 120 s. The mean value of the bending strength is determined as 56.6 N/mm^2 with a coefficient of variation (COV) of 7.0 %. The characteristic value of the bending strength according to ÖNORM EN 14358 (CEN, 2007) is 49.3 N/mm^2 . The mean value of the local modulus of elasticity is determined as $8,612 \text{ N/mm}^2$ and the mean value of density is determined as 648 kg/m^3 .

Table 15 summarizes the determined bending properties of sample B-A1, as well as the moisture content and density.

Table 15: Bending properties, moisture content and density of sample B-A1 (FW)

	F_{max} [kN]	f_m [N/mm ²]	$E_{m,local}$ [N/mm ²]	ρ [kg/m ³]	u [%]
number of specimens [-]	22	22	22	22	22
mean value	48.3	56.6	8,612	648	8.7
standard deviation	3.4	4.0	292	8.0	0.6
COV [%]	7.0 %	7.0 %	3.4 %	1.2 %	6.3 %
characteristic value (EN 14358)	--	49.3	--	--	--

3-1.2 SAMPLE B-A2 (EW)

The failure of these samples was similar to that of sample B-A1 with the FW orientation of the lamellae. In 18 out of 22 test specimens, the failure of a longitudinal joint of the bamboo strip was obvious. All specimens satisfied the demanded testing time of 300 ± 120 s and were considered in the analysis.

The mean value of the bending strength is determined as 61.7 N/mm^2 with a COV of 4.6 %. The characteristic value of the bending strength is 56.4 N/mm^2 . The mean value of the local modulus of elasticity is determined as $9,093 \text{ N/mm}^2$. The mean value of density is determined as 696 kg/m^3 .

Further results are given in Table 16 and Figure 27 provides images of the typical failure mode due to bending for both samples, A1 (FW) and A2 (EW).

Table 16: Bending properties, moisture content and density of sample B-A2 (EW)

	F_{max} [kN]	f_m [N/mm ²]	$E_{m,local}$ [N/mm ²]	ρ [kg/m ³]	u [%]
number of specimens [-]	22	22	22	22	22
mean value	53.8	61.7	9,093	696	9.8
standard deviation	2.8	2.8	458	13	0.6
COV [%]	5.1 %	4.6 %	5.0 %	1.8 %	5.9 %
characteristic value (EN 14358)	--	56.4	--	--	--



B-A1
FW



B-A2
EW



Figure 27: Typical failure mode due to bending (left) B-A1 (FW); (right): B-A2 (EW)

3-2 TEST RESULTS OF SERIES C90 – COMPRESSION PERPENDICULAR TO THE GRAIN

3-2.1 SAMPLE C90-H1 (EW)

The end of the testing process was defined as a certain displacement criterion which was set as 1.5 mm mean deformation, measured by the sensors of type DD1. A material failure is not required to determine the compression strength perpendicular to the grain. All tested specimens did not show a material failure until the abort criterion was attained.

20 of 21 test specimens satisfied the demanded testing time of 300 ± 120 s according to ÖNORM EN 408. The specimen C90-H1-02 was tested with a lower testing speed which resulted in a longer testing time (714 s). Nevertheless, the specimen was included in the analysis as the exceedance of 294 s of the testing time does not significantly distort the results for modulus of elasticity as well as compressive strength.

Test specimen C90-H1-15 showed a completely different behaviour in relation of load and displacement and delivered the highest result of compression strength perpendicular to the grain in this series. Additionally, a linear behaviour of the load-displacement curve occurred not until a load of approximately $0.27 \cdot F_{c,90,max}$ was applied. Due to the fact that no material failure occurred and the modulus of elasticity determined was just within range, the result was taken into the statistical evaluation.

The mean value of the compression strength perpendicular to the grain is determined as 12.1 N/mm^2 with a COV of 10.3 % and the mean value of the local modulus of elasticity is determined as $1,219 \text{ N/mm}^2$.

Table 17 shows the results of the compression tests perpendicular to the grain, density and moisture content.

Table 17: C90 properties, moisture content and density of sample C90-H1 (EW)

	F_{max}	$f_{c,90}$	$E_{c,90}$	ρ	u
	[kN]	[N/mm ²]	[N/mm ²]	[kg/m ³]	[%]
number of specimens [-]	21	21	21	21	21
mean value	38.6	12,1	1219	647	9,4
standard deviation	4.0	1,2	120	11	0,6
COV [%]	10,3 %	10,3 %	9,8 %	1,7 %	6,5 %
characteristic value (EN 14358)	--	9,9	--	--	--

3-2.2 SAMPLE C90-H2 (FW)

At time of testing the average moisture content of sample C90-H2 was 9.3 %.

Like for the sample C90-H1, the end of the testing process was defined with a displacement criterion of 1.5 mm mean deformation, measured by the displacement sensors. All 21 test specimens satisfied the demanded testing time of 300 ± 120 s.

The mean value of the compression strength perpendicular to the grain is determined as 10.4 N/mm^2 with a COV of 6.9 %. The characteristic value of the compression strength perpendicular to the grain is 9.1 N/mm^2 . The mean value of the local modulus of elasticity is determined as 1295 N/mm^2 . The mean value of density is determined as 700 kg/m^3 . Further results are provided in Table 18.

Table 18: C90 properties, moisture content and density of sample C90-H2 (FW)

	F_{max}	$f_{c,90}$	$E_{c,90}$	ρ	u
	[kN]	[N/mm ²]	[N/mm ²]	[kg/m ³]	[%]
number of specimens [-]	21	21	21	21	21
mean value	33.7	10.4	1,295	700	9.3
standard deviation	23.4	0.7	90	34	0.4
COV [%]	6.9 %	6.9 %	7.0 %	4.9 %	4.7 %
characteristic value (EN 14358)	--	9.1	--	--	--

3-3 TEST RESULTS OF SERIES T90 – TENSION PERPENDICULAR TO THE GRAIN

3-3.1 SAMPLE T90-G1 (EW)

At time of testing, the average moisture content of sample T90-G1 was 9.0 %.

19 of 20 test specimens satisfied the demanded testing time of 300 ± 120 s. Specimen T90-G1-15 reached the maximum load and failure in a testing time of 434 s.

All 20 test specimens showed a tension failure perpendicular to the grain of the bamboo. However, some specimens cracked partially in the glue line between the bamboo test specimen and the Norway spruce. According to ÖNORM EN 408, the test result shall be disregarded where the failure occurs in the connection between test specimen and the load input element and the surface of the break is more than 20 % in the glued area. Specimens T90-G1-18 and T90-G1-22 have approximately 20 % of the surface of the break in the glued area (see images of the fractured samples in appendix D) but results did not have to be excluded from the calculation

To avoid a damage of the inductive displacement sensors (DD1) they had to be taken off the specimen before the failure occurred. To take off the sensors the load was kept at a constant level (for the first specimens 8 kN, then 6 kN).

The mean value of the tension strength perpendicular to the grain is determined as 3.8 N/mm^2 with a COV of 21.6 %. The characteristic value of the tension strength perpendicular to the grain is 2.3 N/mm^2 .

The mean value of the local modulus of elasticity is determined as 1,279 N/mm². The mean value of density is determined as 640 kg/m³.

Table 19 shows the results of the tension tests perpendicular to the grain of sample T90-G1, as well as the moisture content and density.

Table 19: T90 properties, moisture content and density of sample T90-G1

	F_{max}	$f_{t,90}$	$E_{t,90}$	ρ	u
	[kN]	[N/mm ²]	[N/mm ²]	[kg/m ³]	[%]
number of specimens [-]	20	20	20	20	20
mean value	11.9	3.8	1,279	640	9.0
standard deviation	2.6	0,8	89	10	0.6
COV [%]	21.7 %	21.6 %	7.0 %	1.5 %	6.4 %
characteristic value (EN 14358)	--	2.3	--	--	--

3-3.2 SAMPLE T90-G2 (FW)

At time of testing the average moisture content of sample T90-G2 was 9.2 %.

All 20 test specimens showed a tension failure perpendicular to the grain of the bamboo.

18 of 20 test specimens satisfied the demanded testing time of 300 ± 120 s. The test specimen T90-G2-20 and T90-G2-22 reached the maximum load and failure in a testing time of 428 s and 437 s respectively.

As in sample T90-G1 the displacement sensors had to be taken off the specimen before the failure occurred. Therefore, the load was kept at a constant level (at 10 kN and later 8 kN) for 10 seconds.

The mean value of the tension strength perpendicular to the grain is determined as 4.2 N/mm² with a COV of 24.2 %. The characteristic value of the tension strength perpendicular to the grain is 2.5 N/mm². The mean value of the local modulus of elasticity is determined as 1,443 N/mm². The mean value of density is determined as 679 kg/m³.

Table 20 summarizes the results obtained for sample T90-G2 and images of typical failure mode due to tension perpendicular to the grain (EW and FW) can be seen in Figure 28

Table 20: T90 properties, moisture content and density of sample T90-G2

	F_{max}	$f_{t,90}$	$E_{t,90}$	ρ	u
	[kN]	[N/mm ²]	[N/mm ²]	[kg/m ³]	[%]
number of specimens [-]	20	20	20	20	20
mean value	13.4	4.2	1,443	679	9.2
standard deviation	3.3	1.0	93	12	0.7
COV [%]	24.2 %	24.2 %	6.5 %	1.8 %	7.3 %
characteristic value (EN 14358)	--	2.5	--	--	--

T90-G1
EW

T90-G2
EW

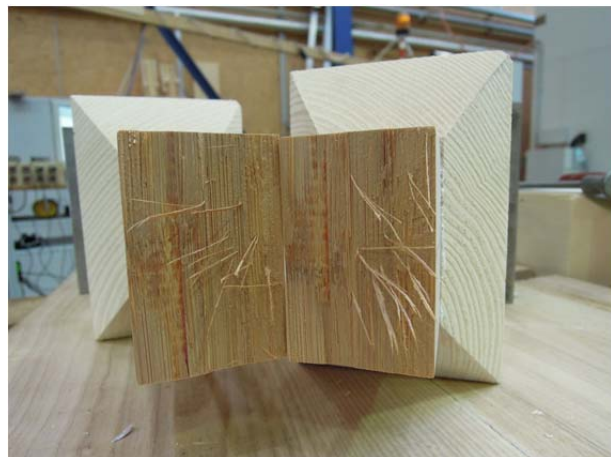


Figure 28: Typical failure mode due to tension perpendicular to the grain (left) T90-G1 (EW); (right) T90-G2 (FW)

3-4 TEST RESULTS OF SERIES T-C AND PT-T0– TENSION PARALLEL TO THE GRAIN

3-4.1 SAMPLE T-C

The average moisture content of sample T-C was 7.7 % at time of testing. All 44 test specimens showed a failure in the longitudinal joint of the bamboo strips as the cause of rupture. The failure behaviour is brittle as the load increases linear with displacement until failure. All specimens satisfied the demanded testing time of 300 ± 120 s.

The mean value of the tension strength parallel to the grain is determined as 39.1 N/mm^2 with a COV of 10.8 %. The characteristic value of the tension strength parallel to the grain is 31.8 N/mm^2 . The mean value of the local modulus of elasticity is determined as $8,062 \text{ N/mm}^2$. The mean value of density is determined as 639 kg/m^3 .

Table 21 shows the results of the tension tests parallel to the grain to determine the mechanical properties of sample T-C, as well as the moisture content and density are provided. Images of typical failure due to tension can be seen in Figure 29. The smooth areas in the fracture zone indicate the joints. The lower pictures show that the joint fails due to shearing off the hitch

Table 21: Tension properties, moisture content and density of sample T-C

	F_{max}	$f_{t,0}$	$E_{t,0}$	ρ	u
	[kN]	[N/mm ²]	[N/mm ²]	[kg/m ³]	[%]
number of specimens [-]	44	44	44	44	44
mean value	101.0	39.1	8,062	639	7.7
standard deviation	10.9	4.2	424	17.0	0.4
COV [%]	10.8 %	10.8 %	5.3 %	2.7 %	4.9 %
characteristic value (EN 14358)	--	31.8	--	608	--

3-4.2 SAMPLE PT-T0

The average moisture content of sample PT-T0 was 8.4 % at time of testing. All ten test specimens showed a brittle failure in the longitudinal direction of the bamboo mostly combined with a splintering of the lamellae or bundles of lamellae from one another (see Figure 30).

The mean value of the tension strength parallel to the grain is determined as 70.0 N/mm^2 with a COV of 14.8 %. The characteristic value of the tension strength parallel to the grain is 49.9 N/mm^2 . The mean value of the local modulus of elasticity is determined as $8,800 \text{ N/mm}^2$. The mean value of density is determined as 595 kg/m^3 . Figure 30 provides images of the failure due to tension parallel to the grain.

Table 22: Tension properties, moisture content and density of sample PT-T0

	F_{max}	$f_{t,0}$	$E_{t,0}$	ρ	u
	[kN]	[N/mm ²]	[N/mm ²]	[kg/m ³]	[%]
number of specimens [-]	10	10	10	10	8
mean value	161.4	70.0	8,800	595	8.4%
standard deviation	24.2	10.4	920	41	0.2%
COV [%]	15.0%	14.8%	10.5%	6.8%	2.4%
characteristic value (EN 14358)	--	49.9	--	--	--

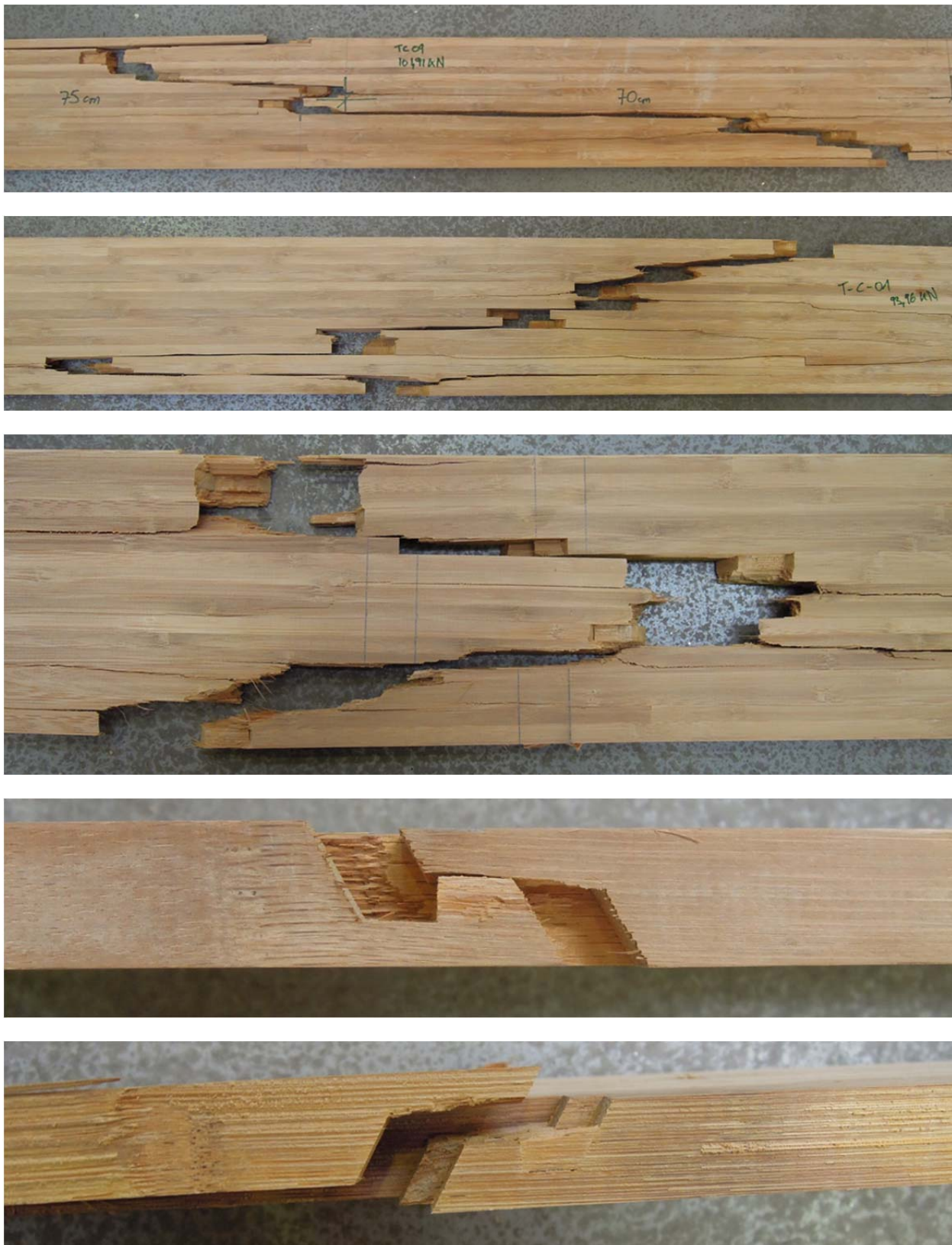


Figure 29: Typical failure pattern due to tension parallel to the grain

RESULTS

Test Results of series T-C and PT-T0– Tension parallel to the grain



Figure 30: Typical failure pattern due to tension; detail of torn out fibres

CHAPTER 4: DISCUSSION

4-1 STRESS STRAIN RELATIONSHIPS IN BAMBOO

Stress-strain diagrams, normally based on way-controlled tests, are used to describe properties and the behaviour of a material. The diagram shows the relationship between stress (e.g. tension, compression, bending, shear) and modulus of elasticity or shear modulus. In an experimental study performed by Dongsheng et al. (2013) it was found that the properties of parallel strand bamboo, such as modulus of elasticity and the load-bearing behaviour itself, is different in tension and compression.

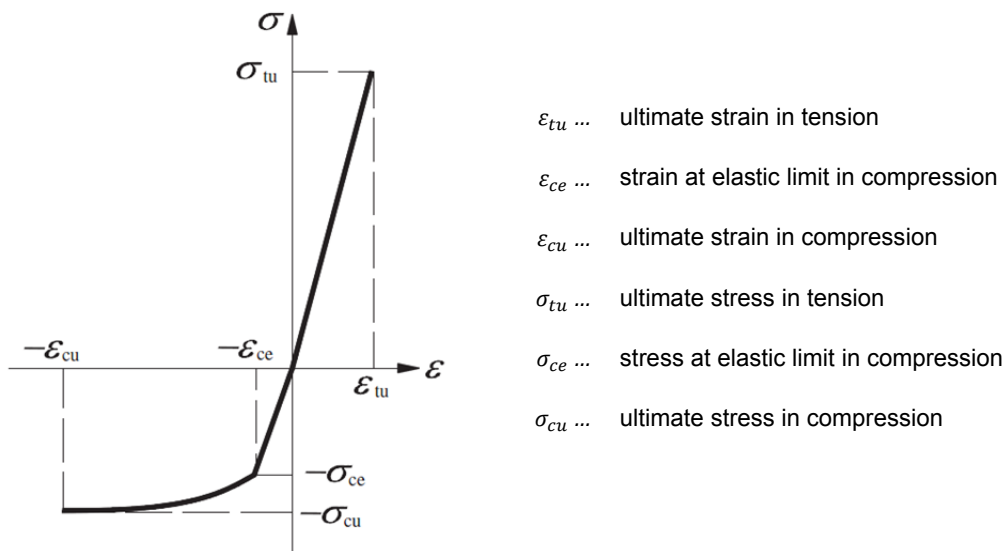


Figure 31: Uniaxial stress-strain relationships (Dongsheng, et al., 2013)

The test for the tensile properties was performed on “clear wood” specimens and the prism for the compression test had a cross section of 105 x 105 mm² and was 315 mm high. Unfortunately, there was no information stated about the bamboo species and no average density of the specimens tested. Only properties parallel to the grain were included in this study. The failure mode of the tensile specimen was due to a broke in the middle section whereas the failure of the compressive specimen was due to local buckling of the fibres. At a low level, there is a linear relationship for both kinds of load, tension and compression, hence the Hooke’s law appears to be applicable at least for the linear-elastic part. However, when this load level (proportional limit) is exceeded, the mechanical behaviour in compression and tension are clearly different as the tension zone fails brittle with a very low strain and the compression zone shows a ductile failure with a long non-linear stress-strain relationship before collapse. The proportion limit for compression was found at a stress level of approximately 35 N/mm² which corresponds to approximately 55 % of the ultimate limit stress. Further test results can be seen in Table 23.

Table 23: Results (Dongsheng, et al., 2013)

	mean [N/mm ²]	COV [%]		mean [‰]
$E_{c,0}$	11,450	3.8	ϵ_{ce}	~3
$f_{c,0}$	62.8	5.6	ϵ_{cu}	~30
$E_{t,0}$	13,680	5.4	ϵ_{tu}	~10
$f_{t,0}$	138	10.5	--	--

In addition, bending tests were conducted. The free span was 1,400 mm and the cross section was 80 mm wide and 108 mm high. Besides the deformation sensor at midspan, five electrical strain gauges were attached symmetrically distributed over the height of the cross section. It can be said, that the longitudinal stain is linear over the cross section. Thus, the strain is proportional to the distance to the neutral axis, but which moves down in direction of the tension zone when the stress exceeds the linear-elastic part of the stress-strain relationship in compression parallel to grain. The failure finally occurred on the bottom of the beams when the ultimate tensile strength in grain was reached (Dongsheng, et al., 2013).

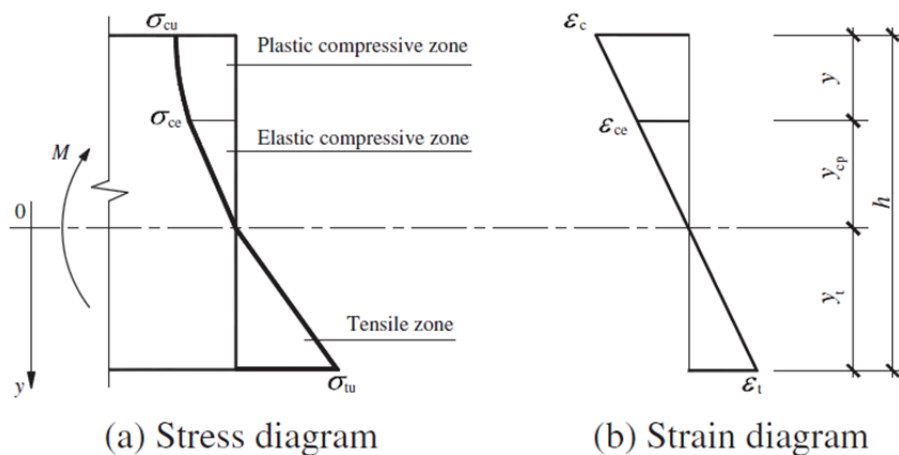


Figure 32: Stress and strain curve over the cross section due to bending

4-2 STRENGTH CHARACTERISTICS IN WOOD

Wood research is further advanced than the research in bamboo. Since wood and bamboo have some certain similarities or even bamboo is often mislabelled as a wood species, it makes sense to consider analogies between these two materials in the discussion.

The structure of wood is characterized by the annual growth rings. The growth layer in softwoods generally consists of a layer thin-walled, wide pore wood cells that are formed at the beginning of the growing season (early wood). These cells are mainly serving the transfer of water and nutrients. The subsequent layer is formed by thick-walled wood cells with narrow pores, which arise at the end of the growing season (late wood). They have the task to strengthen or reinforce the tree. For example in Norway spruce, the density of the early wood layer is about 300 kg/m³, that of late wood is about 1,000 kg/m³. In between there is a continuous transition. Due to the structure there is a directionality of the mechanical parameters (parallel to the fibre, radial (normal to the annual growth rings) and tangential (tangential to the annual rings) (see Table 24 and Figure 33).

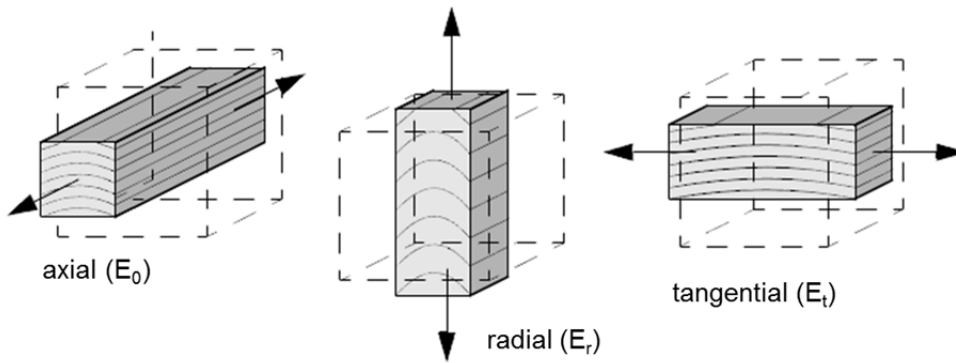


Figure 33: Definition of the directions perpendicular to the grain in wood: axial, radial and tangential (Schickhofer, 2006)

According to Noack and Schwab (1986) the relation of the moduli of elasticity in the different directions to the grain is $E_t : E_r : E_l = 1 : 2.1 : 27$. As stated from Neuhaus (1981) the ratio is $1 : 1.9 : 28.5$.

The considerably higher modulus of elasticity in radial direction, compared with tangential direction, can be explained due to the influence of wood rays that serve as reinforcement that holds together the fibres and prevents them from buckling. However, wood has the lowest stiffness when it is loaded in an angle of 45° to the growth ring. This is due to the effect called “shear coupling” where rolling shear occurs between the early wood and the late wood layers. The rolling shear modulus (G_{rt} ; see Table 24) is much lower than E_t and E_r . Due to that, planks that are sawn from the central part of a log have the lowest modulus of elasticity perpendicular to the grain (Shipsha & Berglund, 2007).

The deviation in the $E_t : E_r$ ratios may also be influenced by differences in the width of the annual tree ring.

Table 24: Elastic constants of Norway spruce and Oregon Pine (Dinwoodie, 2000)

	Moduli of elasticity [N/mm ²]			Moduli of shear [N/mm ²]		
	E_0	E_r	E_t	G_{rt}	G_{0t}	G_{0r}
Norway spruce	10,700	710	430	23	620	500
Oregon Pine	16,400	1,300	900	79	1,180	910

The compressive strength perpendicular to the grain is also dependent of the angle between annual growth ring and load direction. However, the strength values show the opposite trend then stiffness values, as the flatter the angle of the growth rings was within the cross section (side cutting) the lower the compressive strength. Summarising the above-mentioned facts it can be said: the $E_{c,90}$ is rising and $f_{c,90}$ is falling from the centre to the external part (Ruli, 2004; Halili, 2008)

Furthermore, a different failure mode and load bearing behaviour of main and side cutting was observed. In the “centre” specimens the failure often occurred before reaching F_{max} , starting from the core, whereas in side cut specimens, due to its high ductility, very high compressions were possible (20 %) without any sign of breakage.

4-3 BENDING

The diagrams in Figure 34 show the influence of density, which indicates a high amount of fibres, on the bending modulus of elasticity.

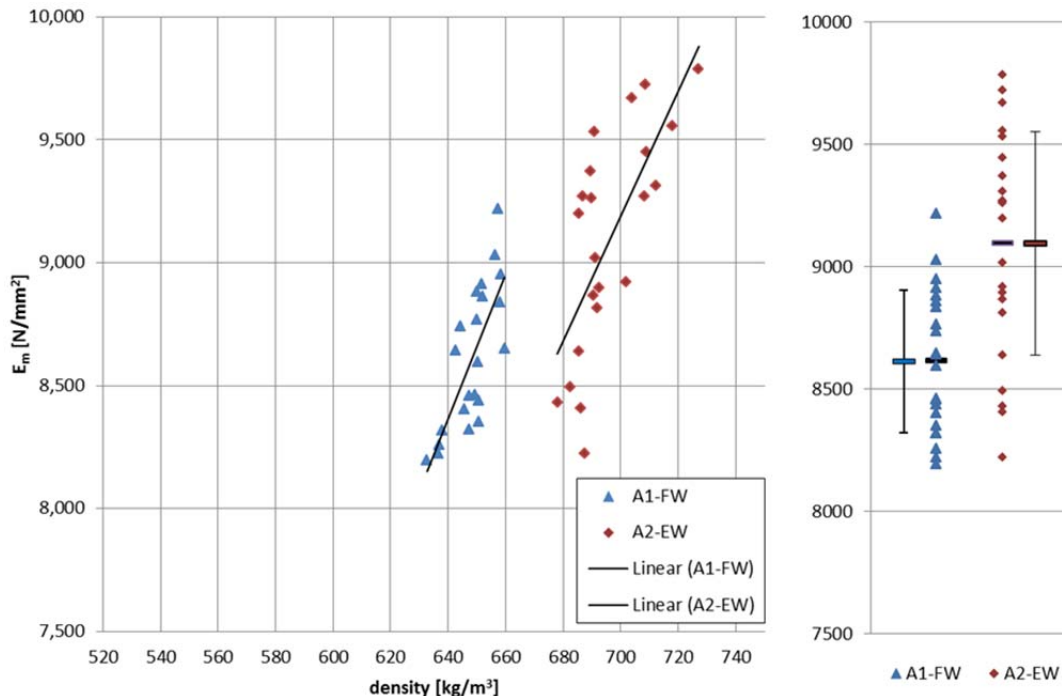


Figure 34: (left) E_m plotted vs. density; (right) range of single values, mean value & standard deviation

In general, material properties are subject of variation and especially natural materials like wood have a higher dispersion in characteristics. For the description of these distributions, different statistical distributions are available. Logarithmic normal distribution is commonly used for characteristics like density, strength and modulus of elasticity. In the relationship between two log-normally distributed properties for regression analysis the use of a power model is meaningful (Brandner, 2012). As samples investigated in this study only cover a certain part of the whole distribution expected in a population the assumption of lognormal distributed properties has to be proven. However, the sample sizes do not present an adequate amount for clear decisions in that respect. Thus, interested only in visualising some tendencies in the relationships between two parameters only linear regression models are used further.

The load vs. deflection diagrams (Appendix C) indicate an almost identical bending behaviour for both lamination orientations. Even though the beams with the EW orientation of the bamboo lamellae have a 5.6 % higher mean value for the modulus of elasticity and a 9 % higher mean bending strength. The reason for this may be density, which is noticeably higher for the EW-beams. In addition, the density ranges of the two series do not overlap. A high density is an indicator for a higher amount of fibres and in order to that, a higher strength and modulus of elasticity parallel to the grain. However, effects on density caused by the processing method (bleaching or carbonizing) may counteract this influence.

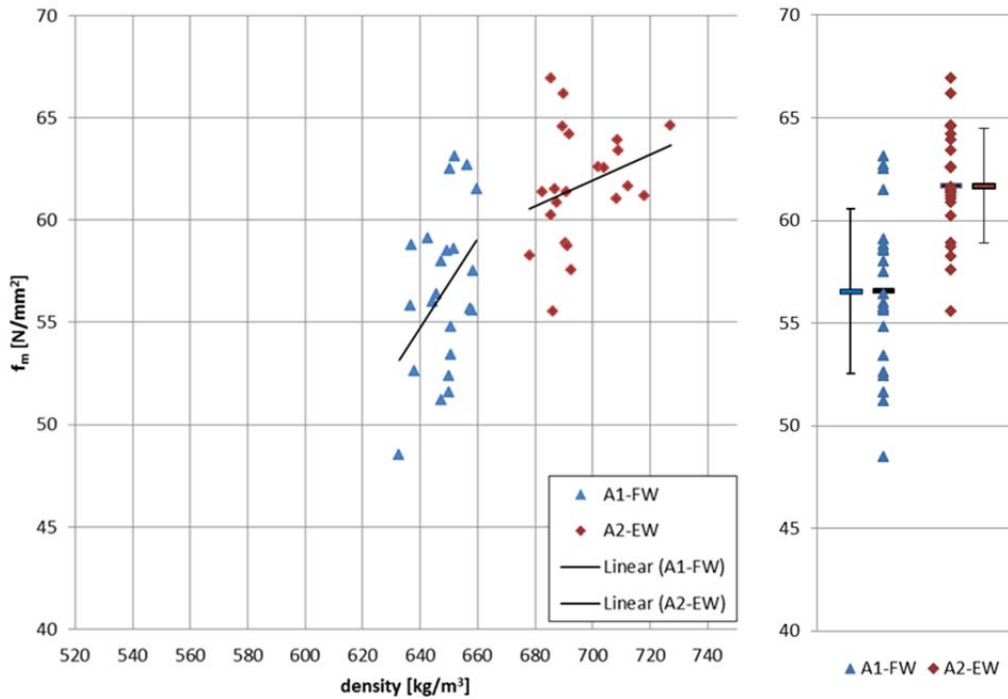


Figure 35: (left) f_m plotted vs. density; (right) range of single values, mean value & standard deviation

However, the data gained from the tension tests parallel to the grain on specimens with joints (Chapter 4-6) do not reflect any relation between tensile strength and density but between modulus of elasticity and density. One explanation given is that the modulus of elasticity is analysed at a lower load level where the joints have a lower influence on the elastic behaviour of the structural members.

Table 25 provides the gradients of the linear regression from the E_m - ρ and f_m - ρ diagrams. The analysis does not show a clear tendency if density has a higher influence on the bending strength or on the modulus of elasticity.

$$\% \text{ - increase} = \frac{k \cdot 100 \text{ kg/m}^3}{X_{mean}} \quad (4.1)$$

X_{mean} in Eq. (4.1) is the mean value of the bending strength or the modulus of elasticity of each sample EW or FW, respectively.

Table 25: Gradient & relative increase of mechanical properties per 100 kg/m³ density

	modulus of elasticity E_m		bending strength f_m	
	k of trend line	%-increase per 100 kg/m ³	k of trend line	%-increase per 100 kg/m ³
A1-FW	29	33	0.21	37
A2-EW	25.5	28	0.06	9

The other effect that is reflected in these diagrams is the so-called “system effect”. This effect occurs when two or more elements are linked together with rigid or flexible connections to act in common as a single structural element. A “compensation” or balancing of material properties is the consequence, as it is very likely that local zones with lower properties are joined by zones in adjacent elements with higher properties (parallel system). Strength properties usually correlate positively with stiffness (see Figure 36). The task of load bearing can therefore be shifted from

the “weaker” to the “stronger” element within the parallel system as the stiffer element attracts the load (Schickhofer, 2006).

Correal et al. (2014) tested laminated bamboo lumber made out of Guadua bamboo. The specimens were produced according to method 1 (see Chapter 1-3.1) with a horizontal lamination of the boards. There were no longitudinal joints within the beams. The dimension of the beams for the static bending tests was $l / h / w = 760 \text{ mm} / 50 \text{ mm} / 50 \text{ mm}$ and the average density of the material tested was 741 kg/m^3 . The authors recorded different main failure modes of the beams with either EW or FW orientation of the bamboo strips. The failure mode identified in the EW-beams was splintering tension on the bottom side of the beam, whereas the FW-beams failed mainly due to horizontal shear. However, they recorded the same trend, as the mean bending strength of the edgewise laminated beams was 19 % higher than for the flatwise laminated specimens. The mean value of the modulus of elasticity was only 4 % higher. The authors state: *“The differences in strength, in which the beams loaded in the tangential direction (note: EW oriented strips within the cross section) were able to sustain the load for larger deflections, are explained by the lamination scheme. In order to have a reduction in the beam capacity, either the shear or the tension failures must propagate through the width of beam. This propagation is harder to reach in the case of vertical lamination since the local failure must propagate not only through the adhesive layer, but also through the different laminae with different properties and defects.”* (Correal, et al., 2014)

The same effect was recorded in various other studies (Lee, et al., 1998; Nugroho & Ando, 2001; Correal, et al., 2014b)

However, extending the trend lines in the density- E_m -diagram the point of intersection will be located in the left of the data cloud of sample A1-FW. This indicates that if both samples would lie in the same range of density distribution, for the sample with flatwise oriented lamellas a higher modulus of elasticity than the edgewise oriented samples is indicated. This contradicts the “system effect”.

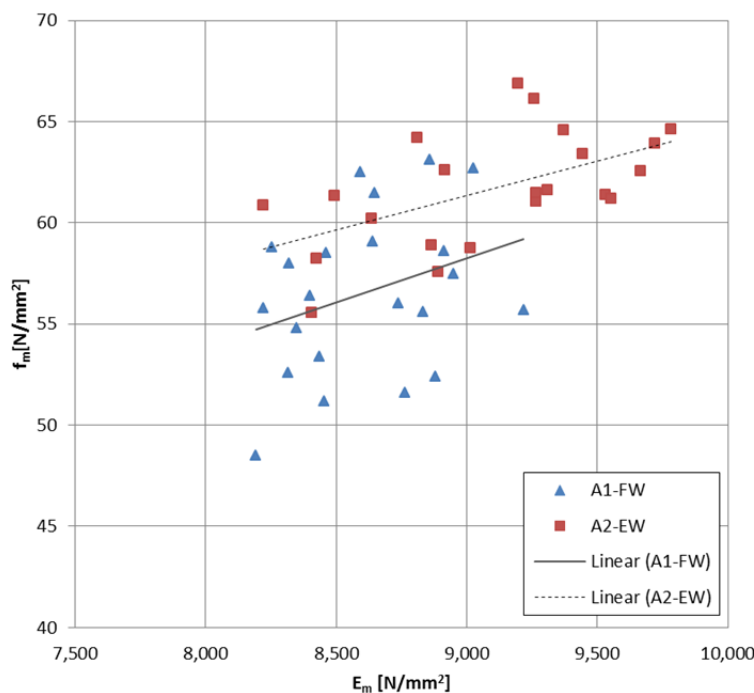


Figure 36: Bending strength plotted against modulus of elasticity

In Figure 36 bending strength is plotted against modulus of elasticity and it is apparent that the FW-samples show a higher variation in bending strength but a lower variation in terms of stiffness. However, the gradient of these trend lines ($k_{FW} \approx 0.004$ and $k_{EW} \approx 0.003$) is also found in bending test analysis of spruce (Brandner & Schickhofer, 2008).

The cumulative distribution functions (CDF) for bending strength and modulus of elasticity are given in Figure 37 right and left, respectively.

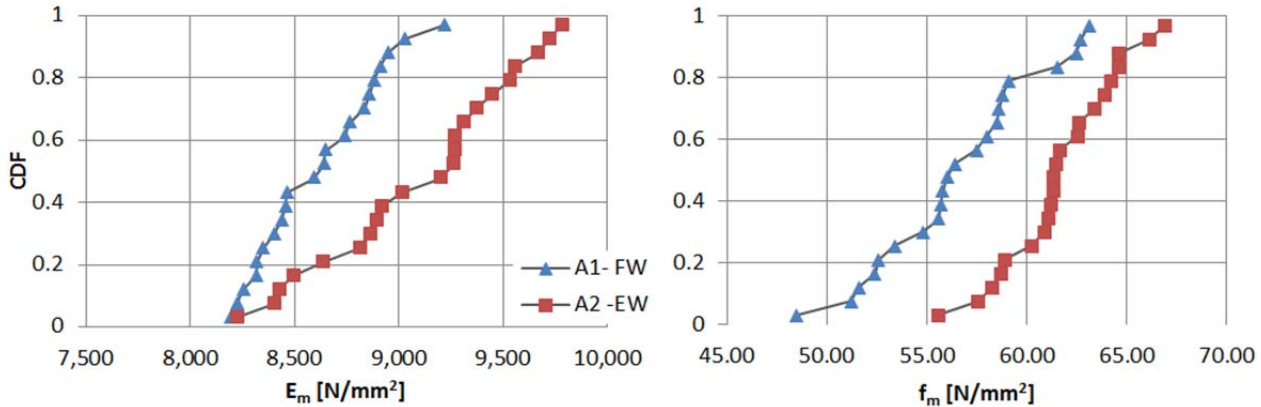


Figure 37: CDFs for the mechanical properties in bending

For the practical implementation of engineered bamboo products, a differentiation between the characteristic properties of edgewise and flatwise laminated beams would not be made, as to keep the product’s application as simple as possible. In Table 26 the test results of sample A1 and A2 are jointly evaluated. The mean value of the bending strength is determined as 59.1 N/mm² with a COV of 7.2 %. The characteristic value of the bending strength $f_{m,k}$ according to ÖNORM EN 14358 (CEN, 2007) is 51.5 N/mm².

Table 26: Common evaluation of test results (A1/FW+A2/EW) of the sample B – bending

	F_{max}	f_m	$E_{m,local}$	ρ	u
	[kN]	[N/mm ²]	[N/mm ²]	[kg/m ³]	[%]
number of specimens [-]	44	44	44	44	44
mean value	51.1	59.1	8852	672	9.25%
standard deviation	4.2	4.3	451	26.3	0.80%
COV [%]	8.1%	7.2%	5.1%	3.90%	8.40%
characteristic value (EN 14358)	--	51.5	--	--	--

4-4 COMPRESSION PERPENDICULAR TO THE GRAIN

For the interpretation of the test results of the sample compression perpendicular to the grain two different approaches have been adopted. One is to find similarities to soft wood specimens where the cross section with FW-oriented strips is related to a side cut wood specimen, which is loaded in radial direction (normal to the annual growth rings) and the EW-specimen, which is comparable to a wood with standing tree rings parallel to the load direction. The other approach is based on the findings of Dixon and Gibson (2014) that the bamboo loaded in transverse direction fails by crushing of the vessels in the vascular bundles (see Figure 7 and Figure 8 in chapter 1-2.2).

Though the average modulus of elasticity is higher for the FW specimens, which have the higher density, there is no positive correlation between $E_{c,90}$ and density within the sample (as can be seen in Figure 38). Figure 39 shows the compressive strength perpendicular to the grain plotted against density.

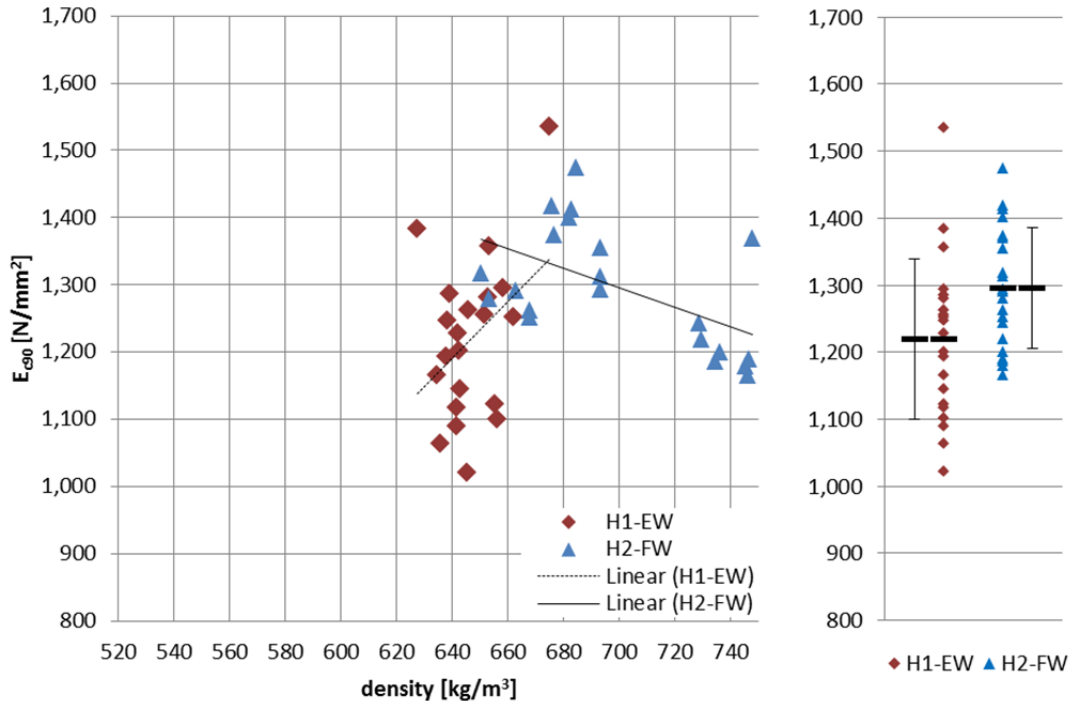


Figure 38: (left) $E_{c,90}$ plotted vs. density; (right) range of single values, mean value & standard deviation

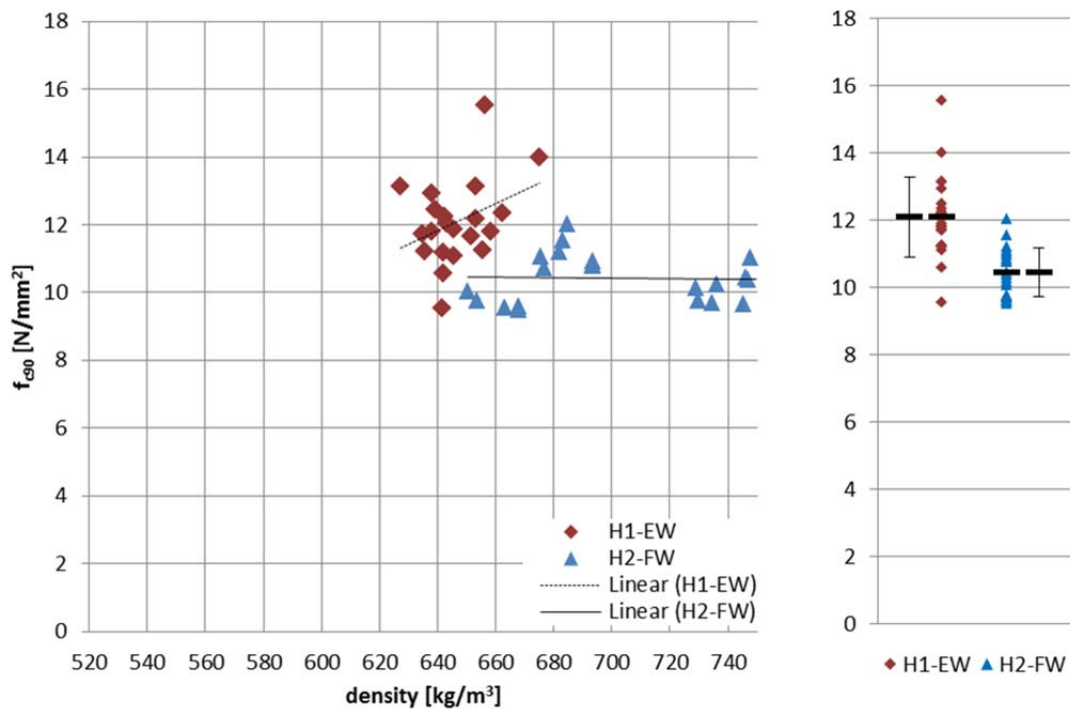


Figure 39: (left) $f_{c,90}$ plotted vs. density; (right) range of single values, mean value & standard deviation

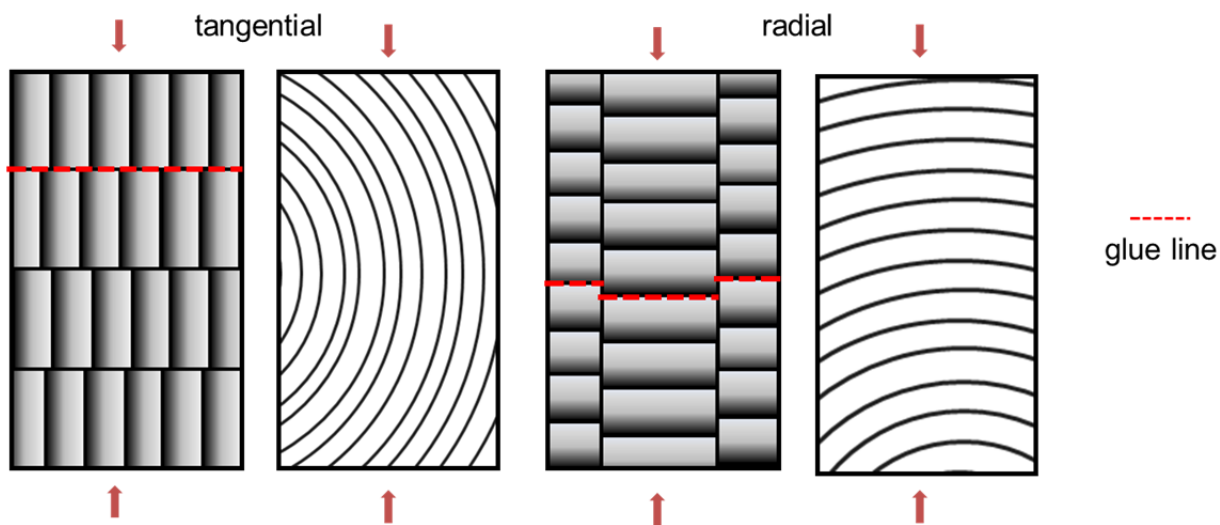


Figure 40: Tangential and radial orientation of the specimens

Halili (2008) found out that in Norway spruce timber there is no correlation between compressive strength perpendicular to the grain and density and only a slight increase of the modulus of elasticity with increasing density. Both, the strength value and the modulus of elasticity perpendicular to the grain are rather influenced by the original position of the sawn timber within the stem and consequently the orientation of the annual growth rings. Additionally the presence of branches can positively affect the compressive characteristics.

For the FW-oriented bamboo specimens there is no dependence between compressive strength perpendicular to the grain and density whereas the modulus of elasticity and density are actually negatively correlated. On the contrary, E_{c90} and f_{c90} show a positive correlation with density for the EW-specimens.

Taking the structure of the specimens into closer consideration, it is notable that, irrelevant if it is bamboo or wood, the specimens loaded in tangential direction (EW) show a higher compressive strength but a lower modulus of elasticity than the specimens loaded in radial direction (FW). However the relation $E_t : E_r$ in softwoods is approximately 1 : 1.9 and therefore shows a clearer directional dependence of the stiffness than in bamboo. The mean moduli of elasticity gained in the tests are in a 1:1.06 relationship, $E_{t,(EW)} : E_{r,(FW)}$ respectively. This may be attributable to the fact that bamboo itself is a more heterogeneous material than wood and due to the composition of the cross section that results in an additional homogenization. This leads to a more constant stress distribution over the cross section in load direction and additionally the shear-coupling effect does not have such a high influence than in wood. The bamboo specimens' structure comes close to the limiting state described in Stuefer (2011) where the annual growth rings are lying plane-parallel to the edge of the plank. Whereas in real wooden planks, stress peaks occur within the cross section due stiffness differences over the width (especially centre-cut specimens). Moreover, the lower differences in radial and tangential direction can also be attributed to the system effect.

Compressive strength is defined at a certain yield point but this does not reveal the behaviour of the specimen under further loading. Figure 41 shows the compressive strength and the further load bearing behaviour of Norway spruce in dependence of the angle of the annual growth rings. It can be realised that the values of the compressive yield point are better in tangential loading direction but a further load increase is not possible as a stability failure of the growth

rings occurs. On the contrary, wood specimens with lying growth rings can bear much higher forces without being ruptured (Schickhofer, 2009). It will be of interest in further studies on bamboo if a similar behaviour can be observed.

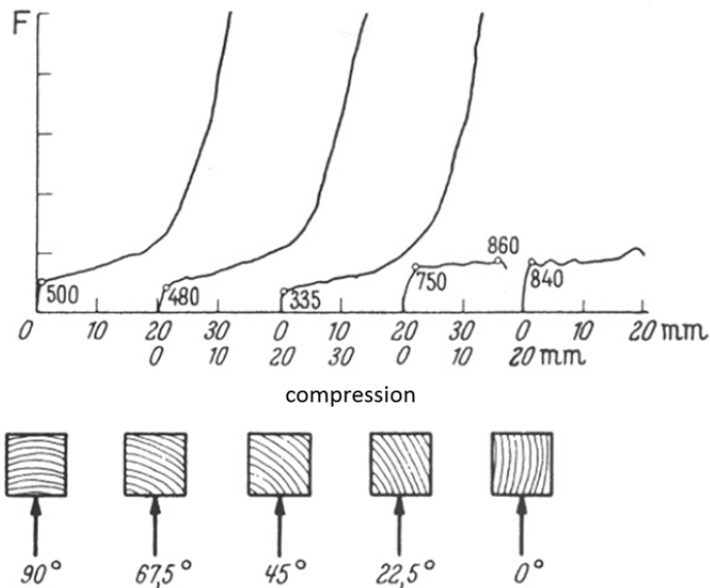


Figure 41: Dependence between compressive strength and orientation of the growth rings in Norway spruce (SIA, 1981)

Another characteristic in the structure of the EW-bamboo specimens is the glue area, which is a continuous straight surface perpendicular to the loading direction, which comes from the composition of vertically laminated sheets. The FW-oriented strips are arranged staggered in this plane.

The second approach for interpreting the test results is based on the findings of Dixon and Gibson (2014). The volume fraction of the vessels can be assumed as almost constant with density and radial position within the culm wall, which would result in a rather consistent compressive strength as the bamboo loaded in transverse direction fails by crushing of the vessels in the vascular bundles (see Figure 7 and Figure 8 in chapter 1-2.2). However, this approach is not in agreement with the test results.

When the bamboo specimen is loaded in radial (FW) direction, there may be an additional factor that can be considered. Similar to how branches affect material properties perpendicular to the grain in wood, the nodal area with fibres running transversely to the growth direction (when they enter the diaphragm) may influence the characteristics in bamboo.

Figure 42 shows the transverse compressive strength plotted against modulus of elasticity. The mean compressive strength of the FW-specimens is lower whereas E_{c90} is within the same range of the EW-specimens. A positive correlation can be determined for both samples. The correlation in softwoods is normally negative.

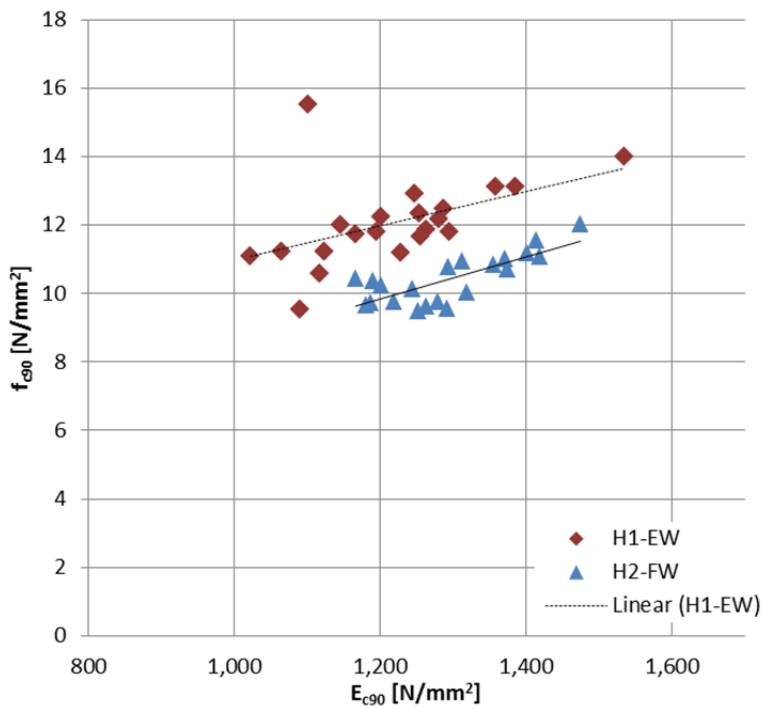


Figure 42: f_{c90} plotted vs. E_{c90}

Table 27 provides the test results of EW and FW samples jointly evaluated. The characteristic value for the compressive strength decreases from 9.9 N/mm² and 9.1 N/mm², EW and FW respectively, to 9.1 N/mm² due to the higher COV. The mean modulus of elasticity is 1,257 N/mm².

Table 27: Common evaluation of test results (H1/EW+H2/FW) of the sample C90

	F_{max}	$f_{c,90}$	$E_{c,90}$	ρ	u
	[kN]	[N/mm ²]	[N/mm ²]	[kg/m ³]	[%]
number of specimens [-]	42	42	42	42	42
mean value	36,138	11.3	1,257	673	9.3
standard deviation	4,053	1.3	112	37	0.5
COV [%]	11.2	11.6	8.9	5.5	5.7
characteristic value (EN 14358)	--	9.1	--	--	--

4-5 TENSION PERPENDICULAR TO THE GRAIN

Transverse tension stresses occur in curved beams and beams with various section heights like saddle-roof shaped beams as in cross connections, notches and breakthroughs. In timber and in bamboo the tension failure perpendicular to the grain is very brittle and the tension strengths show a wide dispersion. 95 % of the load displacement curves in Appendix C: do not show any signs of a beginning damage but the load increases linear with displacement until failure. Only two specimens (T90-G1-04 and T90-G2-12) show a momentary load drop before load increases again until the specimens fail abruptly.

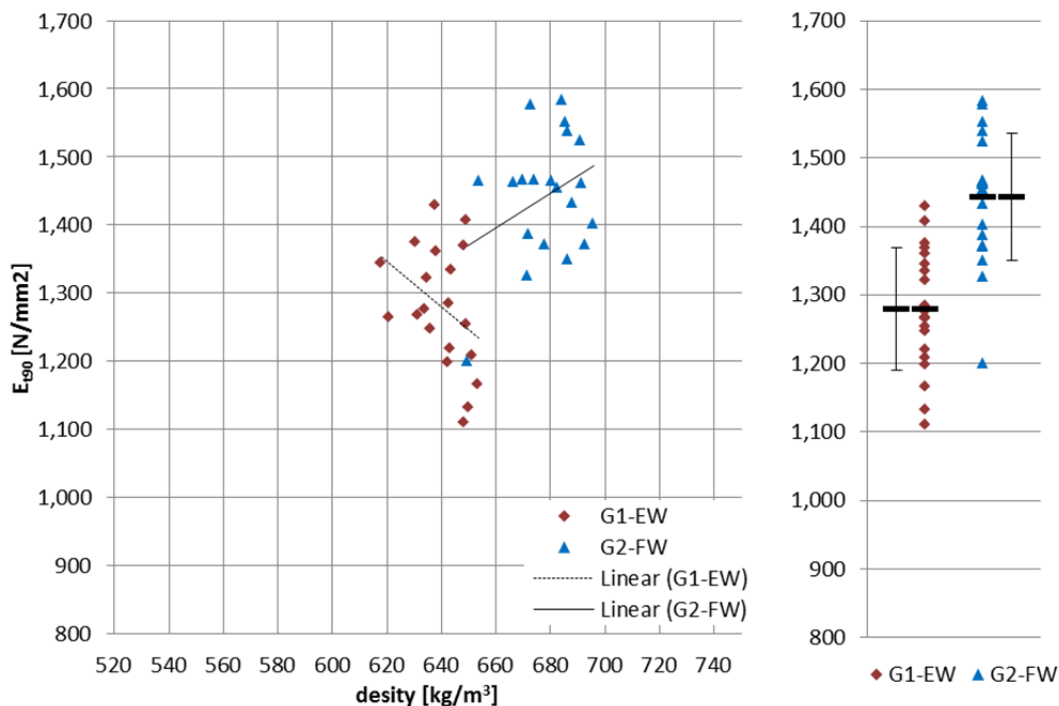


Figure 43: (left) E_{190} plotted vs. density; (right) range of single values, mean value & standard deviation

The structure of the specimens is the same than for the test in compression perpendicular to the grain but they are twice as high. Therefore, one can apply the same analogy with wood. The tangential and the radial modulus of elasticity stand in a relationship of $E_{t(EW)} : E_{r(FW)} = 1 : 1.13$. Again, the modulus of elasticity is higher in radial (FW) direction. However, the density difference between the two test series makes it difficult to assign influences on the mechanical properties either to density or the orientation of the lamellae within the cross section. The coefficient of variation of the strength properties was for both test samples, EW and FW, higher than 20 % whereas the modulus of elasticity showed a lower deviation (COV approximately 7 %).

In finite element analysis and various experiments, it was found out that in glulam, tensioned perpendicular to the grain, the maximum stresses are approximately in the middle of the wood lamellas depending on the radius of the growth rings and the distance of the sawn plank from the pith. In load direction, the stress peaks are close to the glue line. This is why most specimens fail in the interface area and the crack runs through two lamellas (Stuefer, 2011).

A similar observation has been made for the EW test sample where 16 out of 20 specimens tested showed a partial failure in the glued area between two bamboo strips. The glue area is not continuous though, as the cross section is composed of vertically laminated sheets (see the images of the fracture in Appendix D:).

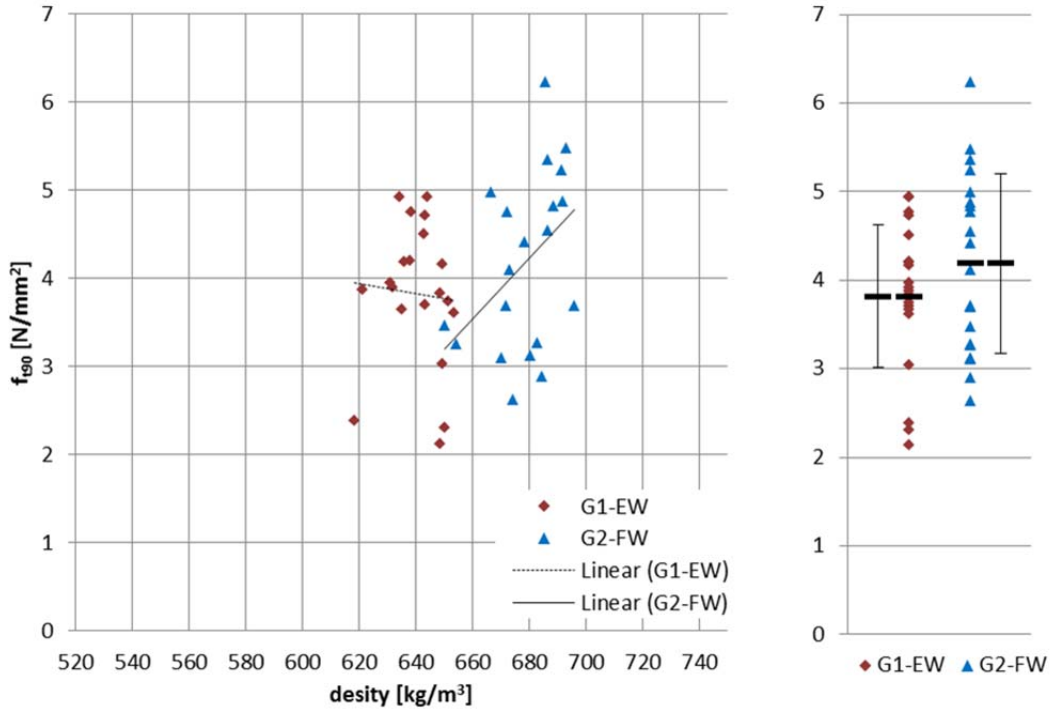


Figure 44: f_{t90} plotted vs. density; (right) range of single values, mean value & standard deviation

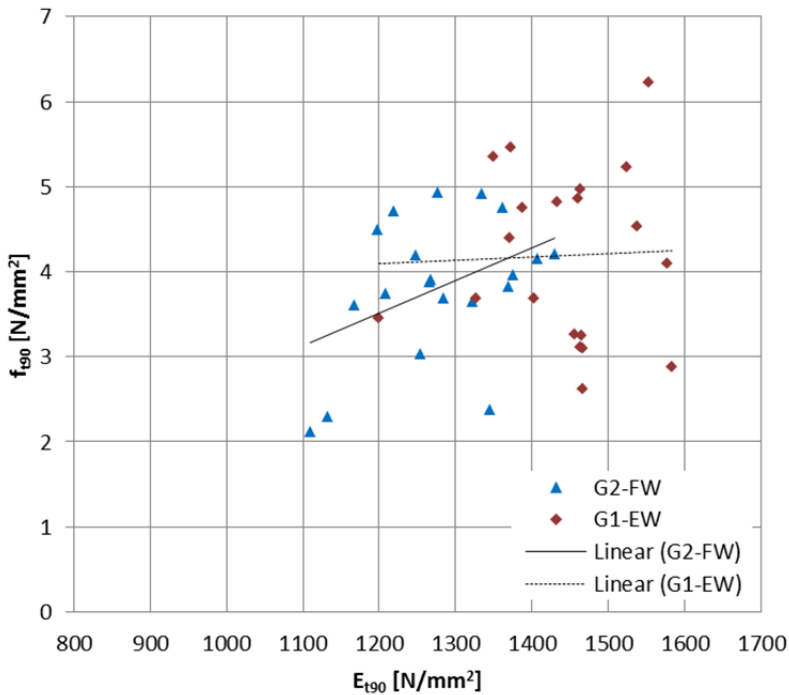


Figure 45: f_{t90} plotted vs. E_{t90}

In the samples with FW oriented bamboo strips (loaded in radial direction) the modulus of elasticity and compressive strength correlate positively with density, whereas the EW-specimens show a negative correlation with $E_{t,90}$ and almost no density relation for $f_{c,90}$. Though, the data series of both properties, $f_{t,90}$ and $E_{t,90}$, and both samples show rather “dot-clouds” than a distinct trend (see Figure 44).

Figure 45 shows the transverse compressive strength plotted against modulus of elasticity. No conclusive correlation between these two properties can be found due to the large deviation of both values.

Table 28 provides the test results of EW and FW samples jointly evaluated. The characteristic value for tension strength perpendicular to the grain is 2.5 N/mm^2 .

Table 28: Common evaluation of test results (G1/EW+G2/FW) of the sample T90

	F_{max}	$f_{t,90}$	$E_{t,90}$	ρ	u
	[kN]	[N/mm ²]	[N/mm ²]	[kg/m ³]	[%]
number of specimens [-]	40	40	40	40	40
mean value	12,690	4.0	1.361	660	9.1
standard deviation	3,003	0.9	123	22	0.6
COV [%]	23.7	23.3	9.0	3.4	0.6
characteristic value (EN 14358)	--	2.5	--	--	--

4-5.1 E_{90} – CHARACTERISTIC VALUE

The mean values for the moduli of elasticity in compression and tension perpendicular to the grain are located in the same bandwidth between approximately $1,200$ and $1,450 \text{ N/mm}^2$, which corresponds to 14 to 17 % of the modulus of elasticity in grain direction.

For the design and dimensioning of a timber or bamboo structure, the E_{90} is of only minor importance. It can be useful for calculating the compression deformation at the supports of a supporting structure in case of SLS design. Furthermore, it is of interest in cross-layered structural members to consider the stiffness of the overall system more exactly.

It is an attempt of the structural engineer to avoid tension perpendicular to the grain as timber as well as bamboo shows the lowest strength properties at this load. Additionally the compressive modulus of elasticity perpendicular to the grain is experimentally more reliable due to the more constant stress distribution within the cross section. It is suggested to use the commonly evaluated $E_{c,90}$ from both samples, EW and FW, as modulus of elasticity perpendicular to the grain (E_{90}). The mean value is $1,257 \text{ N/mm}^2$.

4-6 TENSION PARALLEL TO THE GRAIN

Whereas a relation between density and the tensile modulus of elasticity was found, a relationship between density and the tensile strength was not indicated. Possible reasoning for this last observation is seen by results influenced by the joints between the bamboo lamellas. On the one hand, as the cross section of one single strip is reduced to approximately 40 % of the cross-sectional area at the joints, the ultimate load bearing capacity decreases. On the other hand, the weakest-link model can be applied, which means, that the failure from one element causes the whole structure to fail (“A chain is as strong as the weakest link”). In case of a single jointed bamboo strip (as a serial system) the maximum tensile strength is as high as the weakest part or rather the net section within the joint area. However, the specimens tested were composed cross sections with several strips laminated to a parallel system (one layer of vertically laminated boards) which means that the stress can shift from the lamella with the local weakening to the lamellae next to it. However, it should be noted, that this realignment of forces results in an eccentricity that causes an additional bending moment in the boards and reduces the tensile strength.

Figure 46 shows that the modulus of elasticity of both test samples correlates positively with density and that both trends are almost parallel. Nevertheless, it can be expected from the trend lines that the boards without longitudinal joints have a higher E_0 compared to longitudinally jointed boards with the same density.

The material without longitudinal joints shows a clear dependency between density and tensile strength (Figure 47). This was to be expected due to the higher volume fraction of fibres and is consistent with the existing experience based on literature research (see subchapter 1-2.2). The strength values of the T-C sample do not show a correlation with density.

The larger deviation of the mechanical properties from the “defect free” sample can be attributed to the higher variation of density, as the COV in sample T-C is only 2.7 % and in sample PT-T0 6.8 %.

The mean value of tension strength of the material with joints was 39.1 N/mm^2 and for the material without joints 70.0 N/mm^2 . The reduction from 70.0 N/mm^2 to 39.1 N/mm^2 corresponds to a loss of 44 %. The average density was 595 kg/m^3 and 639 kg/m^3 respectively. To adjust the influence of density on the mechanical properties, the modulus of elasticity and tensile strength of a bamboo board without longitudinal joints and with a density of 639 kg/m^3 are calculated using the gradient of the trend line ($k_E = 17$ and $k_{ft} = 0.22$) of the pre-test sample. The calculated value for tensile strength and modulus of elasticity parallel to the grain is 79.5 N/mm^2 and $9,540 \text{ N/mm}^2$, which corresponds to an increase of more than 100 % in tension strength and 13 % in stiffness. The difference of the mechanical properties between the boards with and without joints with reference to an identical density is more evident (see dashed arrow in Figure 46 and Figure 47).

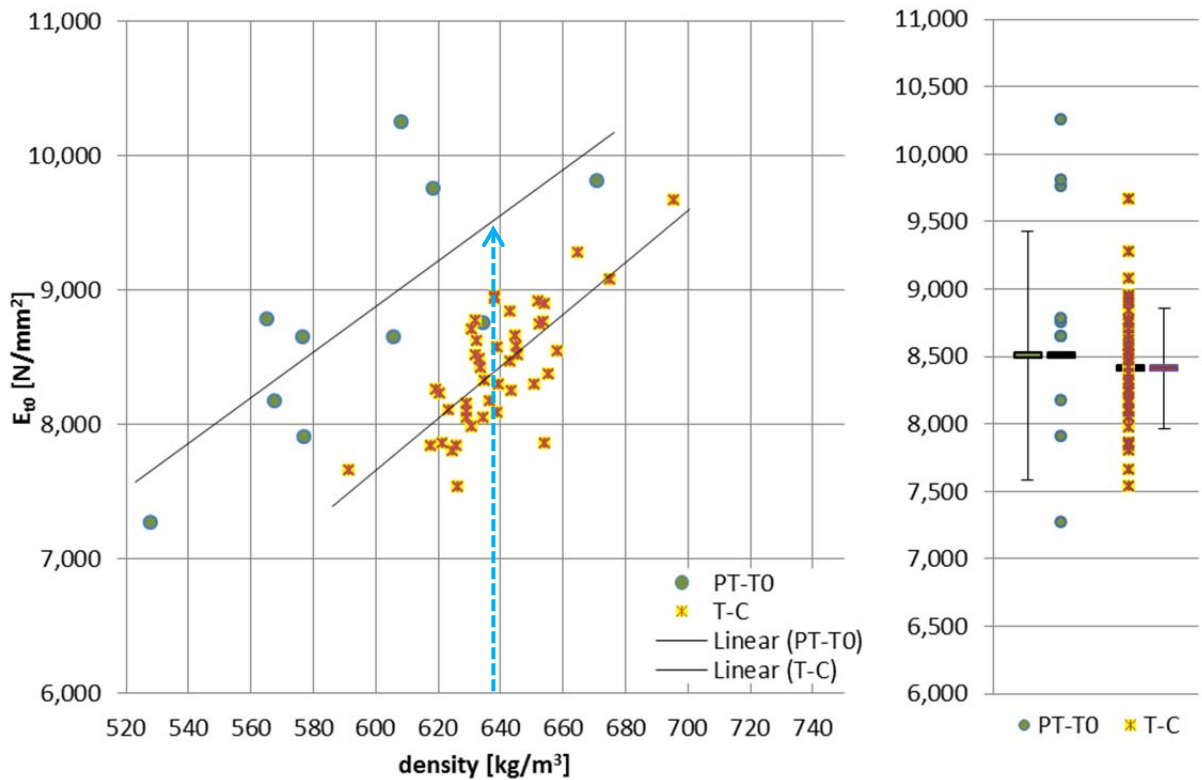


Figure 46: (left) $E_{t,0}$ plotted vs. density; (right) range of single values, mean value & standard deviation

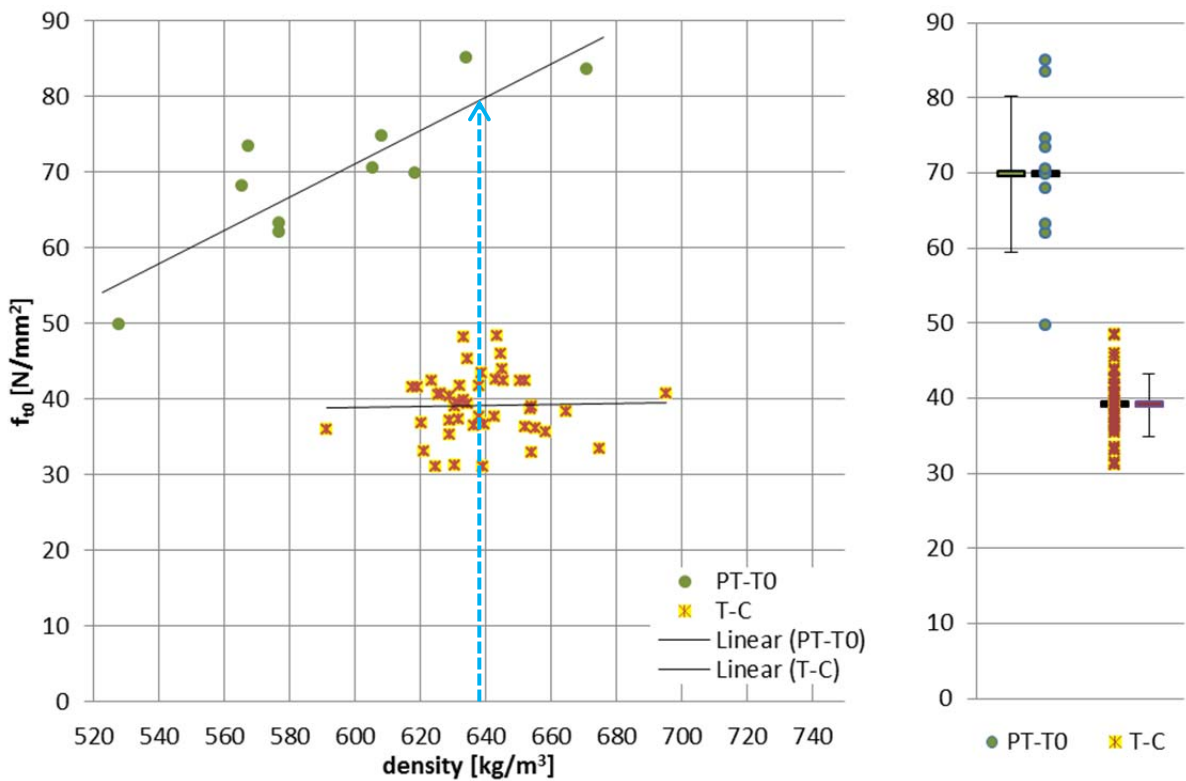


Figure 47: (left) $f_{t,0}$ plotted vs. density; (right) range of single values, mean value & standard deviation

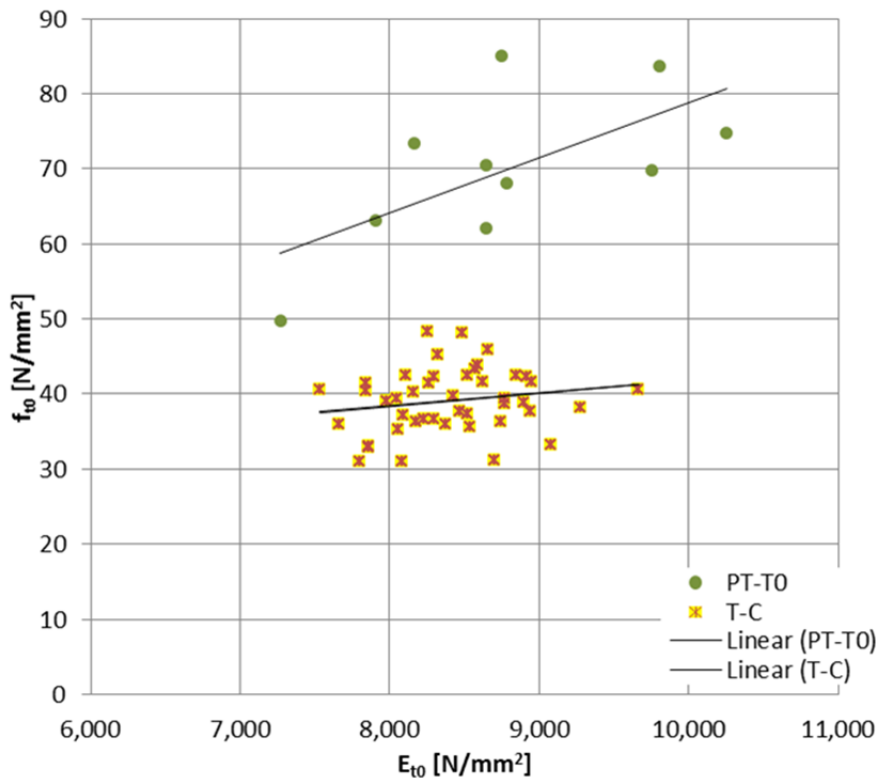


Figure 48: f_{t0} plotted vs. E_{t0}

The analysis in Figure 48 of the specimens without jointed strips shows a more distinct relationship between E_{t0} and f_{t0} than that for the sample composed of specimen with longitudinally jointed strips. This regression is expected as in timber the modulus of elasticity is a common indicator for the grading in strength classes. However, the bamboo boards with longitudinal joints do not show this trend, which is attributable to the influence caused by the joints, which probably counteract relationships between material properties.

4-7 JOINTS

The joints within the bamboo lamellae were identified the main cause of failure in bending and in tension tests. In Figure 49 the flow of forces is depicted. There is not only the reduction of the cross sectional area but due to the joints geometry, a bending moment ($F \cdot e$) occurs in the net-section. Furthermore, the entire force (F) has to be transferred by shear stresses in the joint.

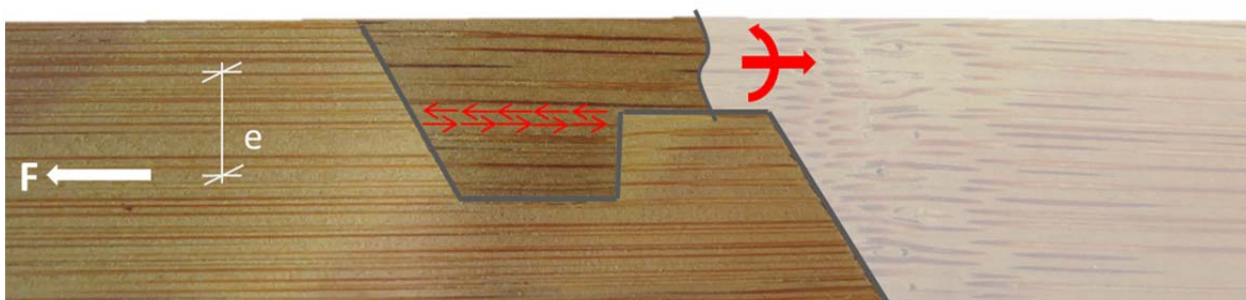


Figure 49: Joint in the bamboo lamella and internal forces due to tension

At the University of Los Andes, Columbia, the department of Civil and Environmental Engineering conducted a comprehensive study to determine mechanical properties of glued laminated Guadua members. The experimental test methods followed the ASTM standards for wood and wood products as no particular standard for bamboo products has been established. The material tested was produced out of a four-year-old Guadua augustifolia Kunth culm that was grown in Columbia. It is South America's most important bamboo and besides Moso the most common bamboo for industrial processing.

The production technique equals method 1 (see section 1-3.1.1) with the strips laminated horizontally (narrow faces glued together) to form the sheets. Then the bamboo sheets were bonded on the wide faces to form glue laminated Guadua (GLG) sections of approximately 30 mm thickness and 110 mm width. In a further processing step the defect-free sections with a length of 1,200 mm were assembled longitudinally by producing finger joints with an effective depth of 11 to 13 mm, adhesive resin application and applying a pressure. Through this joining technique theoretically an "endless" bamboo plank is received that can be stacked together to form the desired cross section.

However, the main failure mode was identified as tension in the finger joint close to midspan and the crack extended through the horizontal glue line. The mean bending strength obtained in four point bending tests were 42.9 N/mm² for the edgewise orientation and 48.9 N/mm² for the flatwise orientation of the lamellae within the cross section. The free span in the test was 3,100 mm and the dimensions of the cross section were w / h = 100 mm / 200 mm (Correal, et al., 2014b).

The performance potential of a finger joint depends primarily on the geometry and further on the production quality. The experience from research projects that have been conducted on the Institute of Timber Engineering and Wood Technology at the Graz University of Technology have shown that the performance of finger joints tested in tension in clear wood specimens is about two-thirds of the tensile strength of the base material (Brandner, 2015). Assuming the similar performance for bamboo and taking the value for $f_{t,0} = 79.5 \text{ N/mm}^2$ from the previous calculation, the tensile strength of the finger jointed bamboo board would result in 53 N/mm², according to Eq. (4.2).

$$f_{t,FJ} = \frac{2}{3} \cdot f_{t,0} \quad (4.2)$$

$f_{t,FJ}$... tensile strength of the finger joint
 $f_{t,0}$... tensile strength of the bamboo board

This would improve the performance of the members' tensile strength by 35 %. Processing finger joints for longitudinal joints of bamboo sheets, not single lamellas, is considered the best solution in respect to load bearing capacity as well as production process. Finger jointing is the state of the art joining technique for the production of glulam and other engineered timber products for construction purposes.

4-8 COMPARISON OF PROPERTIES

Even though no grading of the base material is taking place, as known for timber, the COVs within the single test samples are found to be relatively low for an organically grown construction material, which is a consequence of homogenisation. These low COVs have a positive effect on the characteristic strength values.

To find out about the competitive position of laminated bamboo lumber in regard to mechanical properties evaluated in this study, a comparison with commonly graded structural timber (C24) appears meaningful. The material tested shows superior strength properties but the mean modulus of elasticity is 31 % lower than that of the most commonly used structural timber of the strength class C24.

Table 29: Comparison of mechanical properties between LBL and timber (C24)

property			laminated bamboo lumber		timber - C24		
			[N/mm ²]	%	[N/mm ²]	%	
strength	bending tension strength	$f_{m,k}$	51.5	100%	24	47%	
	tension	parallel	$f_{t0,k}$	31.8	100%	14	44%
		perpendicular	$f_{t90,k}$	2.47	100%	0.4	16%
	compression	parallel	$f_{c0,k(est)}$	51.2	100%	21	41%
		perpendicular	$f_{c90,k}$	9.1	100%	2.5	27%
stiffness	E-modulus	parallel	$E_{0,mean}$	8,410	100%	11,000	131%
		perpendicular	$E_{90,mean}$	1257	100%	370	29%

the value of the compressive strength was estimated as 80 % of the averaged value (64 N/mm²) of Table 2 - according to Sharma, et al. (2015)

Additionally, the performances of the building materials steel (S235) and concrete (C30/37) are provided in Table 30. The specific strength is a material's strength divided to its density (e.g. breaking length). It can be seen that laminated bamboo lumber has, compared to timber, steel and concrete the favourable strength to density ratio. However, the stiffness to density ratio is poor and comparable to that of concrete.

Table 30: Mechanical properties of LBL, timber, steel and concrete adopted from Schickhofer (2006)

property	unit	LBL - in grain direction		C24 - in grain direction		steel - S235		concrete - C30/37	
		%	%	%	%	%	%		
E-modulus	$E_{0,mean}$ [N/mm ²]	8,410	100	11,000	131	210,000	2497	32,000	380
tension strength	$f_{t,k}$ [N/mm ²]	31.8	100	14	44	235	739	2	6
compressive strength	$f_{c,k(est)}$ [N/mm ²]	51.2	100	21	41	235	459	30	59
bending tension strength	$f_{m,k}$ [N/mm ²]	51.5	100	24	47	235	456	2.9	6
density	ρ_{mean} [kg/m ³]	670	100	350	52	7,850	1172	2,400	358
breaking length	$f_{t,k}/\rho_{mean}$ [m]	4,750	100	4,000	84	2,990	63	83	2
strength/density	$f_{c,k(est)}/\rho_{mean}$ [m]	7,640	100	6,000	79	2,990	39	1,250	16
stiffness/density	$E_{0,mean}/\rho_{mean}$ [km]	1,255	100	3,143	250	2,675	213	1,333	106

the values $E_{t,0,mean}$ and $f_{t,k}$ for bamboo is taken from the T-C-sample (with longitudinal joints)
the value of the compressive strength was estimated as 80 % of the averaged value (64 N/mm²) of Table 2 - according to Sharma, et al. (2015)

CHAPTER 5: CONCLUSION

5-1 PRACTICAL RELEVANCE & POTENTIAL APPLICATION

The product investigated in this study has a great potential for applications as structural building material. The strength properties are promising in comparison to structural timber and glued laminated timber of timber species typically used in Central Europe. However, its maximum potential of load bearing capacity is not exploited in every case investigated. One of the main potential for optimization is seen in the joints commonly used to connect bamboo lamellas. These joints represent a weak spot within the structural members in particular if loaded in tension parallel to grain and in bending.

A disadvantage for the use of engineered bamboo members as ceiling construction is the low modulus of elasticity as, especially in residential building, the verification of the serviceability limit state (SLS) according to EC 0 (CEN, 2013) may become the crucial verification. That and additionally the higher dead weight of the material will make difficult to compete with traditional structural timber and timber products. The $E_{0,mean}/\rho_{mean}$ ratio is 150 % higher for structural timber of the strength class C24 than for laminated bamboo lumber.

To reduce dead weight and to save raw material one way could be to produce profiles that are similar to the profiles known from steel construction. Smart designed profiles would allow showing comparable stiffness than solid products by using less material. This approach is also known from products made out of timber and wood materials like timber formwork beams. Though, bamboo is appropriate for building up designed cross sections as only strips with small cross sections can be gained from the hollow bamboo culm.

A possibility to make use of high strength properties of bamboo is to use it as reinforcement in composite beams. When timber is under bending stress, the failure normally occurs in the bending tension zone as consequence of local imperfections. This failure manifests, similar to the failure in tension, as a brittle failure. Bamboo has a similar mechanical behaviour (see stress-strain relationship diagram in chapter 4-1) but a higher tensile strength compared to soft wood, such as Norway spruce, and an excellent formability. Therefore a bamboo sheet could be laminated either to the tension or to the tension and compression side of the glulam beam and ensure extensive deformation, due to a higher (bending) tensile (and compressive) strength, before the ultimate limit state of the composite member is reached. The advantage to use bamboo as reinforcement material is the similarity between physical properties of softwood and bamboo. Therefore, additional stresses between the composite materials due to swelling and shrinking or temperature will be lower compared to commonly used reinforcing materials such as steel. Additionally, the difference in modulus of elasticity between timber commonly used in Central Europe and bamboo is not too big. Therefore, none of the components does attract unnecessarily and disproportionately more load. As a result, the possibility increases that the fracture occurs not in the outermost lamellas but closer to the centre of the cross section.

To gain some quantification a calculation where an equivalent glulam beam represents the bamboo-timber composite girder is conducted by means of the rigid composite theory. An ordinary glulam beam built up from C24 timber planks is calculated for comparison. The calculation is based on a single span girder with a six meter free span and beam dimensions of $b / h = 120 \text{ mm} / 240 \text{ mm}$. The cross section of the beams was composed of six 40 mm high planks. Beam I is produced from sawn timber planks of the quality class C24 whereas in beam II the top and the bottom lamella are replaced with a 40 mm high bamboo plank.

beam I	b	h	E-Modulus	n	beam II	b	h	E-Modulus	n
	[mm]	[mm]	[N/mm ²]	[-]		[mm]	[mm]	[N/mm ²]	[-]
lamella 1	120.0	40	11000	1.00	lamella 1	120.0	40	8850	0.80
lamella 2	120.0	40	11000	1.00	lamella 2	120.0	40	11000	1.00
lamella 3	120.0	40	11000	1.00	lamella 3	120.0	40	11000	1.00
lamella 4	120.0	40	11000	1.00	lamella 4	120.0	40	11000	1.00
lamella 5	120.0	40	11000	1.00	lamella 5	120.0	40	11000	1.00
lamella 6	120.0	40	11000	1.00	lamella 6	120.0	40	8850	0.80
	Σ	240				Σ	240		

$$E I_{\text{BEAM}_I} = 1.52\text{E}+12 \text{ N} \cdot \text{mm}^2$$

$$E I_{\text{BEAM}_{II}} = 1.31\text{E}+12 \text{ N} \cdot \text{mm}^2$$

Figure 50: Build-up of the beams and bending stiffness

At a line load of 6 kN/m ($M = 27 \text{ kNm}$) the timber beam reaches its ultimate load bearing capacity as the edge fibres reach their maximum bending resistance of 24 N/mm^2 . The calculated deflection at midspan is at that point 6.66 cm ($l / 90$). In comparison, the bamboo-timber composite beam has a deflection of 7.72 cm ($l / 78$; + 14 %) at the same load which is due to the lower bending stiffness ($E \cdot I$). However, the bamboo-composite beam has not yet reached its ultimate limit state as the stress has not reached the bending strength neither of the bamboo lamella nor of the C24 planks (see Figure 51). The load can be increased to 8 kN/m, which corresponds to a maximum bending moment $M = 36 \text{ kNm}$, where the edge stress of the timber planks complies with the bending strength of 24 N/mm^2 . At this point the stress in the edge lamellas is close above 29 N/mm^2 , which corresponds to a utilization factor of the tensile bending strength (51.5 N/mm^2) of 56 %. The maximum load carrying capacity of the composite beam is therefore 25 % higher than of the conventional glulam beam.

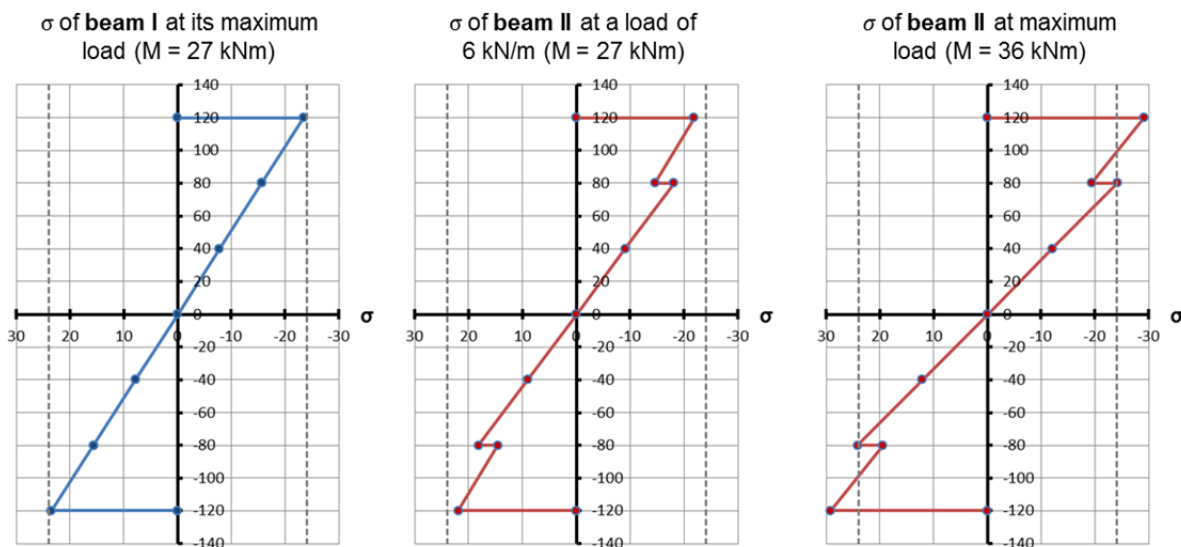


Figure 51: Stresses of beams I and II at various load stages

Even though LBL is an excellent product, there are some major disadvantages as the requirement for accuracy of the geometry and the production itself is very stringent. Hand in hand with that goes a small yield of the material (which means lower production efficiency). In thin-layer lamination, the requirements of bamboo are less stringent which makes it more cost-efficient. Another advantage of using thin bamboo strips for the production is the chance to customize the layout of the bamboo slivers corresponding to the strength design (Xiao & Yang, 2012). This approach rather follows the principle of the processing laminated veneer lumber.

Furthermore, it is possible to form the (bamboo) veneer sheets in shaped moulds to create sheets similar to trapezoidal profiled sheets. This may be a seminal development for structural timber engineering but this is currently a subject of research.

Bamboo is a material available globally, the plantations and forests can be managed sustainably and the processing for engineered bamboo products reaches from very simple methods to high tech industry. Furthermore, bamboo is of interest as it is a natural material, which has the advantage of being biodegradable as well as for carbon sequestration to mitigate greenhouse gas carbon dioxide. For all those reasons, it shall be used as a building material.

Appendix A: Directories

A-1 References

- [1] **Amada, S. et al., 1995.** Fiber texture and mechanical graded structure of bamboo. pp. 13-20.
- [2] **ASTM International, 2013.** *ASTM D5456: Standard specification for evaluation of structural composite lumber.* West Conshohocken, PA, USA: ASTM International.
- [3] **Bamboo Garden, 2006.** <http://www.bamboogarden.com/>. [Online] Available at: <http://www.bamboogarden.com/>; [Zugriff am 16 April 2015].
- [4] **Brandner, R., 2012.** *Stochastic System Actions and Effects in Engineered Timber Products and Structures.* Graz: Verlag der Technischen Universität Graz.
- [5] **Brandner, R., 2015.** *Dipl.-Ing. (FH) Dr. techn* [Interview] (20 May 2015).
- [6] **Brandner, R. & Schickhofer, G., 2008.** Glued laminated timber in bending: new aspects concerning modelling. *Wood Science and Technology*, 42(5), p. 401–425.
- [7] **CEN, 1994.** *ÖNORM ISO 3130:1994-10-01. Wood - Determination of moisture content for physical and mechanicals.* Brussels: European committee for standardization.
- [8] **CEN, 2007.** *ÖNORM EN 14358:2007-04-01. Timber structures - Calculation of characteristic 5-percentile values and acceptance criteria for a sample.* Brussels: European committee for standardization.
- [9] **CEN, 2010.** *ÖNORM EN 384:2010-05-15 Structural timber - Determination of characteristic values of mechanical properties and density.* Brussels: European committee for standardization.
- [10] **CEN, 2010.** *ÖNORM EN 408:2010-12-01. Timber structures - Structural timber and glued laminated timber - Determination of some physical and mechanical properties.* Brussels: European committee for standardization.
- [11] **CEN, 2013.** *Eurocode 0 EC 1990 Eurocode - basis of structural design.* Brussels: European Committee for Standardization.
- [12] **Correal, J. F., Echeverry, J. S., Ramirez, F. & Yamin, L. E., 2014.** Experimental evaluation of physical and mechanical properties of Glued Laminated *Guadua augustifolia* Kunth. ***Construction and Building Materials, Band 73, pp. 105-112.***
- [13] **Correal, J. F., Echeverry, J. S., Yamin, L. E. & Ramirez, F., 2014b.** Experimental behaviour of structural size glued laminated *Guadua* bamboo members. *WCTE*.
- [14] **Dinwoodie, J. M., 2000.** *Timber: its nature and behaviour.* 2. Hrsg. London: Spon.
- [15] **Dixon, P. G. & Gibson, L. J., 2014.** The structure and mechanics of Moso bamboo material. *Journal of Royal Society Interface*, pp. 1-12.
- [16] **Dizman Tomak, E., Topaloglu, E., Ay, N. & Yildiz, U. C., 2011.** Effect of accelerated aging on some physical and mechanical properties of bamboo. *Wood Science and Technologie*, Issue 46, pp. 905-918.

- [17] **Dongsheng, H., Aiping, Z. & Yuling, B., 2013.** Experimental and analytical study on the non linearbending of parallel strand bamboo beams. *Cunstruction and building materials*, Band 44, pp. 585-592.
- [18] **Dunkelberg, K., 1985.** *Bambus/Bamboo*. 4. Hrsg. Stuttgart: Karl Krämer Verlag.
- [19] **Falk, R. H., 2010.** Wood as Sustainable Building Material. In: U. D. o. Agriculture, Hrsg. *Wood handbook*. Madison, Wisconsin: U.S. Department of Agriculture, pp. 1.1 - 1.6.
- [20] **Food and agriculture organization of the United Nations, 2010.** *Global Forest Resources Assesment 2010*, Rome: FAO.
- [21] **Forestry Comission, 2008.** <http://www.forestry.gov.uk/>. [Online]
Available at:
[http://www.forestry.gov.uk/pdf/PF2011_Tree_Species.pdf/\\$FILE/PF2011_Tree_Species.pdf](http://www.forestry.gov.uk/pdf/PF2011_Tree_Species.pdf/$FILE/PF2011_Tree_Species.pdf)
[Zugriff am 21 April 2015].
- [22] **Foshan Ying plus earnings Wood Co, 2013.** www.yingjiaying.cn/en. [Online]
Available at: <http://www.yingjiaying.cn/en/news/Bamboo-plywood-is-the-fastest-growing-industry-in-the-sheet-metal-plate-12.html>
[Zugriff am 1 May 2015].
- [23] **Gat6o, A. et al., 2014.** Sustainable structures: bamboo standards and building codes. *Engineering Sustainability*, Band 167, pp. 189-196.
- [24] **Ghavami, K. & Marinho, A., 2001.** Determina7c3o das propriedades mecanicas dos bambus das especies: moso, matake, Guadua angustifolia, Guadua tagoara e Dendrocalamus giganteus, para utiliza7c3o na engenharia. *Eng. Agr6c., Jaboticabal*, 23(3), pp. 415-424.
- [25] **Halili, Y., 2008.** *Versuchstechnische Ermittlung von Querdruckkenngr6o8en von Brettsperrholz*. Graz: TU Graz.
- [26] **Hollee, B. H., 2013.** Laminated Bamboo Structures for a Changing World. *Subtropical Cities 2013, Braving A New World: Design Interventions for Changing Climates: Paper Proceedings*, Fall, ACSA Fall Meeting(-), pp. 195-202.
- [27] **Holzmann, G., Wangelin, M. & Bruns, R., 2012.** *Nat6crlliche und pflanzliche Baustoffe*. 2. Hrsg. Wiesbaden: Springer Vieweg.
- [28] **ISO, 2004a.** *ISO 22156 Bamboo --Structural design*. Geneva: s.n.
- [29] **ISO, 2004b.** • *ISO 22157-1 Bamboo -- Determination of physical and mechanical properties -- Part 1: Requirements*. Geneva: s.n.
- [30] **ISO, 2004c.** • *ISO 22157-2 Bamboo -- Determination of physical and mechanical properties -- Part 2: Laboratory manual*. Geneva: s.n.
- [31] **Kollmann, F., 1951.** *Technologie des holzes und der Holzwerkstoffe*. 2. Hrsg. Berlin: Springer Verlag.
- [32] **Lambo Inc., 2015.** [lambo.us](http://www.lambo.us). [Online]
Available at: <http://www.lambo.us/#!sources-of-bamboo-processes/c24vr>
[Zugriff am 7 May 2015].

- [33] **Lee, A. W., Bai, X. & Bangi, A. P., 1998.** Selectet Properties of Laboratory-Made Laminated-Bamboo Lumber. *Holzforschung*, Band 52, pp. 207-210.
- [34] **Lee, A., Xuesong, B. & Peralta, P., 1994.** Selected physical and mechanical properties of giant timber bamboo grown in South Carolina. *Forest Products Journal*, Issue 44, pp. 40-46.
- [35] **Liese, W., 1985.** Anatomy and Properties of Bamboo. *INBAR*, pp. 196-208.
- [36] **Liese, W., 1992.** The structure of bamboo in relation to its properties and utilization. *International symposium on industrial use of bamboo*.
- [37] **Liese, W., 2003.** Structures of a Bamboo Culm Affecting its Utilization. *International Workshop on Bamboo Industrial Utilization* , pp. 1.1-1.7.
- [38] **Liese, W. & Weiner, G., 1995.** Ageing of Bamboo culms: a Review. *Bamboo, People and the environment*, Band 1, pp. 132-148.
- [39] **Li, X., 2004.** *Physical, chemical and mechanical properties of Bamboo and ist utilization potential for fibreboard manufaturing*, Louisiana: s.n.
- [40] **Mahdavi, M., Clouston, P. & Arwade, S. R., 2012.** A low-technology approach toward fabrication of Laminated Bamboo Lumer. *Construction and Building Materials*, Band 29, pp. 257-262.
- [41] **Nogata, F. & Takahashi, H., 1995.** Intelligent functionally graded material: Bamboo. *Composites Engineering*, Issue Vol. 5, pp. 743-751.
- [42] **Nugroho, N. & Ando, N., 2001.** Development of structural composite products made from bamboo II: fundamental properties of laminated bamboo lumber. *Journal of Wood Science*, Issue 47, pp. 237-242.
- [43] **Obataya, E., Kitin, P. & Yamauchi, H., 2007.** Bending characterisitics of bamboo (*Phyllostachys pubescens*) with respect to its fibre-foam composite structure. *Wood Sci Technol*, Issue 41, pp. 385-400.
- [44] **Puettmann, M. & Wilson, J., 2006.** Gate-to-gate life cycle inventory of glued-laminated timbers production. *Wood and Fibre Science*, 37(CORRIM Special Issue), pp. 99-113.
- [45] **Ramage, M. et al., 2014.** structural bamboo products: a novel engineering material. *WCTE*.
- [46] **Ruli, A., 2004.** *Längs und quer zur Faserrichtung auf Druck beanspruchtes Brettschichtholz*. Graz: TU Graz.
- [47] **Schickhofer, G., 2006.** *Holzbau - Der Roh- und Werkstoff Holz*. 1.2 Hrsg. Graz: Institut für Holzbau und Holztechnologie.
- [48] **Schickhofer, G., 2009.** *Holzbau - Nachweisführung für Konstruktionen aus Holz*. 1.3.1 Hrsg. Graz: Institut für Holzbau und Holztechnologie.
- [49] **Schröder, S., 2014.** *www.guaduabamboo.com*. [Online] Available at: <http://www.guaduabamboo.com/uses/corrugated-bamboo-roofing-sheets> [Zugriff am 1 May 2015].
- [50] **Sharma, B. et al., 2014.** Engineered bamboo: state of the art. *Proceedings of the ICE - Construction Materials*, Issue 167 - Issue 5, pp. 189-196.

- [51] **Sharma, B., Gatóo, A., Bock, M. & Ramage, M., 2015.** Engineered bamboo for structural applications. *Construction and building materials*, Band 81, pp. 66-73.
- [52] **Sharma, B., Gatóo, A. & Ramage, M., 2015.** Effect of processing methods on the mechanical properties of engineered bamboo. *Construction and building materials*, Band 83, pp. 95-101.
- [53] **Shipsha, A. & Berglund, A. L., 2007.** Shear coupling effects on stress and strain distributions in wood subjected to transverse compression. *Composites Science and Technology*, Band 67, pp. 1362-1369.
- [54] **Shrestha, R. & Crews, K., 2014.** Development of engineered bamboo. *WCTE*.
- [55] SIA, 1981. *Einführung in die Norm SIA 164*. Zurich: s.n.
- [56] **Stuefer, A., 2011.** *Einflussparameter auf die Querkzugfestigkeit von BSH-Lamellen*. Graz: TU Graz.
- [57] **Suhaily, S., Khalil, A., Nadirah, W. & Jawaid, M., 2013.** Bamboo Based Biocomposites Material, Design and Applications. *Materials Science - Advanced Topics*, pp. 491-517.
- [58] **van der Lugt, P., 2008.** *Design Interventions for Stimulating Bamboo Commercialization: Dutch Design meets Bamboo as a Replicable Model*. Delft: s.n.
- [59] **Xiao, Y. & Yang, R., 2012.** Discussion of "Development of Laminated Bamboo Lumber: REview of Processing, Performance and Economical Considerations" by M.Mahdavi, P.L. Clouston and S.R. Arwade. *Journal of materials in civil engineering*, Band 24, pp. 1429-1430.
- [60] **Xiao, Y., Yang, R. & Shan, B., 2013.** Production, environmental impact and mechanical properties of glubam. *Construction and Building Materials*, Band 44, pp. 765-773.
- [61] **Xiao, Y., Zhou, Q. & Shan, B., 2010.** Design and Construction of Modern Bamboo Bridges. *Journal of bridge engineering*, Band 15, pp. 533-541.
- [62] **Yu, Y. et al., 2015.** Fabrication, material properties, and application of bamboo scrimber. *Wood Science and Technology*, Band 49, pp. 83-98.
- [63] **Zhang, Y. M., Yu, Y. L. & Yu, W. J., 2013.** Effect of thermal treatment on the physical and mechanical properties of phyllostachys pubescen bamboo. *European Journal of Wood and Wood Products*, Band 71, pp. 61-67.
- [64] **Zhou, A. & Bian, Y., 2014.** Experimental Study on the Flexural Performance of Parallel Strand Bamboo Beams. *The Scientific World Journal*, p. 6.

A-2 List of Figures

Figure 1: Macroscopic geometry of Moso bamboo (Amada, et al., 1995).....	2
Figure 2: Cross section of a bamboo culm; fibre distribution in the culm wall; vascular bundle [left and middle image adopted from (Sharma, et al., 2014), right image adopted from (Schröder, 2014)].....	2
Figure 3: Micrographs; (above) over entire culm wall thickness; (below): a) of inner b) of outer vascular bundles.....	3

Figure 4: Annual growth rings in softwood	3
Figure 5: Density of internodes 5, 11 and 14 vs. radial position.....	4
Figure 6:(left) Volume fraction of vascular bundles (V_{vb}) and (right) solid fraction (S_r) plotted against normalized radial position (Dixon & Gibson, 2014)	4
Figure 7: (left) Typical compressive stress-strain curves; (right) compressive strength vs. density (Dixon & Gibson, 2014)	7
Figure 8: (left) Photomicrographs of the specimen compressed in radial direction; (right) accompanying stress-strain curve (Dixon & Gibson, 2014).....	7
Figure 9: (left) Experimental setup; (middle) M plotted vs. I/r ; (right) types of failure (Obataya, et al., 2007)	8
Figure 10: axial compression stress-strain diagram (Obataya, et al., 2007)	9
Figure 11: Distribution of woody bamboo (Lambooc Inc., 2015).....	10
Figure 12: (left) bamboo rhizomes (Sharma, et al., 2014); (right) longitudinal section of a young bamboo shoot (Bamboo Garden, 2006).....	11
Figure 13: Production process	13
Figure 14: Cross section of bamboo scrimber: (left) natural (right) carbonized (Yu, et al., 2015).....	15
Figure 15: Techniques to receive base-material for LBL (Sharma, et al., 2014).....	16
Figure 16: (left) Bamboo mat board (Foshan Ying plus earnings Wood Co, 2013); (right) roof sheet made from bamboo mats (Schröder , 2014)	17
Figure 17: (left) Geometry of the Joint; (right) orientation of lamellae	20
Figure 18: Beams with joints highlighted.....	20
Figure 19: Test setup for bending according to ÖNORM EN 408	23
Figure 20: Test setup for compression tests perpendicular to the grain according to ÖNORM EN 408	24
Figure 21: Load plotted against deformation to determine $F_{c,90,max}$ according to ÖNORM EN 408 (CEN, 2010)	25
Figure 22: Manufacturing process of the samples for the T90-tests	26
Figure 23: Test setup for tension tests perpendicular to the grain	27
Figure 24: Test setup for tension test parallel to the grain according to EN 408.....	28
Figure 25: Specimen with mounted rods as base line for measuring the local deformation ..	29
Figure 26: Displacement sensors WA 10	29
Figure 27: Typical failure mode due to bending (left) B-A1 (FW); (right): B-A2 (EW).....	32
Figure 28: Typical failure mode due to tension perpendicular to the grain (left) T90-G1 (EW); (right) T90-G2 (FW).....	36
Figure 29: Typical failure pattern due to tension parallel to the grain.....	38
Figure 30: Typical failure pattern due to tension; detail of torn out fibres.....	39
Figure 31: Uniaxial stress-strain relationships (Dongsheng, et al., 2013).....	40

Figure 32: Stress and strain curve over the cross section due to bending.....	41
Figure 33: Definition of the directions perpendicular to the grain in wood: axial, radial and tangential (Schickhofer, 2006)	42
Figure 34: (left) E_m plotted vs. density; (right) range of single values, mean value & standard deviation.....	43
Figure 35: (left) f_m plotted vs. density; (right) range of single values, mean value & standard deviation.....	44
Figure 36: Bending strength plotted against modulus of elasticity	45
Figure 37: CDFs for the mechanical properties in bending	46
Figure 38: (left) $E_{c,90}$ plotted vs. density; (right) range of single values, mean value & standard deviation.....	47
Figure 39: (left) $f_{c,90}$ plotted vs. density; (right) range of single values, mean value & standard deviation.....	47
Figure 40: Tangential and radial orientation of the specimens.....	48
Figure 41: Dependence between compressive strength and orientation of the growth rings in Norway spruce (SIA, 1981).....	49
Figure 42: f_{c90} plotted vs. E_{c90}	50
Figure 43: (left) E_{t90} plotted vs. density; (right) range of single values, mean value & standard deviation.....	51
Figure 44: $f_{t,90}$ plotted vs. density; (right) range of single values, mean value & standard deviation.....	52
Figure 45: f_{t90} plotted vs. E_{t90}	52
Figure 46: (left) $E_{t,0}$ plotted vs. density; (right) range of single values, mean value & standard deviation.....	55
Figure 47: (left) $f_{t,0}$ plotted vs. density; (right) range of single values, mean value & standard deviation.....	55
Figure 48: $f_{t,0}$ plotted vs. $E_{t,0}$	56
Figure 49: Joint in the bamboo lamella and internal forces due to tension	56
Figure 50: Build-up of the beams and bending stiffness	60
Figure 51: Stresses of beams I and II at various load stages	60

A-3 List of Tables

Table 1: Characteristics of sclerenchyma fibres and parenchyma ground tissue	9
Table 2: Mechanical properties of structural bamboo (Sharma, et al., 2015).....	14
Table 3: Mechanical properties of strand woven bamboo.....	15
Table 4: Mechanical properties (Lee, et al., 1998).....	16
Table 5: Material costs and estimated yield per cubic meter of semi-finished material	19

Table 6: Investigation of joint-distribution	21
Table 7: Sample B-A1, B-A2 – bending	22
Table 8: Parameters of the test configuration for sample B-A1 and B-A2.....	22
Table 9: Sample C90 – compression perpendicular to the grain	24
Table 10: Parameters of the test configuration for sample C90-H1 and C90-H2.....	24
Table 11: Sample T90 – tension perpendicular to the grain.....	26
Table 12: Parameters of the test configuration for sample T90-G1 and T90-G2	26
Table 13: Samples T-C and PT-T0 – tension parallel to the grain	28
Table 14: Parameters of the test configuration for samples T-C and PT-T0.....	28
Table 15: Bending properties, moisture content and density of sample B-A1 (FW).....	30
Table 16: Bending properties, moisture content and density of sample B-A2 (EW)	31
Table 17: C90 properties, moisture content and density of sample C90-H1 (EW).....	33
Table 18: C90 properties, moisture content and density of sample C90-H2 (FW).....	34
Table 19: T90 properties, moisture content and density of sample T90-G1	35
Table 20: T90 properties, moisture content and density of sample T90-G2	35
Table 21: Tension properties, moisture content and density of sample T-C	37
Table 22: Tension properties, moisture content and density of sample PT-T0	37
Table 23: Results (Dongsheng, et al., 2013).....	41
Table 24: Elastic constants of Norway spruce and Oregon Pine (Dinwoodie, 2000).....	42
Table 25: Gradient & relative increase of mechanical properties per 100 kg/m ³ density	44
Table 26: Common evaluation of test results (A1/FW+A2/EW) of the sample B – bending...	46
Table 27: Common evaluation of test results (H1/EW+H2/FW) of the sample C90.....	50
Table 28: Common evaluation of test results (G1/EW+G2/FW) of the sample T90.....	53
Table 29: Comparison of mechanical properties between LBL and timber (C24).....	58
Table 30: Mechanical properties of LBL, timber, steel and concrete adopted from Schickhofer (2006).....	58

Appendix B: Tables with detailed test results

B-1 Sample B-A1 (FW)

sample	B-A1 (FW)			
name of test specimen	load max	bending stress	local MoE	shear stress
	F_{\max} [kN]	σ_m [N/mm ²]	$E_{0, \text{lokal}}$ [N/mm ²]	$\tau_{v, 0,90}$ [N/mm ²]
B-A1-01	45,2	53,4	8436	2,69
B-A1-02	49,7	58,5	8461	2,95
B-A1-03	48,0	56,4	8400	2,85
B-A1-04	43,9	51,2	8455	2,59
B-A1-05	44,9	52,4	8879	2,66
B-A1-06	46,5	54,8	8349	2,76
B-A1-07	47,9	55,8	8221	2,84
B-A1-08	43,8	51,6	8764	2,60
B-A1-09	50,5	59,1	8641	2,99
B-A1-10	49,9	58,0	8318	2,95
B-A1-11	41,4	48,5	8192	2,45
B-A1-12	47,9	56,0	8737	2,83
B-A1-13	47,6	55,6	8834	2,82
B-A1-14	54,0	63,1	8857	3,20
B-A1-15	50,8	58,6	8911	3,00
B-A1-16	48,2	57,5	8948	2,87
B-A1-17	47,5	55,7	9217	2,81
B-A1-18	50,0	58,8	8254	2,96
B-A1-19	52,4	61,5	8646	3,10
B-A1-20	53,8	62,7	9026	3,18
B-A1-21	53,1	62,5	8592	3,15
B-A1-22	45,2	52,6	8316	2,67

number of test specimens	22	22	22	22
min	41,4	48,5	8192	2,45
max	54,0	63,1	9217	3,20
mean value	48,3	56,6	8612	2,86
standard deviation	3,4	4,0	292	0,20
COV	7,0%	7,0%	3,4%	7,1%
factor k_s		1,915		
characteristic value of bending strength according to ÖNORM 14358		49,3		

B-2 Sample B-A2 (EW)

sample	B-A2 (EW)			
name of test specimen	load max	bending stress	local MoE	shear stress
	F_{\max} [kN]	σ_m [N/mm ²]	$E_{0, \text{lokal}}$ [N/mm ²]	$\tau_{v, 0, 90}$ [N/mm ²]
B-A2-01	56,9	64,6	9782	3,33
B-A2-02	49,7	57,6	8892	2,93
B-A2-03	56,1	64,2	8812	3,29
B-A2-04	53,9	61,6	9308	3,16
B-A2-05	54,2	62,6	8916	3,19
B-A2-06	57,9	66,2	9260	3,40
B-A2-07	51,8	60,2	8637	3,06
B-A2-08	50,9	58,9	8864	3,00
B-A2-09	54,8	62,6	9667	3,21
B-A2-10	50,7	58,7	9016	2,99
B-A2-11	56,5	64,6	9369	3,31
B-A2-12	56,3	63,9	9719	3,29
B-A2-13	52,3	60,9	8221	3,09
B-A2-14	48,2	55,5	8405	2,83
B-A2-15	53,7	61,1	9267	3,14
B-A2-16	56,0	63,4	9445	3,27
B-A2-17	58,9	66,9	9197	3,44
B-A2-18	53,8	61,4	9530	3,15
B-A2-19	54,3	61,5	9266	3,18
B-A2-20	50,5	58,3	8426	2,97
B-A2-21	53,2	61,4	8492	3,13
B-A2-22	53,6	61,2	9554	3,14
number of test specimens	22	22	22	22
min	48,2	55,5	8221	2,83
max	58,9	66,9	9782	3,44
mean value	53,8	61,7	9093	3,16
standard deviation	2,8	2,8	458	0,16
COV	5,1%	4,6%	5,0%	4,9%
factor k_s		1,915		
characteristic value of bending strength according to ÖNORM 14358		56,4		

B-3 Sample C90-H1 (EW)

sample	C90-H1 (EW)		
	load max	compression stress perp. to grain	local MoE
	F_{\max} [N]	$\sigma_{c,90}$ [N/mm ²]	$E_{c,90}$ [N/mm ²]
C90-H1-01*	-	-	-
C90-H1-02	37760	11,9	1262
C90-H1-03	30452	9,5	1090
C90-H1-04	42016	13,1	1357
C90-H1-05	37420	11,7	1167
C90-H1-06	35797	11,2	1228
C90-H1-07	39315	12,3	1253
C90-H1-08	37902	11,8	1295
C90-H1-09	44737	14,0	1535
C90-H1-10	38930	12,2	1281
C90-H1-11	35898	11,2	1064
C90-H1-12	39705	12,5	1286
C90-H1-13	35739	11,2	1123
C90-H1-14	42097	13,1	1384
C90-H1-15	49512	15,5	1101
C90-H1-16	37137	11,7	1255
C90-H1-17	35583	11,1	1022
C90-H1-18	37743	11,8	1194
C90-H1-19	33763	10,6	1117
C90-H1-20	38259	12,0	1145
C90-H1-21	41170	12,9	1248
C90-H1-22	38945	12,2	1201

number of test specimens	20	21	20
min	33763	9,5	1022
max	49512	15,5	1535
mean value	38971	12,1	1219
standard deviation	3612	1,2	120
COV	9,3%	10,3%	9,8%
Faktor ks		1,923	
characteristic value of compression strength perpendicular to the grain according to ÖNORM 14358		9,9	
* C90-H1-01: failure in the test setup			

B-4 Sample C90-H2 (FW)

sample	C90-H2 (FW)		
name of test specimen	load max	compression stress perp. to grain	local MoE
	F_{\max} [N]	$\sigma_{c,90}$ [N/mm ²]	$E_{c,90}$ [N/mm ²]
C90-H2-01	31875	9,7	1186
C90-H2-02	36357	11,2	1401
C90-H2-03*	-	-	-
C90-H2-04	35703	11,0	1370
C90-H2-05	31092	9,7	1179
C90-H2-06	34885	10,7	1374
C90-H2-07	38896	12,0	1475
C90-H2-08	35100	10,8	1355
C90-H2-09	30883	9,6	1263
C90-H2-10	31752	9,8	1219
C90-H2-11	30823	9,5	1252
C90-H2-12	33338	10,4	1190
C90-H2-13	33602	10,4	1167
C90-H2-14	35313	11,0	1313
C90-H2-15	37316	11,5	1413
C90-H2-16	30896	9,6	1291
C90-H2-17	31552	9,8	1279
C90-H2-18	32708	10,1	1243
C90-H2-19	35847	11,1	1419
C90-H2-20	32365	10,1	1318
C90-H2-21	34783	10,8	1293
C90-H2-22	32822	10,3	1201

number of test specimens	21	21	21
min	30823	9,5	1167
max	38896	12,0	1475
mean value	33710	10,4	1295
standard deviation	2337	0,7	90
COV	6,9%	6,9%	7,0%
Faktor ks		1,923	
characteristic value of compression strength perpendicular to the grain according to ÖNORM 14358		9,1	
*no measurement of the local deformation during the test; specimen is not considered in the calculation			

B-5 Sample T90-G1 (EW)

sample	T90-G1 (EW)		
	load max	tension stress perpend. to grain	local MoE
	F_{\max} [N]	$\sigma_{t,90}$ [N/mm ²]	$E_{t,90}$ [N/mm ²]
T90-G1-01*	-	-	-
T90-G1-02	11244	3,6	1167
T90-G1-03	12925	4,2	1408
T90-G1-04	9489	3,0	1254
T90-G1-05*	-	-	-
T90-G1-06	11603	3,7	1284
T90-G1-07	6623	2,1	1110
T90-G1-08	15407	4,9	1277
T90-G1-09	14749	4,7	1220
T90-G1-10	14841	4,8	1361
T90-G1-11	7176	2,3	1133
T90-G1-12	7393	2,4	1345
T90-G1-13	13066	4,2	1429
T90-G1-14	14096	4,5	1198
T90-G1-15	15375	4,9	1335
T90-G1-16	12108	3,9	1266
T90-G1-17	11424	3,7	1322
T90-G1-18	12207	3,9	1268
T90-G1-19	12349	4,0	1375
T90-G1-20	13131	4,2	1248
T90-G1-21	11710	3,7	1208
T90-G1-22	11976	3,8	1370

number of test specimens	20	20	20
min	6623	2,1	1110
max	15407	4,9	1429
mean value	11945	3,8	1279
standard deviation	2588	0,8	89
COV	21,7%	21,6%	7,0%
Faktor ks		1,932	
characteristic value of tension strength perpendicular to the grain according to ÖNORM 14358		2,3	

*Test specimens T90-G1-01 and T90-G1-05 were not tested.

B-6 Sample T90-G2 (FW)

sample	T90-G2 (FW)		
name of test specimen	load max	tension stress perpend. to grain	local MoE
	F_{\max} [N]	$\sigma_{t,90}$ [N/mm ²]	$E_{t,90}$ [N/mm ²]
T90-G2-01	17067	5,4	1350
T90-G2-02	9376	2,9	1583
T90-G2-03	14661	4,5	1539
T90-G2-04	8362	2,6	1467
T90-G2-05	10399	3,3	1466
T90-G2-06	13105	4,1	1578
T90-G2-07*	-	-	-
T90-G2-08	15446	4,8	1433
T90-G2-09	15329	4,8	1388
T90-G2-10	10931	3,5	1200
T90-G2-11	11825	3,7	1327
T90-G2-12	9976	3,1	1464
T90-G2-13	15646	4,9	1461
T90-G2-14	16019	5,0	1463
T90-G2-15	10592	3,3	1455
T90-G2-16	16615	5,2	1525
T90-G2-17*	-	-	-
T90-G2-18	9929	3,1	1466
T90-G2-19	11691	3,7	1402
T90-G2-20	20167	6,2	1552
T90-G2-21	14071	4,4	1371
T90-G2-22	17529	5,5	1372
number of test specimens	20	20	20
min	8362	2,6	1200
max	20167	6,2	1583
mean value	13437	4,2	1443
standard deviation	3263	1,0	93
COV	24,3%	24,2%	6,5%
factor ks		1,932	
characteristic value of tension strength perpendicular to the grain according to ÖNORM 14358		2,5	
* test specimens T90-G2-07 and T90-G2-17 were damaged before testing			

B-7 Sample T-C

sample name of test specimen	T-C		
	load max	tension stress	local MoE
	F_{\max} [kN]	σ_t [N/mm ²]	$E_{t,0}$ [N/mm ²]
T-C-01	94,0	36,3	7836
T-C-02	109,8	42,5	8498
T-C-03	93,8	36,3	8368
T-C-04	92,0	35,2	7755
T-C-05	106,4	41,4	7565
T-C-06	95,4	37,1	7814
T-C-07	125,2	48,3	7926
T-C-08	101,5	39,5	8391
T-C-09	101,6	39,8	8097
T-C-10	108,2	41,7	8581
T-C-11	85,8	33,1	7509
T-C-12	106,7	41,5	7903
T-C-13	109,6	42,4	8509
T-C-14	101,3	39,0	7634
T-C-15	81,1	31,2	8323
T-C-16	124,8	48,2	8073
T-C-17	112,9	43,8	8216
T-C-18	119,0	45,9	8284
T-C-19	102,1	39,3	7695
T-C-20	103,7	40,4	7521
T-C-21	87,2	33,3	8684
T-C-22	93,3	35,9	7379
T-C-23	100,2	38,7	8386
T-C-24	104,6	40,3	7786
T-C-25	84,8	32,8	7532
T-C-26	110,3	42,4	7798
T-C-27	94,7	36,7	7870
T-C-28	95,6	36,6	7981
T-C-29	104,6	40,7	9291
T-C-30	109,8	42,4	8177
T-C-31	96,1	37,3	8137
T-C-32	97,4	37,7	8652
T-C-33	104,9	40,6	7220
T-C-34	111,9	43,4	8223
T-C-35	107,5	41,7	8237
T-C-36	79,7	31,0	7481
T-C-37	98,8	38,3	8836
T-C-38	96,9	37,6	8133
T-C-39	117,7	45,2	7991
T-C-40	100,5	38,9	8476
T-C-41	110,2	42,4	7410
T-C-42	91,6	35,6	7625
T-C-43	80,1	31,0	7218
T-C-44	92,8	36,0	7475

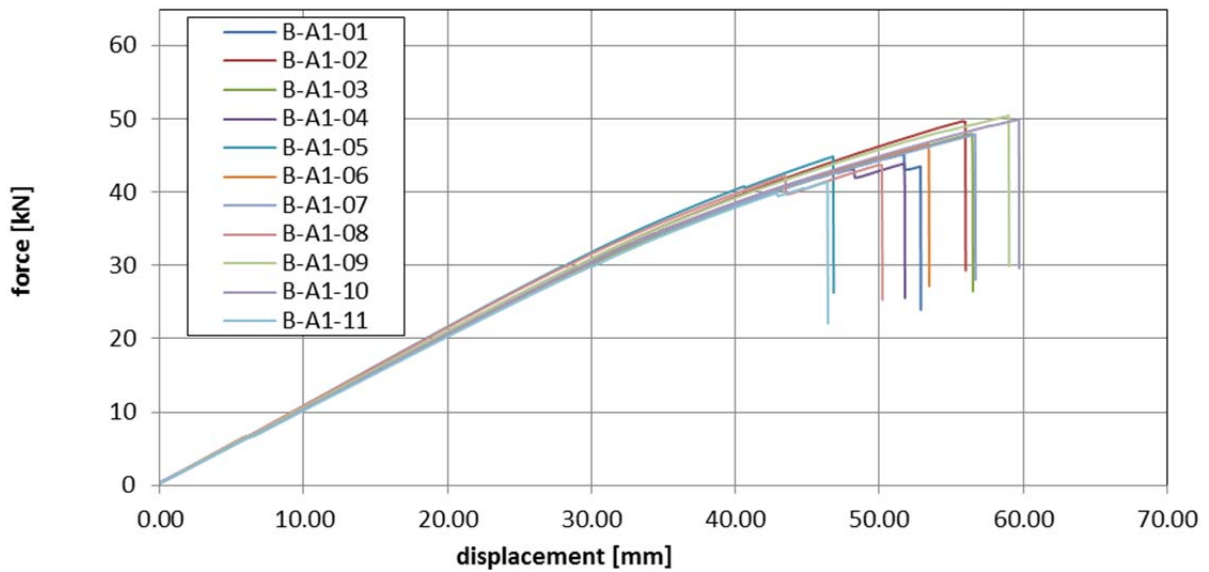
number of test specimens	44	44	44
min	79,7	31,0	7218
max	125,2	48,3	9291
mean value	101,0	39,1	8011
standard deviation	10,9	4,2	462
COV	10,8%	10,8%	5,8%
Faktor k_s		1,824	
characteristic value of tension strength parallel to grain according to ÖNORM 14358		31,8	

Appendix C: Force vs. displacement diagrams

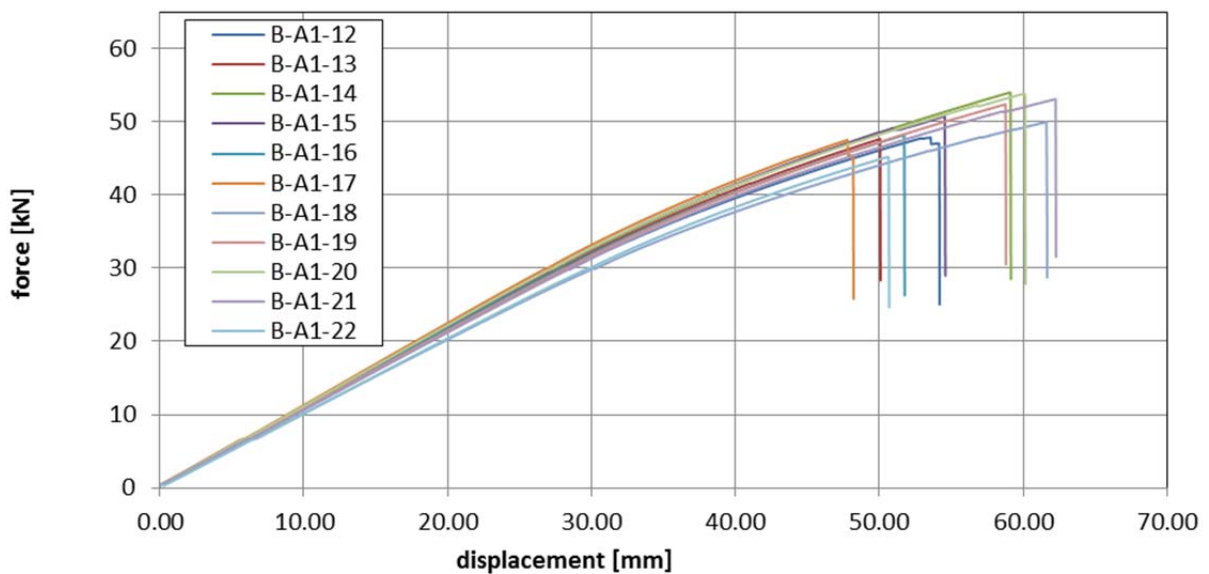
All diagrams show the recorded data from the machines. For the determination of the moduli of elasticity, local measurement systems have been used. However, load-displacement diagrams better illustrate the load bearing behaviour.

C-1 Sample B-A1 (FW)

test samples: B-A1-01 to B-A1-11

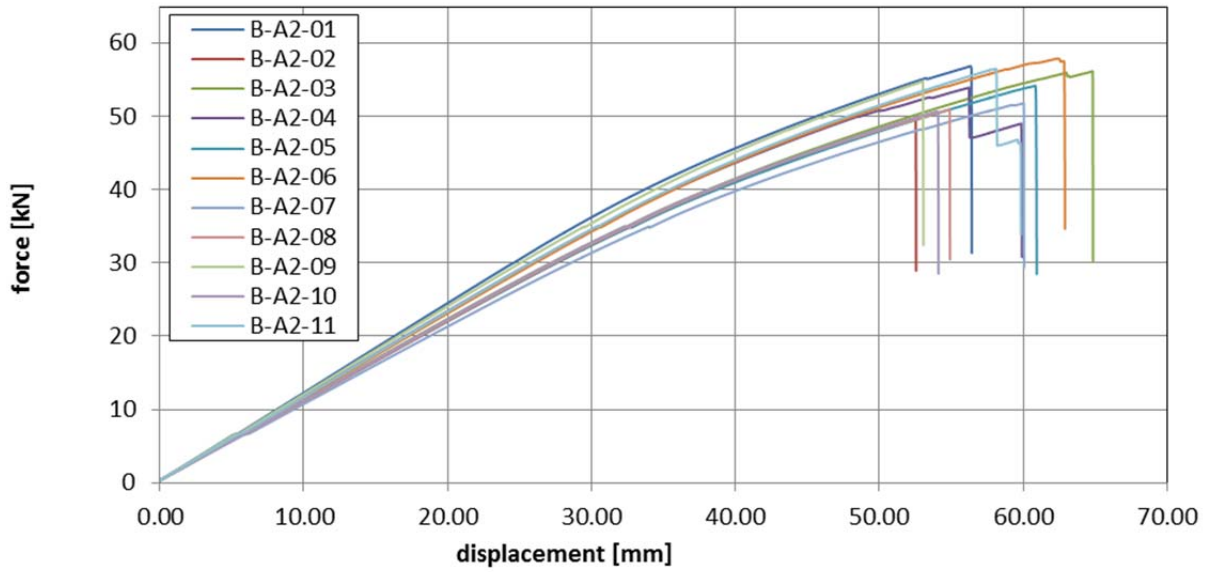


test samples: B-A1-12 to B-A1-22

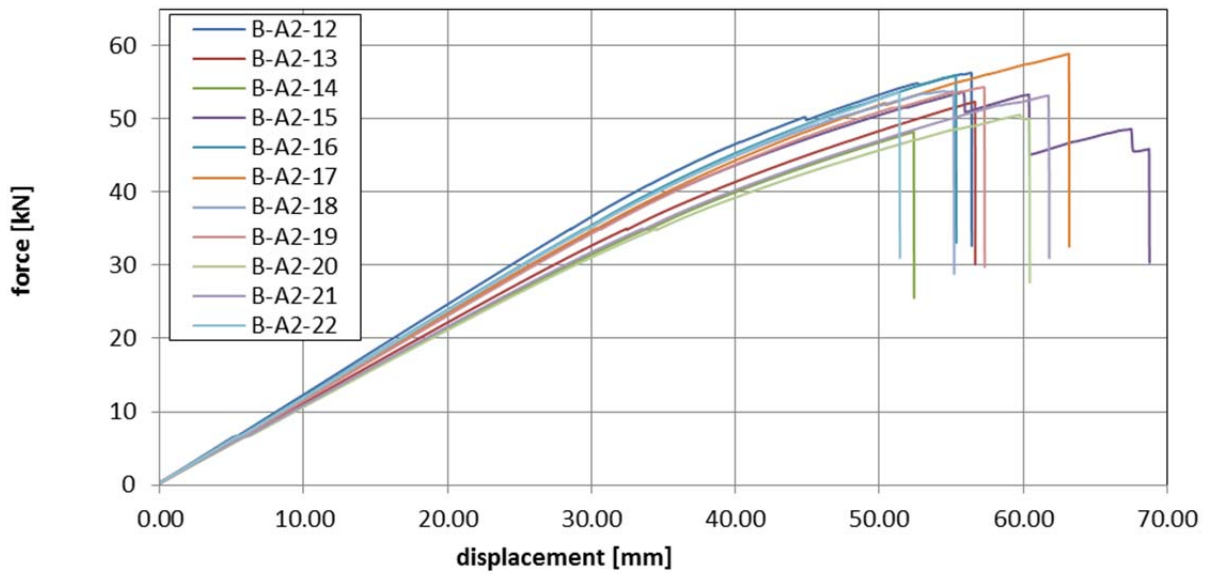


C-2 Sample B-A2 (EW)

specimens: B-A2-01 to B-A2-11

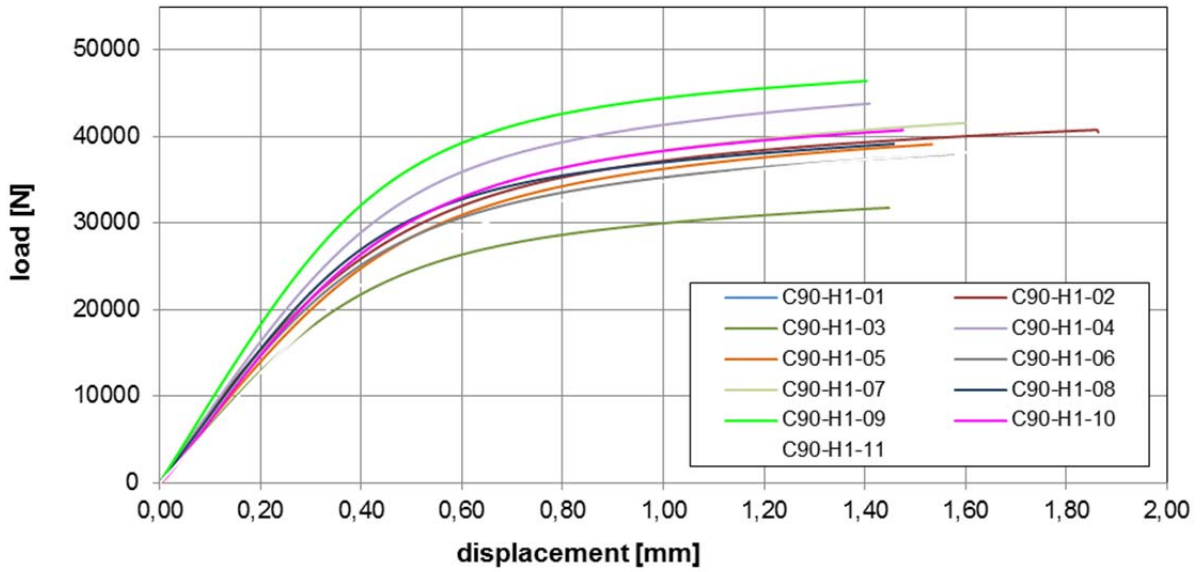


specimens: B-A2-12 to B-A2-22

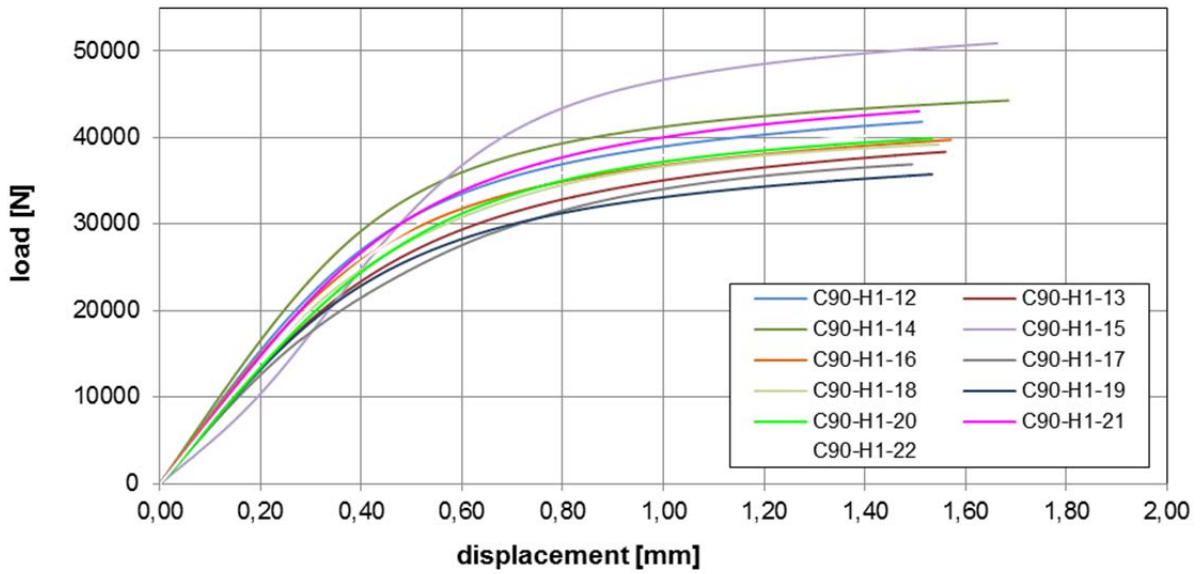


C-3 Sample C90-H1 (EW)

Test sample C90-H1: C90-H1-01 to C90-H1-11

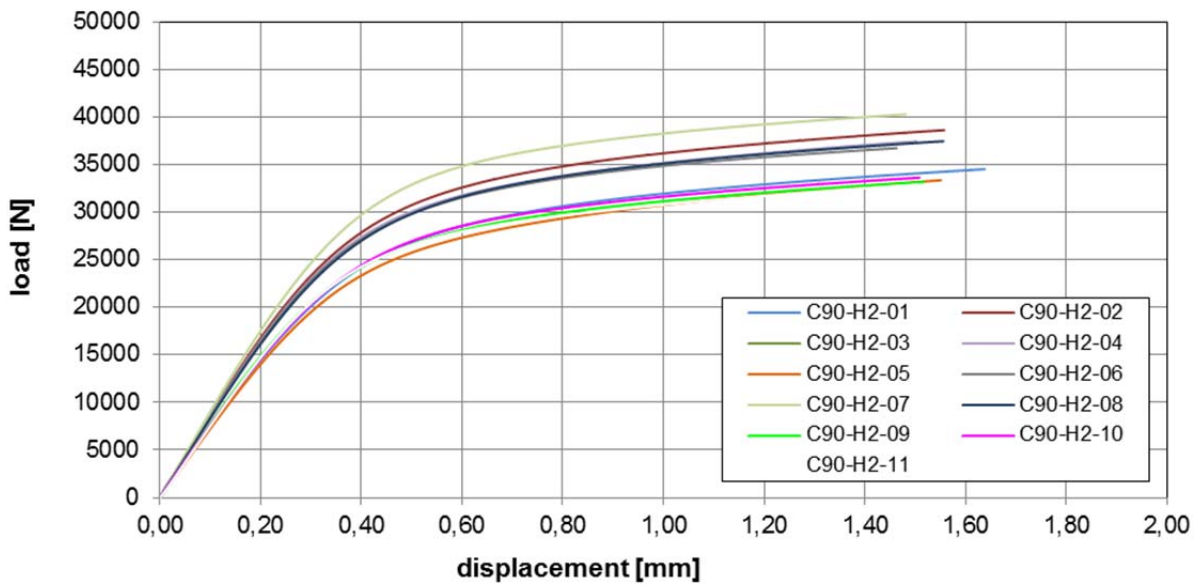


Test sample C90-H1: C90-H1-12 to C90-H1-22

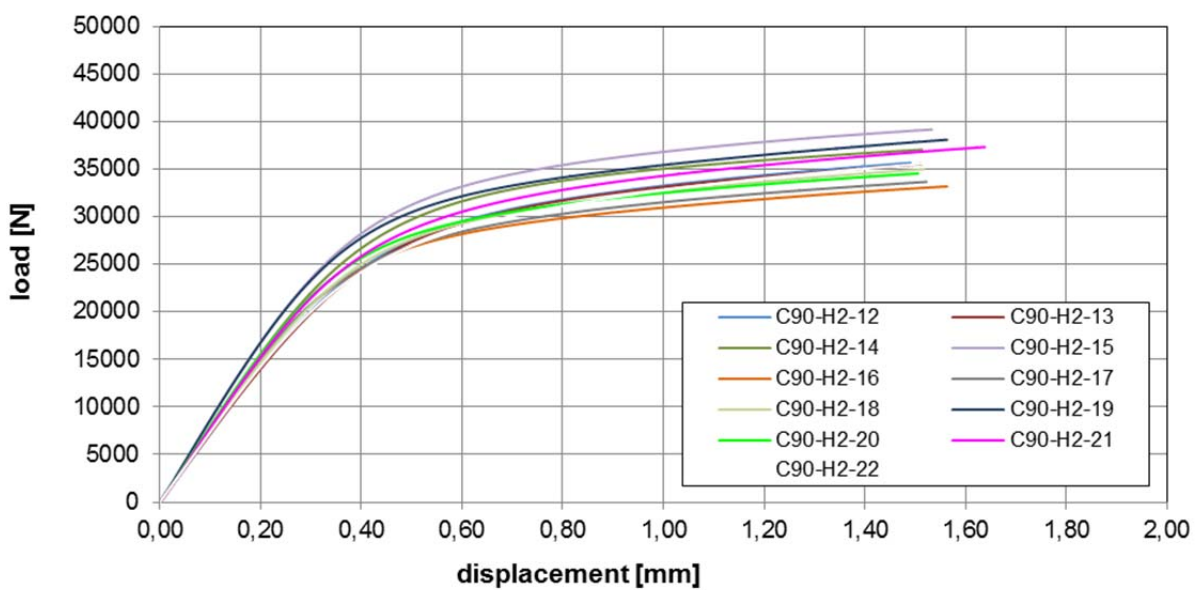


C-4 Sample C90-H2 (FW)

test sample C90-H2: C90-H2-01 to C90-H2-11

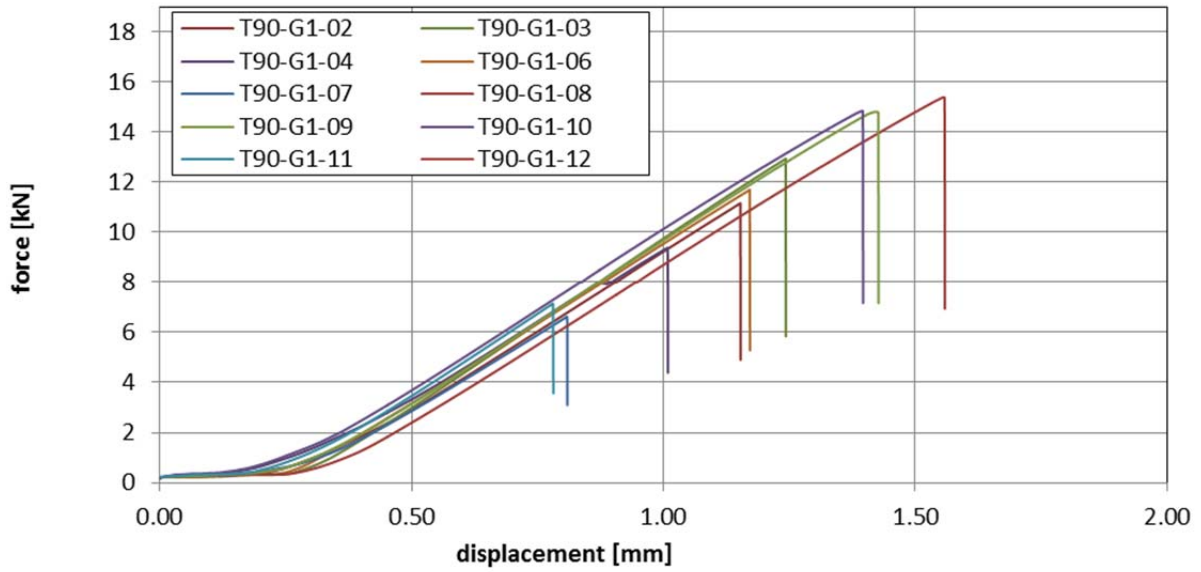


test sample C90-H2: C90-H2-12 to C90-H2-22

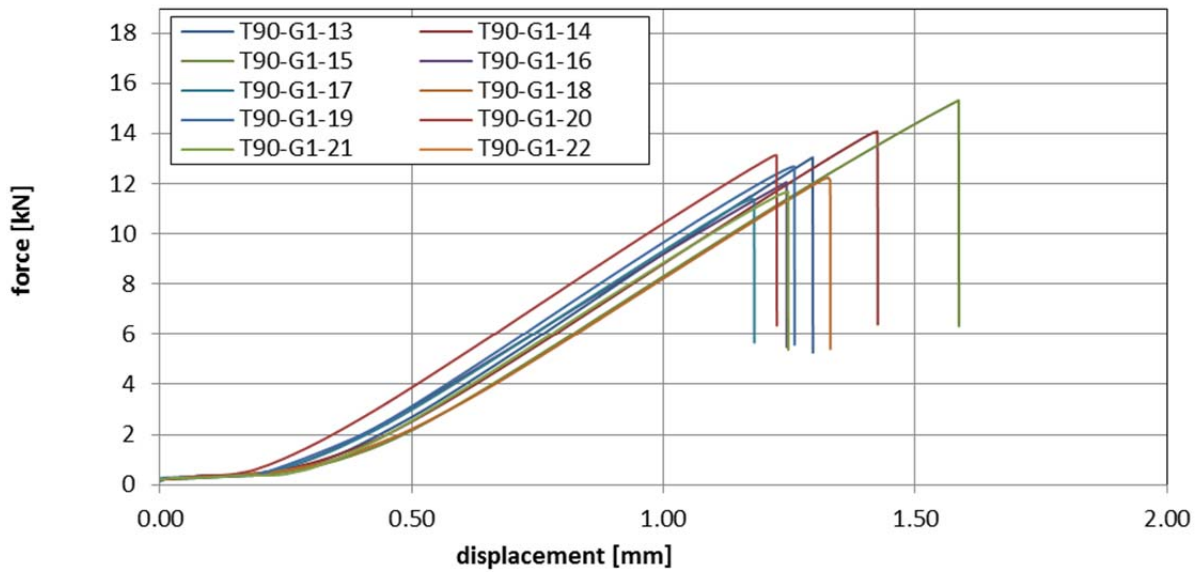


C-5 Sample T90-G1 (EW)

specimens: T90-G1-01 to T90-G1-12

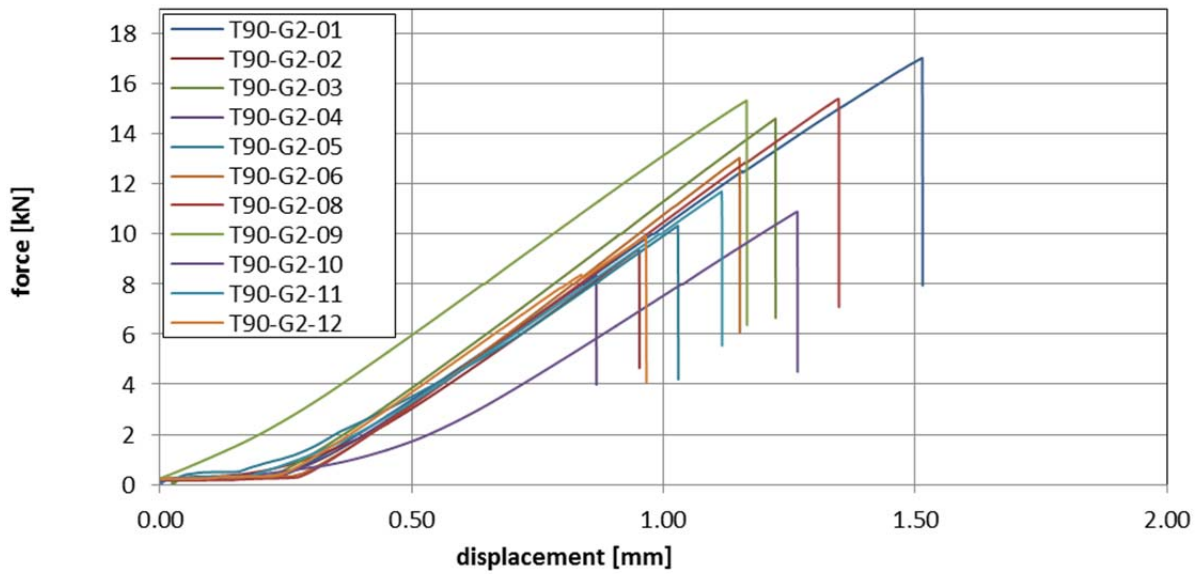


specimens: T90-G1-13 to T90-G1-22

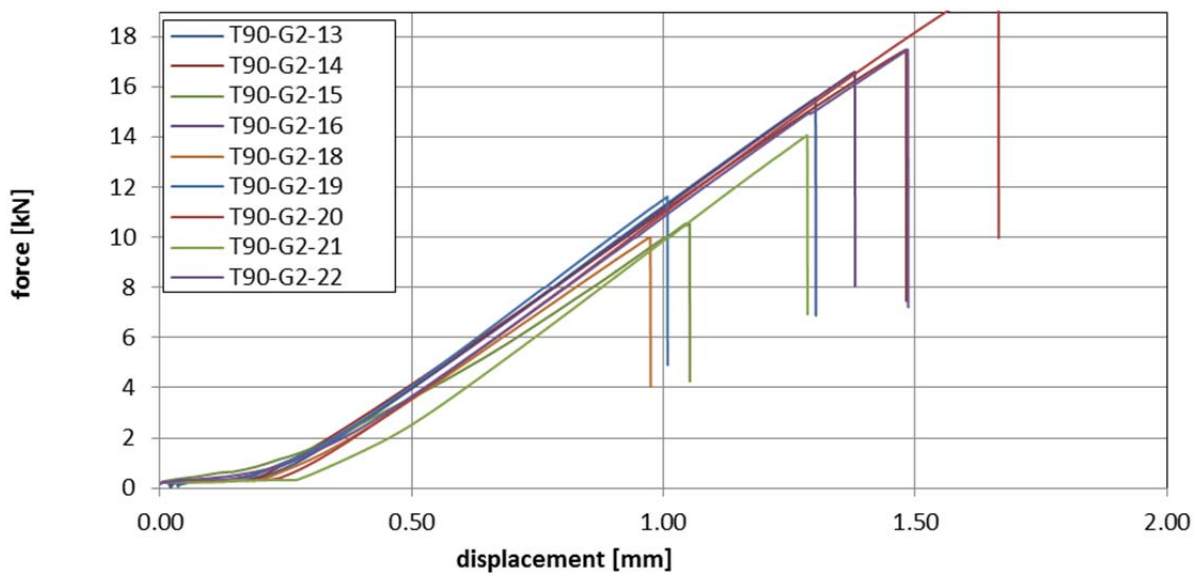


C-6 Sample T90-G2 (FW)

specimens: T90-G2-01 to T90-G2-12



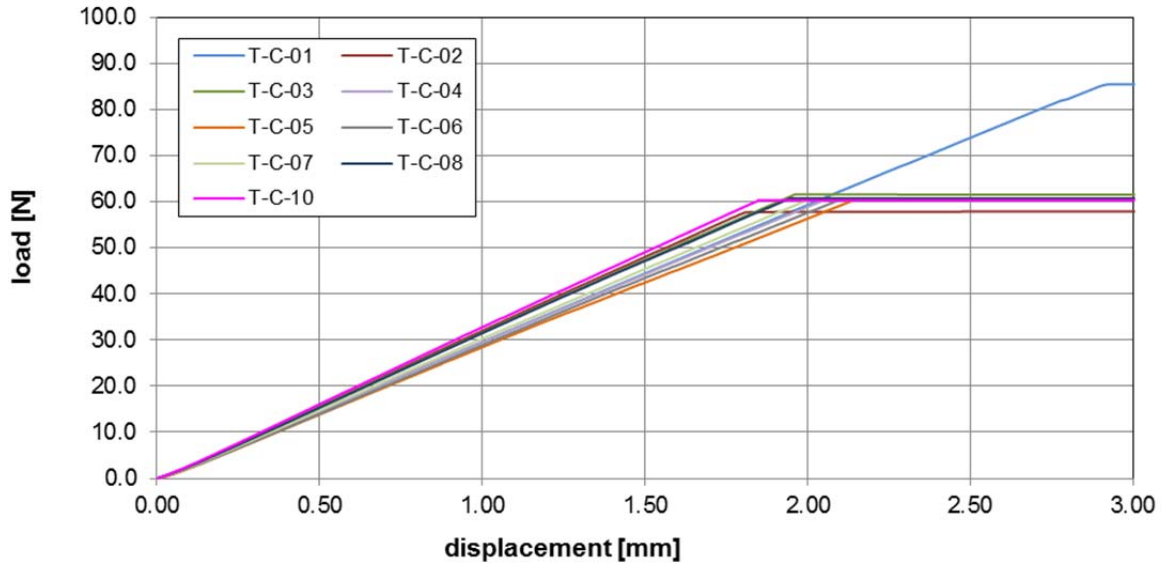
specimens: T90-G2-13 to T90-G2-22



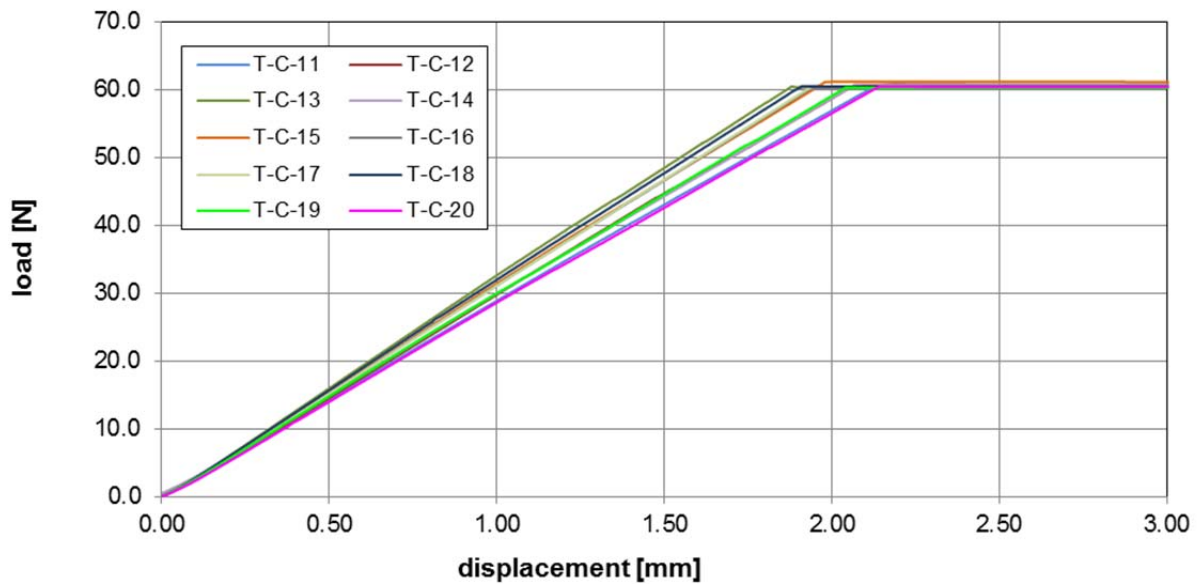
C-7 Sample T-C

As the global displacement was not measured for all test specimens of the samples T-C and PT-T0. For this reason, the following diagrams provide the local displacement measurements.

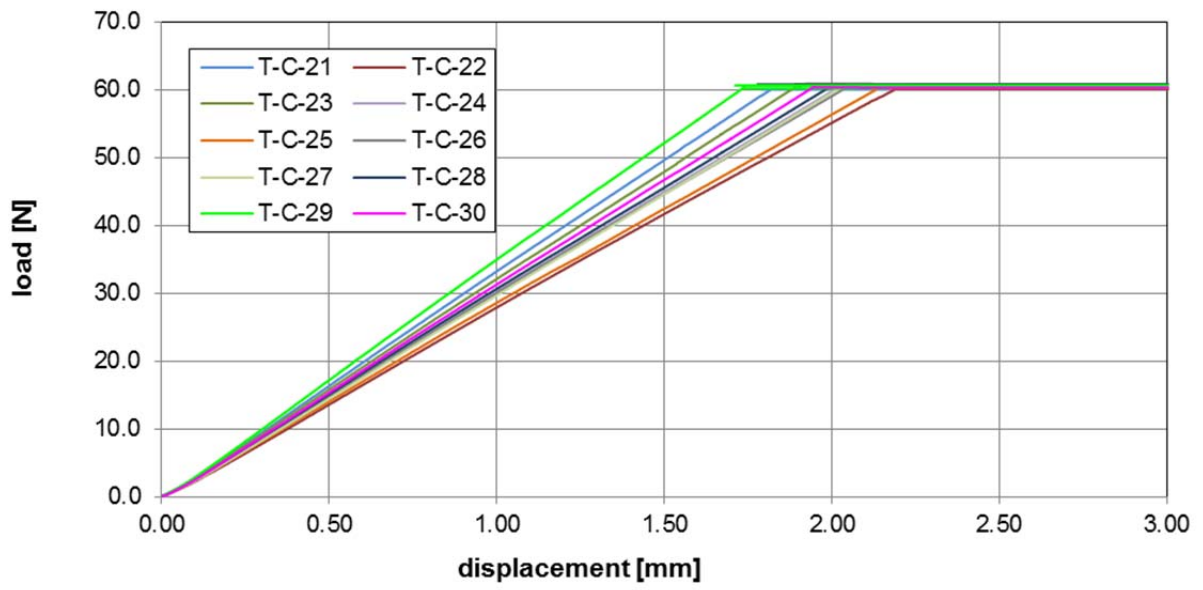
test sample T-C: T-C-01 to T-C-10



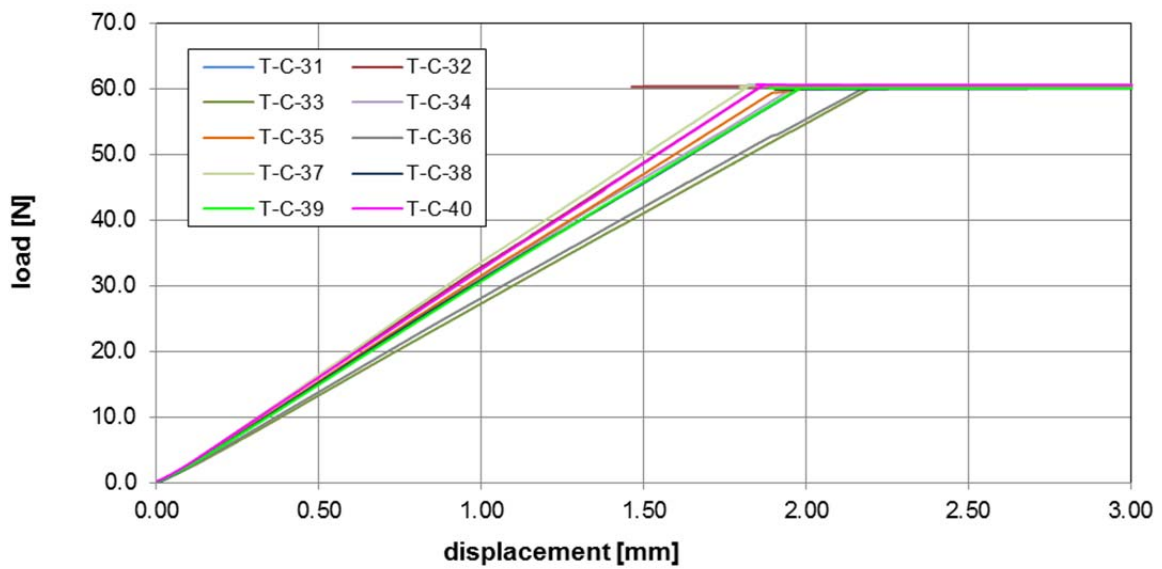
test sample T-C: T-C-11 to T-C-20



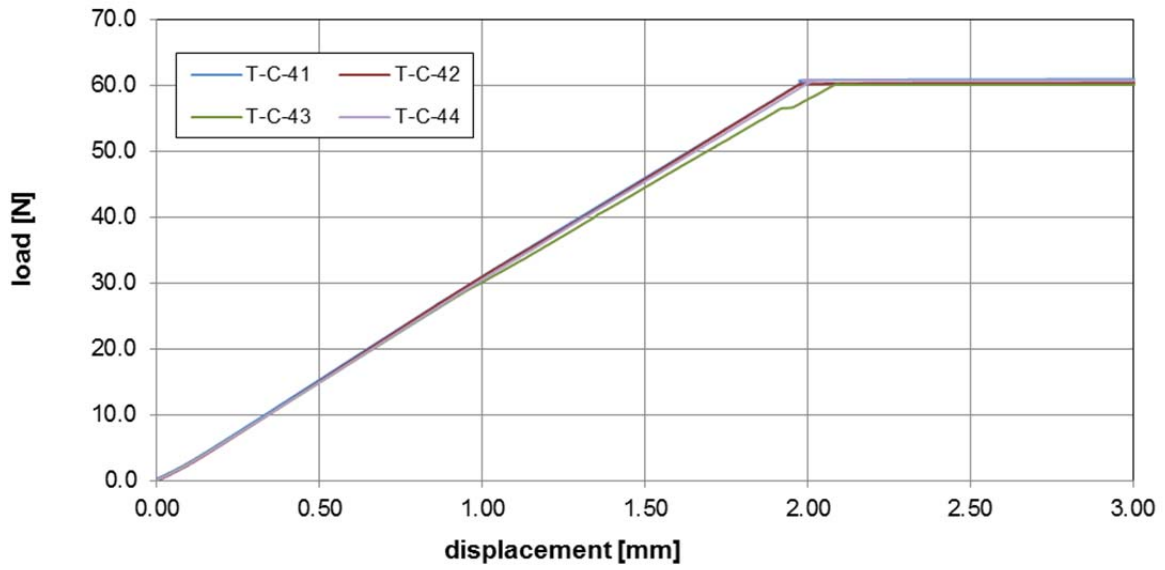
test sample T-C: T-C-21 to T-C-30



test sample T-C: T-C-31 to T-C-40

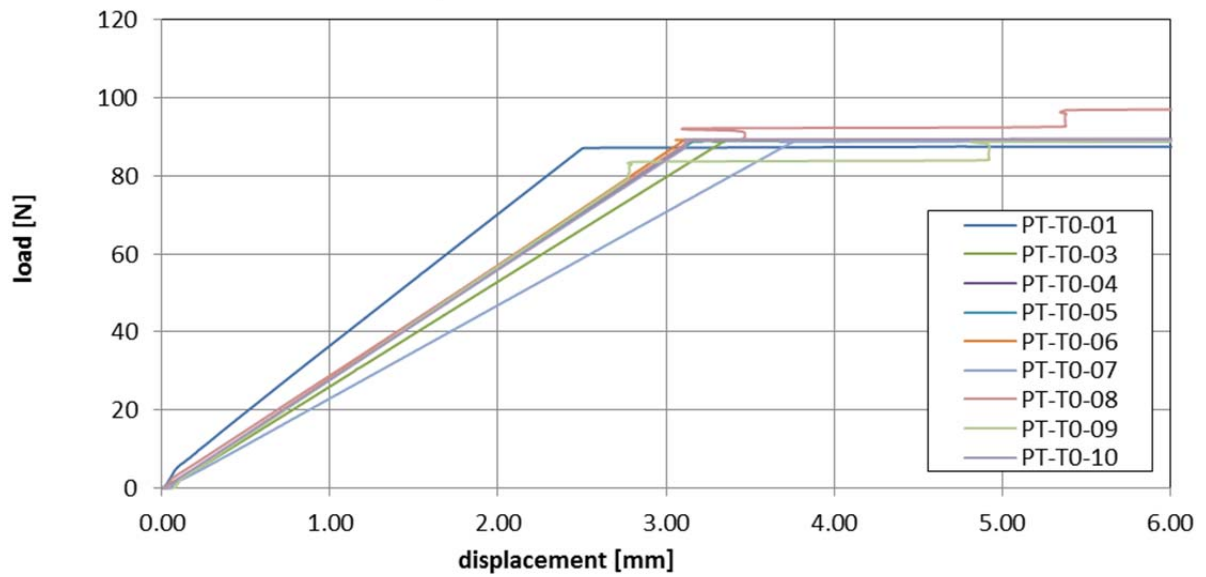


test sample T-C: T-C-41 to T-C-44



C-8 Sample PT-T0

test sample PT-T0: PT-T0-01 bis PT-T0-10



Appendix D: Images of fracture

D-1 Sample B-A1 (FW)

B-A1-01



B-A1-02



B-A1-03



B-A1-04



B-A1-05



B-A1-06



B-A1-07



B-A1-08



B-A1-09



B-A1-10



B-A1-11



B-A1-12



B-A1-13



B-A1-14



B-A1-15



B-A1-16



B-A1-17



B-A1-18



B-A1-19



B-A1-20



B-A1-21



B-A1-22



D-2 Sample B-A2 (EW)

B-A2-01



B-A2-02



B-A2-03



B-A2-04



B-A2-05



B-A2-06



B-A2-07



B-A2-08



B-A2-09



B-A2-10



B-A2-11



B-A2-12



B-A2-13



B-A2-14



B-A2-15



B-A2-16



B-A2-17



B-A2-18



B-A2-19



B-A2-20



B-A2-21



B-A2-22

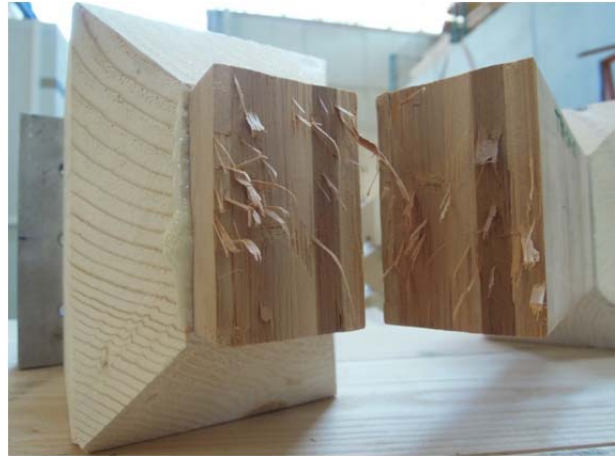


D-3 Sample T90-G1 (EW)

T90-G1-02



T90-G1-02



T90-G1-03



T90-G1-03



T90-G1-04



T90-G1-04



T90-G1-06



T90-G1-06



T90-G1-07



T90-G1-07



T90-G1-08



T90-G1-08



T90-G1-09



T90-G1-09



T90-G1-10



T90-G1-10



T90-G1-11



T90-G1-11



T90-G1-12



T90-G1-12



T90-G1-13



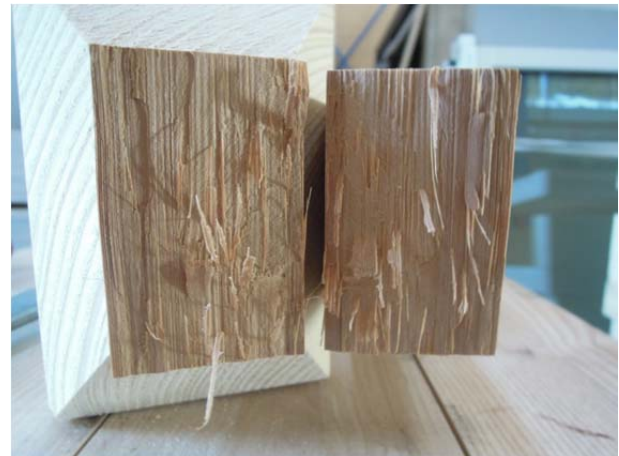
T90-G1-13



T90-G1-14



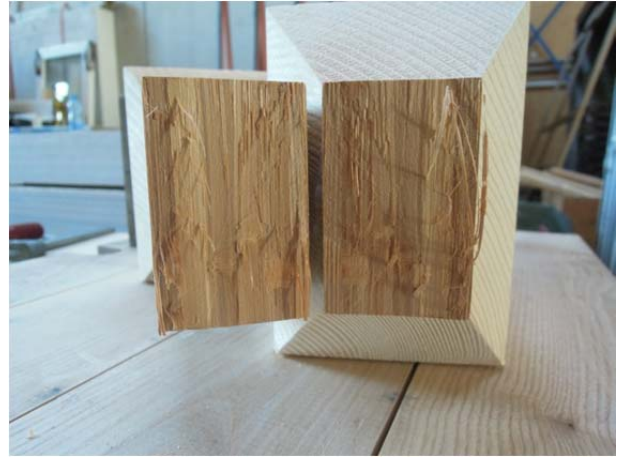
T90-G1-14



T90-G1-15



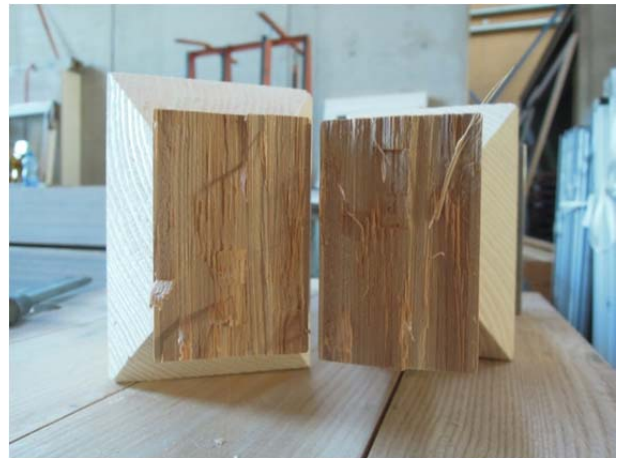
T90-G1-15



T90-G1-16



T90-G1-16



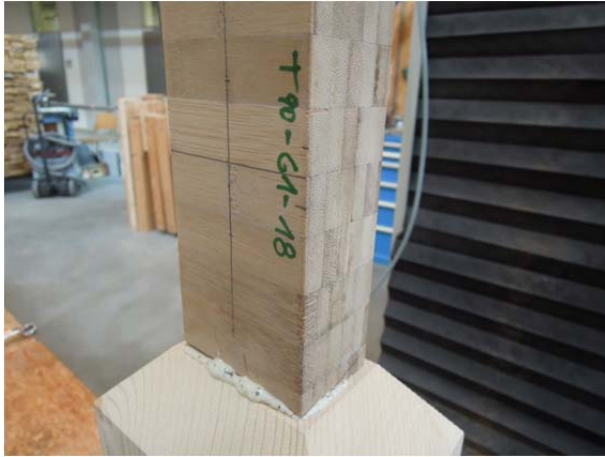
T90-G1-17



T90-G1-17



T90-G1-18



T90-G1-18



T90-G1-19



T90-G1-19



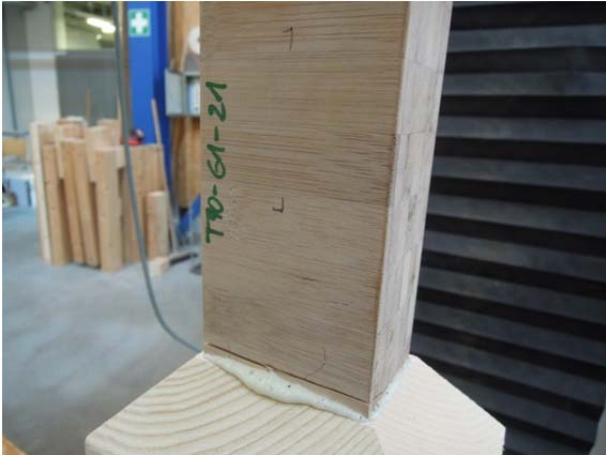
T90-G1-20



T90-G1-20



T90-G1-21



T90-G1-21



T90-G1-22



T90-G1-22



D-4 Sample T90-G2 (FW)

T90-G2-22



T90-G2-22



T90-G2-15



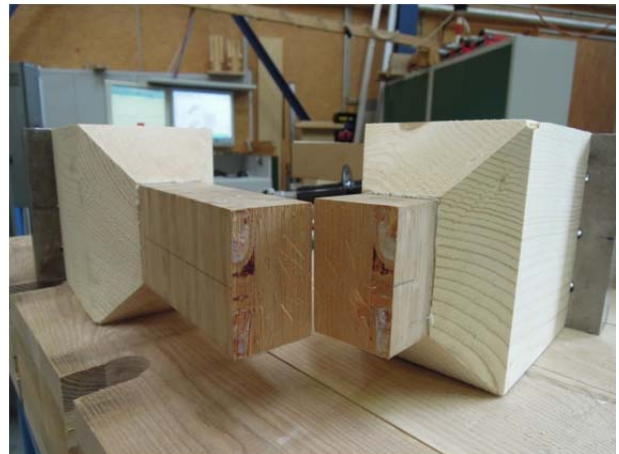
T90-G2-15



T90-G2-18



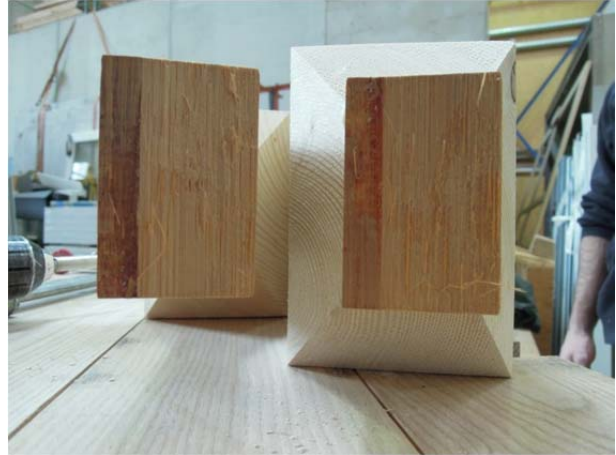
T90-G2-18



T90-G2-11



T90-G2-11



T90-G2-03



T90-G2-03



T90-G2-16



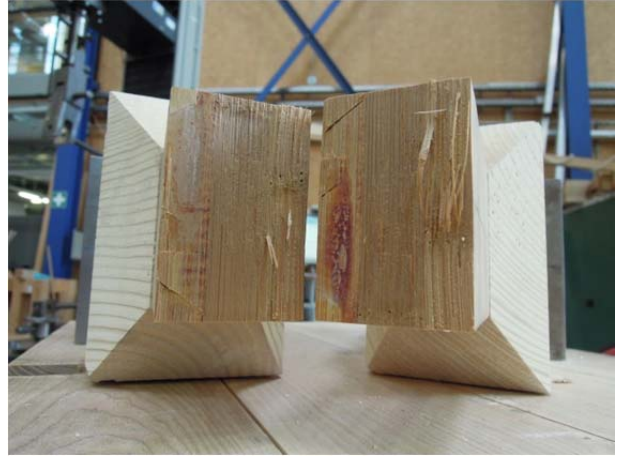
T90-G2-16



T90-G2-12



T90-G2-12



T90-G2-05



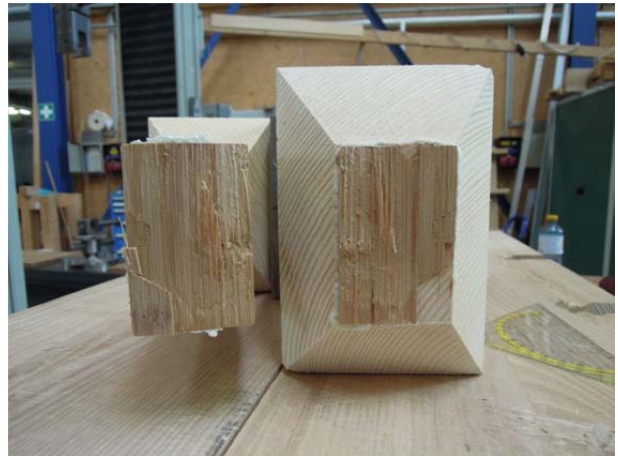
T90-G2-05



T90-G2-20



T90-G2-20



T90-G2-06



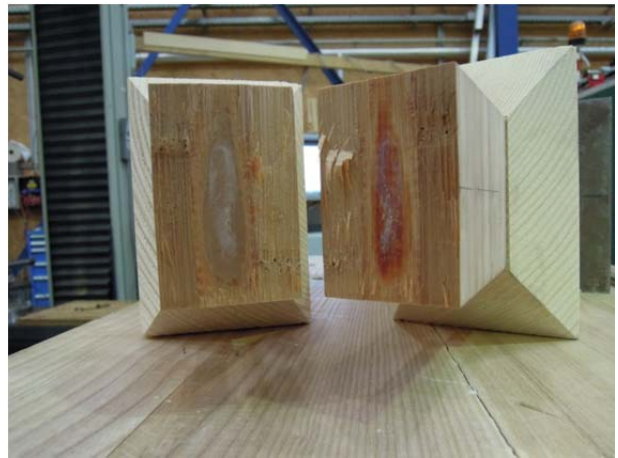
T90-G2-06



T90-G2-04



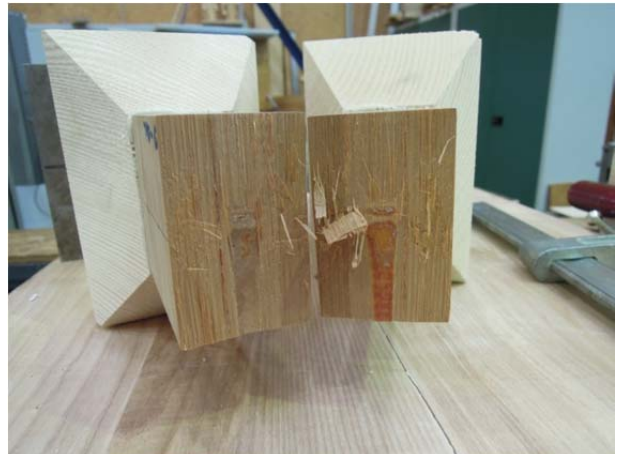
T90-G2-04



T90-G2-10



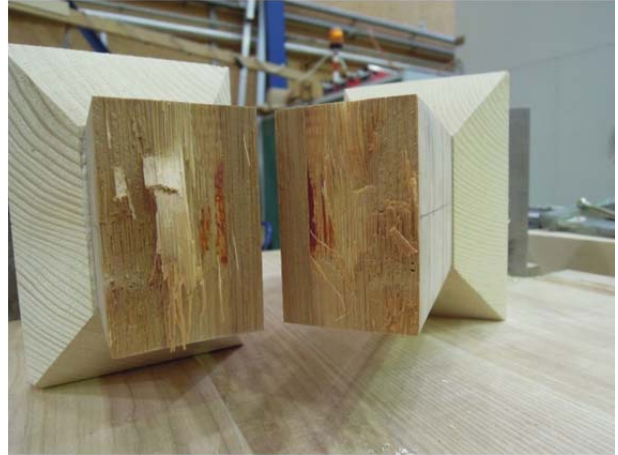
T90-G2-10



T90-G2-13



T90-G2-13



T90-G2-19



T90-G2-19



T90-G2-14



T90-G2-14



T90-G2-09



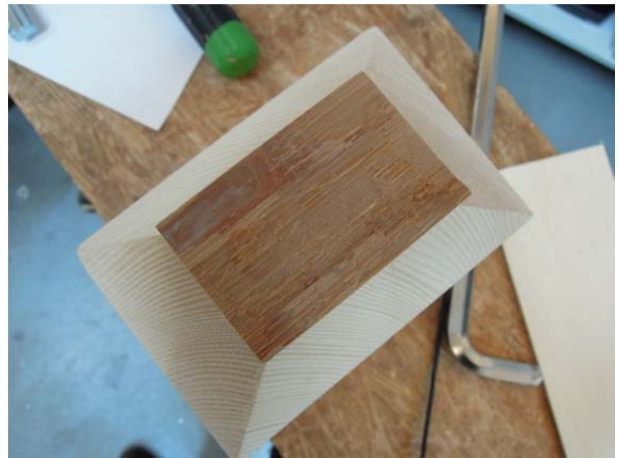
T90-G2-09



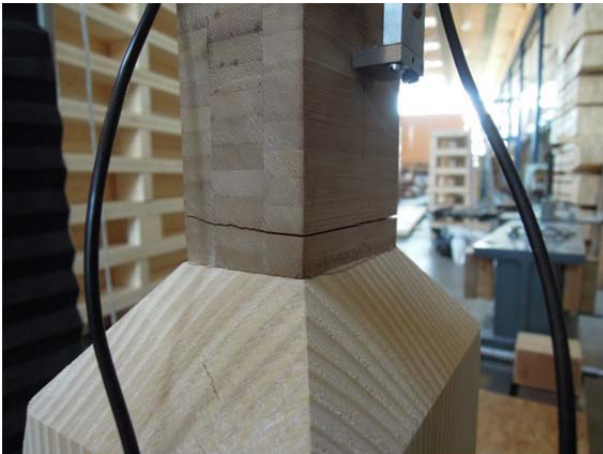
T90-G2-08



T90-G2-08



T90-G2-02



T90-G2-02



T90-G2-21



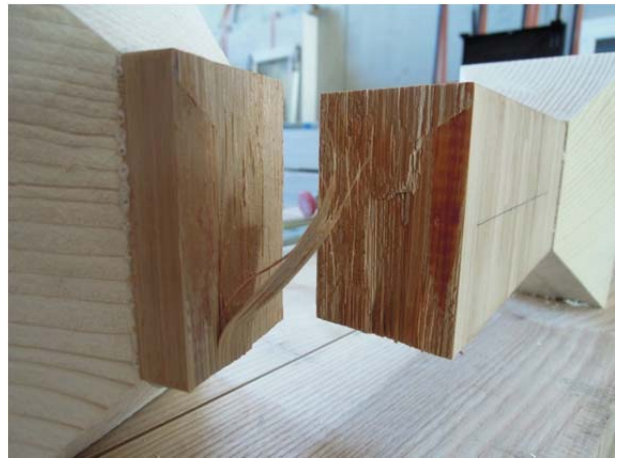
T90-G2-21



T90-G2-01



T90-G2-01



Dies ist eine Veröffentlichung des

FACHBEREICHS INGENIEURBAUKUNST (IBK) AN DER TU GRAZ

Der Fachbereich Ingenieurbaukunst umfasst die dem konstruktiven Ingenieurbau nahe stehenden Institute für Baustatik, Betonbau, Stahlbau & Flächentragwerke, Holzbau & Holztechnologie, Materialprüfung & Baustofftechnologie, Baubetrieb & Bauwirtschaft, Hochbau & Industriebau, Bauinformatik und Allgemeine Mechanik der Fakultät für Bauingenieurwissenschaften an der Technischen Universität Graz.

Dem Fachbereich Ingenieurbaukunst ist das Bautechnikzentrum (BTZ) zugeordnet, welches als gemeinsame hochmoderne Laboreinrichtung zur Durchführung der experimentellen Forschung aller beteiligten Institute dient. Es umfasst die drei Laboreinheiten für konstruktiven Ingenieurbau, für Bauphysik und für Baustofftechnologie.

Der Fachbereich Ingenieurbaukunst kooperiert im gemeinsamen Forschungsschwerpunkt „Advanced Construction Technology“. Dieser Forschungsschwerpunkt umfasst sowohl Grundlagen- als auch praxisorientierte Forschungs- und Entwicklungsprogramme.

Weitere Forschungs- und Entwicklungskooperationen bestehen mit anderen Instituten der Fakultät, insbesondere mit der Gruppe Geotechnik, sowie nationalen und internationalen Partnern aus Wissenschaft und Wirtschaft.

Die Lehrinhalte des Fachbereichs Ingenieurbaukunst sind aufeinander abgestimmt. Aus gemeinsam betreuten Projektarbeiten und gemeinsamen Prüfungen innerhalb der Fachmodule können alle Beteiligten einen optimalen Nutzen ziehen.

Durch den gemeinsamen, einheitlichen Auftritt in der Öffentlichkeit präsentiert sich der Fachbereich Ingenieurbaukunst als moderne Lehr- und Forschungsgemeinschaft, welche die Ziele und Visionen der TU Graz umsetzt.

Nummerierungssystematik der Schriftenreihe

S – Skripten, Vorlesungsunterlagen | F – Forschungsberichte
V – Vorträge, Tagungen | M – Masterarbeiten

Institutskennzahl:

1 – Allgemeine Mechanik | 2 – Baustatik | 3 – Betonbau
4 – Holzbau & Holztechnologie | 5 – Stahlbau & Flächentragwerke
6 – Materialprüfung & Baustofftechnologie | 7 – Baubetrieb & Bauwirtschaft
8 – Hochbau & Industriebau | 9 – Bauinformatik

Fortlaufende Nummer pro Reihe und Institut / Jahreszahl